Chemical-genetic profiling to investigate cross-resistance and collateral sensitivity between antimicrobial peptides

Ph.D. Thesis

Pramod Kumar Jangir

Supervisors: Csaba Pál, Ph.D., Bálint Kintses, Ph.D.

Doctoral School of Biology

Biological Research Centre of the Hungarian Academy of Sciences

Institute of Biochemistry

Synthetic and Systems Biology Unit

University of Szeged

Faculty of Natural Sciences and Informatics

Szeged

2019

Abstract

Antimicrobial peptides (AMPs) are crucial components of the host immune system and have been proposed as promising novel anti-infectives. However, there is a serious concern that therapeutic application of AMPs would drive bacterial cross-resistance to our own immunity peptides. Our knowledge of cross-resistance between AMPs remains extremely limited. To address this gap, we used chemical-genetic approaches to uncover the resistance determinants of *E. coli* against 15 different AMPs. This comprehensive compendium revealed multiple and functionally diverse genes that modulate bacterial susceptibility to different AMPs. Interestingly, AMPs differ considerably in their resistance determinants, and resistance-enhancing genes overlap only to a limited extent between AMPs. As a consequence, collateral sensitivity effects were common: numerous genes decreased susceptibility to one AMP while simultaneously sensitized to others. Finally, by integrating laboratory evolution approach, we showed that our chemical-genetic map informed on the cross-resistance interactions between AMPs. In the future, the chemical-genetic map could inform efforts to avoid cross-resistance between therapeutic and human host AMPs.

Table of content

List of abbreviations

AMPs	Antimicrobial peptides
AP	Apidaecin IB
BAC5	Bactenecin 5
BAC7	Bactenecin 7
CAP18	CAP18
CP1	Cecropin P1
HBD-3	Human beta-defensin-3
IND	Indolicidin
LL37	LL-37 human cathelicidin
PGLA	Peptide glycine-leucine amide
PEX	Pexiganan
PLEU	Pleurocidin
PXB	Polymyxin B
PROA	Protamine
R8	R8
TPII	Tachyplesin II
RND transporter	Resistance-nodulation-division transporter
HNP-1	Human neutrophil peptide-1
hLF-1-11	Human lactoferrin
α-MSH	α-melanocyte stimulating hormone peptide
IL-6	Interleukin-6
TNF-α	Tumor necrosis factor-alpha
LPS	Lipopolysaccharide
PL	Phospholipid
PG	Phosphatidylglycerol
PE	Phosphatidylethanolamine
CL	Cardiolipin

MOA	Mode of action
ORF	Open reading frame
MS	Minimal salt medium
HIP	HaploInsufficiency profiling
NVI	Normalized variation of information
DAmP	Decreased abundance by mRNA perturbation
GO	Gene ontology
FDR	False discovery rate
MIC	Minimum inhibitory concentration
FITC-PLL	Fluorescein isothiocyanate-labeled poly-L-lysine
CCCP	Cyanide-m-chlorophenylhydrazone
RFU	Relative fluorescence unit
IPTG	Isopropyl β-D-1-thiogalactopyranoside
PCR	Polymerase chain reaction
PBS	Phosphate-buffered saline
COGs	Clusters of Orthologous Groups
OM	Outer membrane
IM	Inner membrane
Δψ	Membrane potential

1. Introduction

1.1 Antimicrobial peptides (AMPs): Molecules of host defense system

Antimicrobial peptides (AMPs) are ancient host defense molecules present in all classes of life. These are endogenous antibiotic molecules that protect hosts from a wide variety of pathogens, like bacteria, viruses, fungi[1]. AMPs are generally short (10-50 amino acids) cationic and ribosomally synthesized molecules[1,2]. Because of specific physicochemical properties (cationic property, amphipathicity etc.) of AMPs microbial membrane has been considered as their primary target[3]. Fundamental differences between microbial and mammalian cells make these AMPs specific and active against microbial cells. These differences include membrane composition, membrane potential, structural properties (Figure 1).

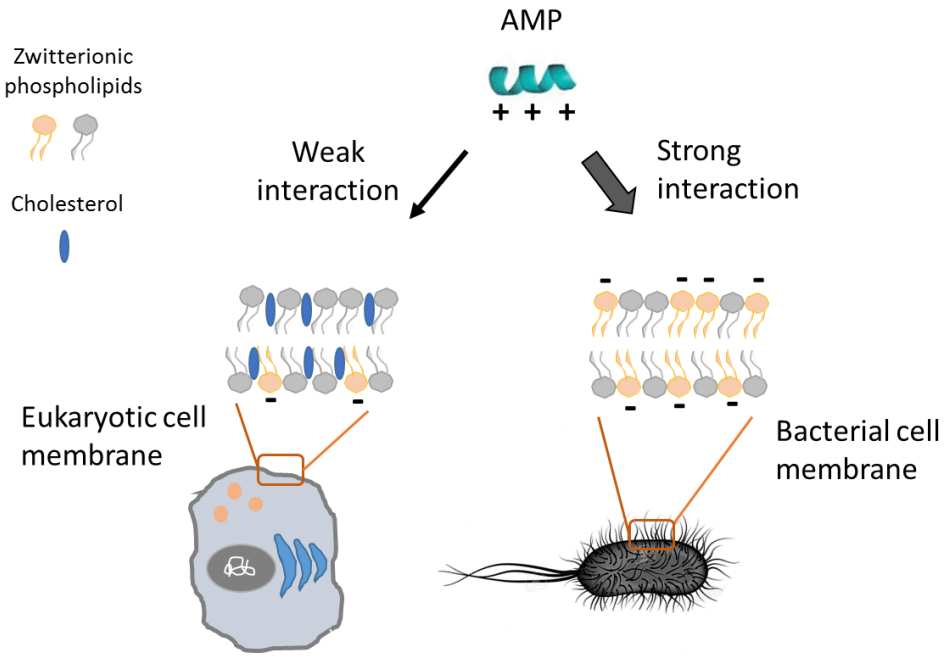

Figure 1. Schematic showing the cell selectivity of AMPs. Specific structural and chemical properties of bacterial membrane, make bacteria more prone to AMPs. For example, negative surface charge on bacterial membrane causes strong electrostatic interaction between bacterial membrane and AMPs. Figure is adapted from *Zasloff, M. (2002), Nature*.

The discovery of lysozyme by Alexander Fleming in 1921 was one of the first reports on AMPs showing their protective role in humans against certain bacterial infections. Later on, in 1939, Gramicidin the first AMP as commercially manufactured antibiotics was discovered from prokaryotic cells (*Bacillus brevis*). Gramicidin exhibits activity against a wide range of Gram-positive bacteria[4]. During the 1990s important new classes of AMPs were discovered in humans, including defensins[5] and cathelicidins[6], and this stimulated research into discovering a variety of human AMPs, and more recently, into their potential applications in antimicrobial therapy to control bacterial infections. AMPs are present not only in human and bacteria but also plants and insects that lack an adaptive immune system suggesting that these are important part of host immune system[2,3]. Because of their broad spectrum of antimicrobial activities, they have been proposed as novel anti-infective compounds[7].

1.2 AMPs: Multifunctional molecules

Many studies have suggested that AMPs possess multiple activities in the host such as antimicrobial, anticancer and immunomodulatory activity[1,2,7] (Figure 2).

Antibacterial AMPs are the well-studied AMPs. These are mostly cationic and amphipathic molecules and the majority of them target bacterial cell membrane. Although there is a great diversity in their physicochemical properties, cationic and amphipathic property allow them to attach to bacterial lipid membrane and penetrate through the membrane to exert their antibacterial activity[8]. Several studies have demonstrated that AMPs can also target bacterial intracellular processes such as cell-wall synthesis, nucleic acid synthesis, protein synthesis, cellular respiration[2]. For example, buforin II[9], and PR39[2] can diffuse into cells and bind to DNA and RNA without damaging the cell membrane. Drosocin, pyrrhocoricin, and apidaecin are other examples of such AMPs[2,10]. Some AMPs (Indolicidin, protamine, pleurocidin etc.) can target both the membrane and intracellular processes[10] (Figure 3).

Some AMPs (β-defensins, lactoferrin, melittin etc.) have been shown to function as a first-line defense against various viruses, these AMPs are called antiviral AMPs[11]. The antiviral activity is mediated through interaction with viral envelopes or by interfering with the binding of virus to host cells.

Several studies showed that some AMPs have an anticancer property and considered as potential chemotherapeutic drugs[12]. The altered membrane property of cancer cells allows AMPs to act efficiently against them. Cancer cells lose the asymmetry between inner and outer

membrane which cause phosphatidylserine exposure, altered membrane fluidity and membrane potential. Presence of heparan sulfates and O-glycosylated mucins on the surface of tumor cells also changes membrane property by increasing the surface negative charge of tumor cells[12]. These changes facilitate the AMPs to exert their activity against cancer cells. Aurein 1.2, a frog AMP, is one of the anticancer peptides which was found to be active against multiple cancer cells in vitro[12]. Similarly, human neutrophil peptide-1 (HNP-1) and pleuricidin 07 have also been demonstrated to show anticancer property with low cytotoxicity against healthy cells[12].

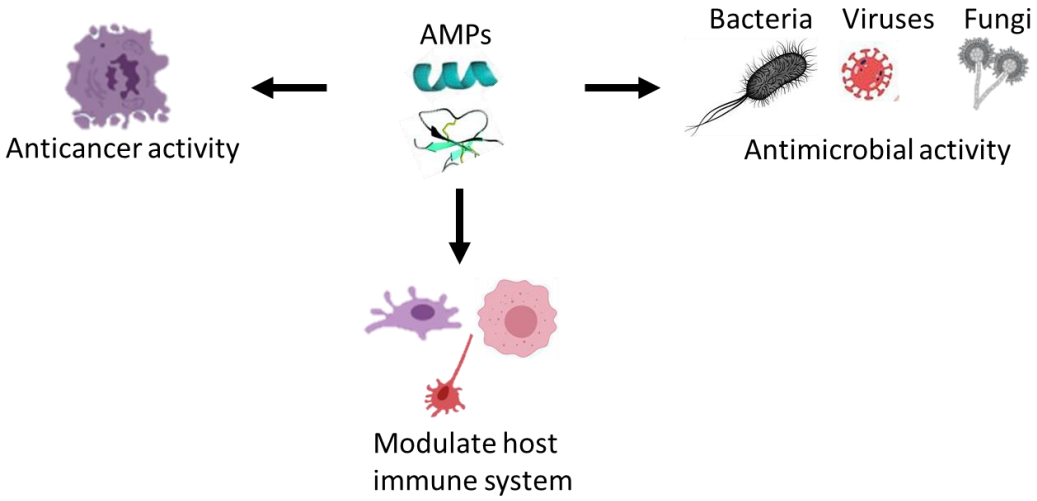

Figure 2. Overview of broad-spectrum activity of AMPs.

In addition to antimicrobial and anticancer activity, AMPs can serve as modulators of the host immune system[7]. AMPs exhibit a broad range of immunomodulatory activity such as stimulation of chemotaxis, alter host gene expression, modulation of immune cell differentiation and response, promote wound healing, contribute to the clearance of microbial infections and anti-endotoxin activity[4,7]. As an example, α-melanocyte-stimulating hormone peptide (α-MSH), lactoferricin and LL37 have been shown to promote the generation of anti-inflammatory cytokines, inhibit the LPS-induced secretion of interleukin-6 (IL-6) and tumor necrosis factor alpha (TNF-α), respectively[13].

1.3 Physicochemical properties and antimicrobial activity of AMPs

In order to design effective therapeutic peptides, considerable efforts have been made to understand how the physicochemical properties influence antimicrobial activity of AMPs. The

antimicrobial property of AMPs largely depends on their physicochemical properties such as net charge, amphipathic propensity, hydrophobicity[8]. These properties allow AMPs to bind to negatively charged bacterial membrane and penetrate into the cell[8].

1.3.1 Net charge

Most AMPs are positively charged and this is one of the main properties that determine the initial electrostatic attraction of AMPs to negatively charged bacterial membrane. Bacterial membrane contains acidic phospholipids (like phosphatidylglycerol (PG), phosphatidylethanolamine (PE) and cardiolipin (CL)) that display a net negative charge on the membrane and allow positively charged AMPs to bind on the membrane. For example, a human peptide LL-37 binds to the bacterial membrane through electrostatic interactions, and after the initial electrostatic interaction, the amphipathic property of AMP enables it to insert into the bacterial membrane, forming a pore and leading to lysis of the bacterial cell[2,8]. While several studies have demonstrated that there is a correlation between antimicrobial activity and net charge of AMP, beyond a certain limit, increasing positive charge may not affect antimicrobial activity[8,14]. In the case of magainin 2 analogs, the antibacterial activity was increased when the net positive charge was increased from +3 to +5. However, charge increase beyond +5 resulted in the loss of antibacterial activity[8]. These results suggest that a proper balance of electrostatic interactions between AMP and bacterial membrane is critical for antimicrobial activity of the peptide.

1.3.2 Hydrophobicity

AMP hydrophobicity has also been considered as an important feature that influences the activity and selectivity of AMP molecules. The amino acid sequences of natural AMPs are mostly rich in hydrophobic residues. Bacterial membrane permeabilization by AMPs greatly depends on their hydrophobicity[8,15]. Similar to net charge, there is an optimal range where an increase in hydrophobicity of an AMP can increase its antibacterial activity. Interestingly, change in hydrophobicity can also alter the target range of AMPs. For example, some synthetic analogs of magainin peptide with higher hydrophobicity can kill both the Gram-positive and Gram-negative bacteria while Magainin is only active against Gram-negative bacteria[16].

1.3.3 Amphipathicity

Amphipathicity is another crucial parameter of AMPs that facilitates AMP binding to membrane and membrane permeabilization[8,15]. Amphipathicity reflects a property in which AMP can fold into a structure that displays both hydrophobic and hydrophilic surface. Hydrophobic moment is one of the quantitative measures of amphipathicity. Hydrophobic moment can be calculated using R package (Peptides) for data mining of AMPs which uses the standardized Eisenberg scale[17]. Increase in hydrophobic moment has been shown to increase the membrane permeabilization and hemolytic activities of AMPs. Since amphipathicity is more important than other physicochemical features, it should be considered when designing novel AMPs for therapeutic purpose.

1.3.4 Solubility and aggregation propensity

In order to penetrate the bacterial lipid bilayer, AMPs should be soluble and have low aggregation propensity in solution. Importantly, aggregation in solution (in vitro) has a clearly different effect on AMP activity compared to in vivo (i.e. bacterial membrane) aggregation[14]. Aggregation in solution makes AMPs less effective while in vivo aggregation helps AMPs to exert their activity on bacterial membrane[8,14]. Several studies have demonstrated the importance of solubility in AMP action. For example, V_{681} a synthetic AMP showing a higher tendency to aggregate in solution resulted in weaker membrane permeabilization and increased hemolytic activity[18].

1.4 Mode of action of AMPs

As described above, cationic AMPs bind to negatively charged bacterial membrane and cause cell lysis. However, recent studies have shown that AMPs can also target intracellular processes such as DNA and RNA synthesis, translation, cell wall biosynthesis and septum formation[2,10] (Figure 3). Adding more complexity, some AMPs can have multiple targets including cell membrane and intracellular processes, and these AMPs are called dirty drugs.

AMPs can be divided into two groups on the basis of their mode of action, a) membrane disrupting (pore formers) AMPs and b) intracellular-targeting AMPs.

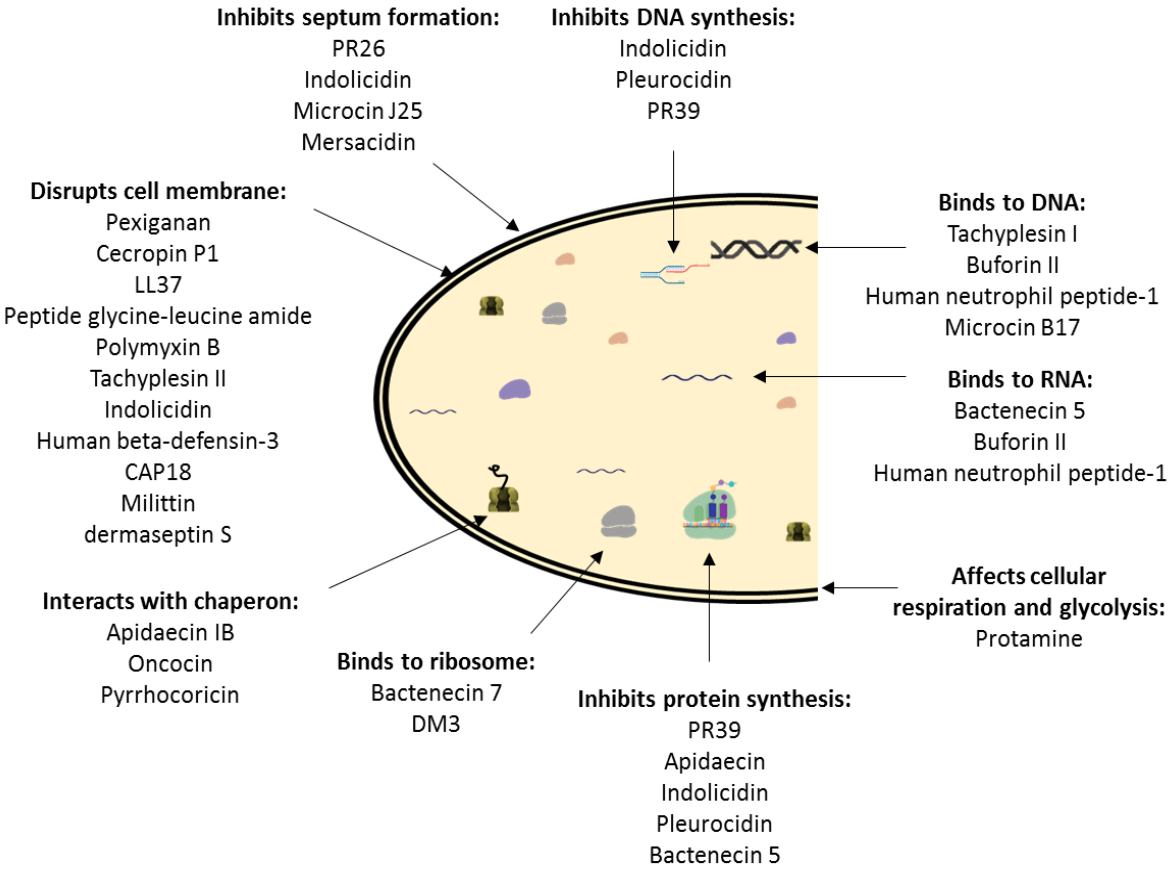

Figure 3. Mode of action of AMPs. This figure shows diverse cellular processes targeted by AMPs. Figure is adapted from *Brogden, K. A., Nat. Rev. Microbiol. (2005).*

1.4.1 Membrane disrupting AMPs (pore formers)

It is widely believed that AMPs show a rapid antibacterial killing by creating pores in the bacterial membrane, resulting in cytoplasmic leakage and cell death. The above described physicochemical properties (such as net charge, amphipathicity, hydrophobicity and solubility) ensure the initial binding and insertion of AMPs into bacterial lipid membrane[8,15]. The initial binding is due to electrostatic interaction between positively charged AMPs and negatively charged LPS or phospholipids of the bacterial membrane. After initial binding, AMPs can start aggregating on the membrane and disrupt the physical integrity of the cell membrane. Different models have been proposed to explain AMP-induced pore formation[2,8]: i) the barrel-stave model, shows that AMPs (example, alamethicin) aggregates and penetrate perpendicularly into the lipid membrane[19,20] (Figure 4A); ii) in the carpet mechanism, AMPs (examples, cecropin,

melittin dermaseptin S etc.) accumulate on the bacterial membrane, and after reaching critical concentration, induce detergent-like effect to disrupt the lipid membrane[2,13](Figure 4B); and iii) the toroidal pore model, proposes that AMP helices insert in the membrane and lipid molecules bend inwards to form transmembrane pores (Figure 4C). Magainin, protegrin and LL37 are well studies AMPs that create toroidal pores in the lipid membrane[2].

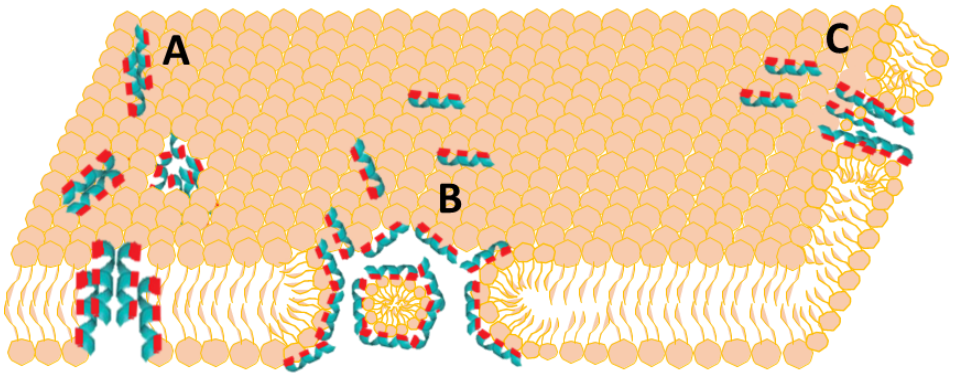

Figure 4. Schematic representation of different models of AMP-induced pore formation in bacterial membrane. A: barrel-stave model, **B:** carpet model, **C:** toroidal pore model. Figure is adapted from *Brogden, K. A., Nat. Rev. Microbiol. (2005).*

These different mechanisms of membrane disruption depend on multiple factors, for example, physicochemical properties of AMPs, bacterial membrane type and composition (Gram-negative and Gram-positive). For example, LL37 a human peptide preferentially inserts into phosphatidylglycerol (PG) rich membrane and shows weaker interaction with other lipids like phosphatidylethanolamine (PE) and phosphatidylcholine (PC).

1.4.2 Intracellular targeting AMPs

Previously, membrane disrupting mechanism was considered as the only mechanism of bacterial killing. However, recent work has demonstrated that some AMPs can kill bacteria without creating pores in the membrane[2]. Such AMPs can inhibit intracellular processes like DNA replication, transcription, translation, cell wall synthesis and metabolism[2,10] (Figure 3). For example, proline-arginine rich AMPs (PR39, bactenecin 5, bactenecin 7 etc.) inhibits RNA and

protein synthesis. Similarly, mersacidin and microcin J25 inhibits cell-wall synthesis and septum formation, respectively[2,10]. Interestingly, some of the intracellular targeting AMPs can target multiple cellular processes. For example, seminalplasmin inhibits RNA synthesis[21] and induce autolysis in the target cell[22,23]. Intracellular targeting AMPs use different mechanisms of cellular uptake to translocate themselves inside the cell. Membrane potential-driven transporters have been shown to be involved in cellular uptake of AMPs. A well-known example is *sbmA*, a peptide antibiotic transporter[24]. Other examples of AMP-uptake mechanisms include *yejABEF* operon which encodes an inner membrane ABC transporter in *Salmonella Typhimurium*[25] and *bacA gene* (peptide transporter) in *Sinorhizobium meliloti*[26]. The *yejABEF* operon and *bacA* have been shown to involve in the uptake of protamine[25] and proline-arginine rich AMPs (example, bactenecin 7)[26].

While these studies draw a complex picture of the mode of action of AMPs, our understanding of their actual mechanism of killing remains limited. Future investigations of their complex mechanism of action are needed to develop AMPs as novel therapeutic agents.

1.5 AMP resistance mechanisms

AMPs differ considerably in their physicochemical properties and mechanisms of killing and correspondingly bacteria have evolved different resistance mechanisms against them. These resistance mechanisms involve a variety of changes in bacterial cell membrane, intracellular processes and even targeting AMPs[27,28] (Figure 5). Bacterial resistance mechanisms can be divided into two main categories, intrinsic and acquired mechanism.

Intrinsic resistance can occur either due to the inherent property of bacterial cell (for example, having more positively charged membrane) known as a passive mechanism or due to adaptive/inducible molecular modifications[27]. In the case of inducible mechanisms, bacterial membrane and intracellular targets can be modified to circumvent AMP killing. A well-known AMP resistance mechanism is the alteration of membrane properties (surface charge, permeability etc.) that cause reduced electrostatic interactions and binding of AMPs. For example, bacterial two-component systems like PmrAB and PhoPQ modify lipid membrane by changing net negative surface charge and increase bacterial survival under AMP stress[29,30] (Figure 5). Deletion of these two-component systems results in not only increased susceptibility to AMPs but also attenuated virulence[31]. Several studies showed that these two-component systems regulate expression of many genes, for example, *pagP*[32], genes of the *arnBCADTEF*

operon, *eptA*, *eptB*, *lpxT*[33]. Most of these genes modify LPS and phospholipids to make the membrane less negatively charged and therefore provide resistance to AMPs[27,28,33].

Beside membrane and intracellular target modification, bacteria also have other AMP resistance mechanisms such as proteolytic degradation or elimination of the AMPs from the cell by efflux pumps[27] (Figure 5).

The well-known AMP degrading proteases are *ompT*[34] and *pgtE*[35] in *E. coli* and *Salmonella Typhimurium*, respectively (Figure 5 and Supplementary Table 1). Stumpe *et al*. demonstrated that expression of OmpT in *E. coli* correlates with increased resistance against protamine. PgtE, an outer membrane endopeptidase, having structural features identical to OmpT, has also been shown to be associated with resistance to alpha-helical peptides[35]. ATP-binding cassette transporters and RND efflux pumps also play an important role in AMP resistance. For example, SbmA, an ABC superfamily transporter in *E. coli* is involved in the uptake of proline-rich AMPs[36] and deletion of *sbmA* causes resistance to these AMPs, like bactenecin 7, arasin, PR39[36–38].

The aforementioned examples of genetic determinants are part of intrinsic resistome, i.e., the collection of genes that contribute to resistance at their native expression levels[39]. Intrinsic resistome can be explored by testing the drug hypersensitivity of gene knockout mutants. Both the genome-wide and targeted screening approaches have been considered as potential tools to characterize the intrinsic resistome[39,40].

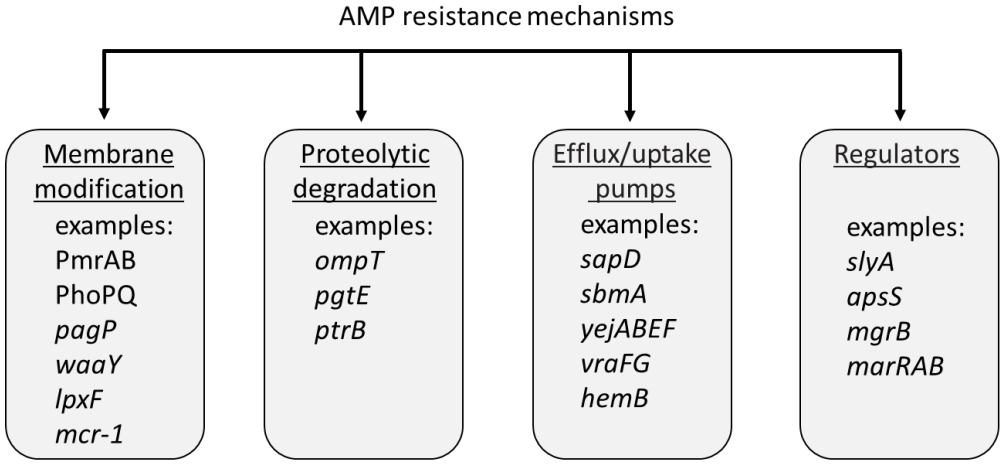

Figure 5: AMP resistance mechanisms in bacteria. For a full list of literature curated AMP resistance genes, see Supplementary Table 1.

A genetic screen for drug resistance (using gene overexpression) can provide some extra information compare to genetic screen for drug hypersensitivity[39] (i.e. intrinsic resistome). Gene overexpression causes nonoptimal expression which can protect bacteria from drug stress, and collectively, these genes can be called as latent resistome[39]. Interestingly, some studies have shown that overlap in resistance genes between intrinsic and latent resistome is rare, which further suggest that intrinsic and latent resistome provide different biological meaning about resistance mechanisms in bacteria[39].

Besides intrinsic resistance, bacteria can acquire resistance through horizontal gene transfer (transfer of genetic material between bacteria via transformation, phages transduction and conjugation)[41]. Recently, it was found that a plasmid containing the *mcr-1*, a colistin resistance gene is spreading in different bacterial species. The first report on *mcr-1* was in *E. coli* from a pig in China and within 1-2 years' time, several studies reported the presence of *mcr-1* in different bacterial species in more than 30 countries[42,43].

While most of the studies on AMPs has been carried out using a targeted approach focusing on single AMP or gene, a genome-wide systematic study is still lacking. Therefore, there is an urgent need to comprehensively map the relationships between the modes of action of AMPs and the genetic determinants influencing bacterial susceptibility to them.

1.6 Evolutionary trade-offs associated with resistance evolution

Evolution of microbial resistance can result in evolutionary positive (cross-resistance) and negative (collateral sensitivity) trade-offs[44,45]. In the case of cross-resistance, evolution of resistance to one drug can increase bacterial fitness to other drugs while its inverse (decrease bacterial fitness to other drugs) is known as collateral sensitivity (Figure 6). Understanding of cross-resistance and collateral sensitivity interactions can inform on effective drug combinations and treatment strategies like drug cycling[45]. For example, Imamovic *et al.* demonstrated that resistance evolution in *Pseudomonas aeruginosa* in cystic fibrosis patients caused collateral sensitivity to other antibiotics. Authors showed that the drug treatment optimized based on the collateral sensitivity interaction effectively eradicated the resistant subpopulation from the patient's lung[46].

Recent studies have proposed collateral sensitivity as a promising strategy to slow down the resistance evolution and even reverse the pre-existing resistance[46–48]. However, the

underlying principles and molecular mechanism of collateral sensitivity remain poorly understood.

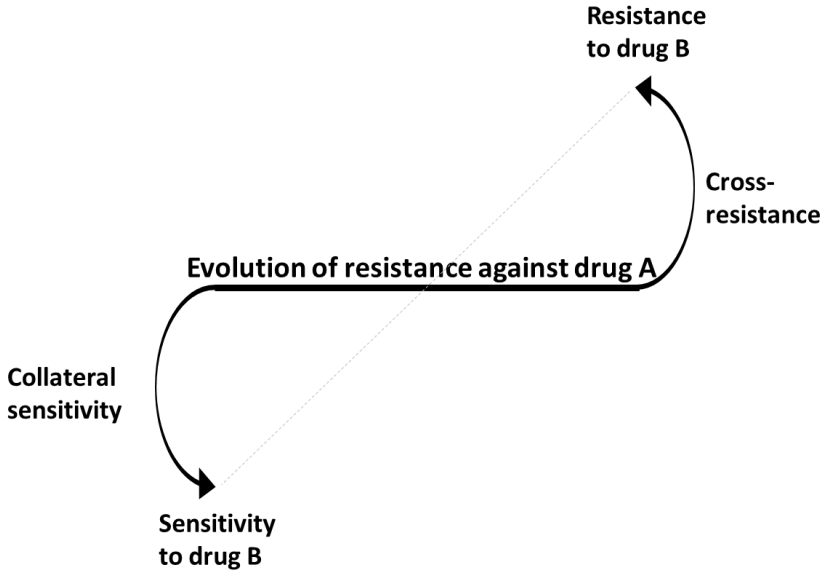

Figure 6. Cross-resistance and collateral sensitivity interactions between antimicrobial drugs. Evolution of antimicrobial resistance to drug A can increase (cross-resistance) or decrease (collateral sensitivity) bacterial susceptibility to drug B.

1.7 Chemical-genetics in dissecting bacterial resistance mechanisms and their evolutionary trade-offs

Chemical-genetic profiling is a high-throughput approach that systematically measures the contribution of each gene to the bacterial fitness upon exposure to different chemical compounds. Genome-wide mutant libraries consist of gain-of-function (overexpression library) or loss-of-function (knockout library) mutants are used for chemical-genetic profiling[40,49–51]. In order to perform this phenotypic screening, one needs to have a quantitative measure of the phenotype of each mutant in the library (pooled or arrayed) (Figure 7). Integrated approaches like next-generation sequencing and gene barcoding, allows to quantify the relative abundance and thus fitness of each mutant upon drug treatment[51,52]. In the case of arrayed libraries, experimental automation, microscopy and image processing tools can be used to quantify the fitness of hundreds of mutants on a single plate (Figure 7)[40,53].

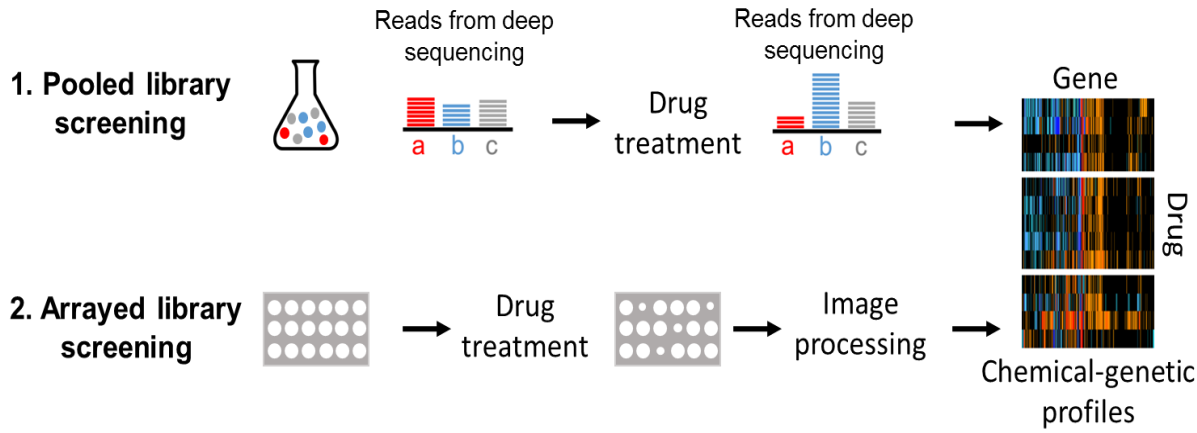

Figure 7. Schematic representation of chemical-genetic approaches. Pooled or arrayed mutant library can be used for the screening. The fitness of each mutant in the library is determined upon drug treatment.

The high-throughput nature of the chemical-genetic approach provides a system-level understanding of drug action and resistance determinants, drug-drug interactions, function of unknown proteins etc[49,54–56]. A well-known example is HaploInsufficiency Profiling (HIP) that was carried out to find drug targets in yeast[57]. In this profiling, heterozygous deletion mutant library was used to reduce the dose of essential genes in the yeast. In the case of haploid organisms like bacteria, overexpression and knockout screening are widely used to map mode of action of a drug and genetic determinants of drug resistance[49,58,59]. Several studies in the model bacterium *E. coli* have provided valuable chemical-genetic data and insights into resistance mechanisms against different antimicrobial compounds. For example, Nichols *et al.* carried out a phenomic profiling by quantifying the response of all single-gene deletion in *E. coli* to more than 300 different chemical/drug stresses[49]. This study generated a comprehensive dataset that provided novel insights into drug action, role of genes in multidrug resistance and function of uncharacterized genes. In addition, to study both the gene and drug function, chemical-genetic approach has been proposed as a useful tool to access the cross-resistance and collateral sensitivity interactions between drugs[40,60]. A recent study showed that chemogenomic profile similarity between antibiotics can predict the cross-resistance spectrum[60]. Altogether these studies show the utility of chemical-genetic approach to explore different aspects of drugs function and cellular responses against them.

Because of the rapid bacterial resistance evolution against conventional antibiotics, there is a growing interest in the clinical development of AMPs as a possible alternative strategy. However, there are two major concerns with therapeutic use of AMPs. First, bacterial potential of resistance development against AMPs[27] and second, therapeutic use of AMPs may select for resistant pathogen showing cross-resistance to human host-defense AMPs[61,62]. These issues need to be carefully investigated as some AMPs (like pexiganan, iseganan, human lactoferrin-1-11) are already under clinical trials[7,63]. While most of our knowledge on AMP resistance is coming from case studies focusing on specific AMP, a systematic study on the extent to which the genetic determinants of resistance differ across AMPs is still lacking. Also, our understanding of cross-resistance and collateral sensitivity between AMPs remains unclear. Given the therapeutic importance of AMPs, a systematic study on AMP resistance, collateral sensitivity and cross-resistance between AMPs may help to rationally choose AMPs for clinical development and to minimize the cross-resistance between therapeutic and human host AMPs.

To address this issue, we applied a genome-wide chemical-genetic approach to map the genetic determinants of AMP resistance. This approach provides a better understanding of how the differences in mode of action of AMPs shape the resistance mechanisms against them. By analyzing these differences, we could identify a number of genes that induce cross-resistance and collateral sensitivity between AMPs. Moreover, by integrating laboratory evolution experiment we demonstrated that chemical-genetic profiles can inform on cross-resistance patterns between AMPs. Our results suggest that the chemical-genetic map could inform on how to choose therapeutic AMPs with minimal cross-resistance to human host AMPs.

2. Objectives

In our research, we aimed to systematically investigate the latent and intrinsic AMP resistome of *E. coli* and to understand how the modes of action of AMPs shape the resistome.

Our particular goals were the following: 1) identifying the resistance determinants of *E. coli* against 15 different AMPs, 2) understanding how the AMPs with different modes of action and physicochemical properties differ in their resistance determinants, 3) investigating whether the differences in AMP's mode of action and resistance determinants advise on cross-resistance and collateral sensitivity interaction between AMPs.

To achieve these goals,

- we established a genome-wide chemical-genetic screening method to measure the effect of overexpression of each of 4,400 *E. coli* genes on bacterial susceptibility against 15 AMPs (latent AMP resistome).

- we explored the intrinsic AMP resistome by performing a chemical-genetic screen with a set of 279 partially-depleted essential genes (hypomorphic alleles) of *E. coli.*

- we examined how the similarity in chemical-genetic profiles inform on mechanism of action of AMPs.

- we interrogated whether the mode of action of AMPs shapes the latent and intrinsic resistome.

- we investigated collateral sensitivity between AMPs and the molecular mechanism underlying collateral sensitivity interactions.

- we investigated whether chemical-genetic profiles can inform on cross-resistance interactions between AMPs**.**

3. Materials and methods

3.1 Growth media, bacterial strains and growth conditions:

Experiments were conducted in minimal salts (MS) medium supplemented with $MgSO_4$ (0.1mM), $FeCl_3$ (0.54 µg/mL), thiamin (1 µg/mL), casamino acids (0.2%) and glucose (0.2%). Luria-Bertani (LB) medium contained tryptone (0.1%), yeast extract (0.05%), and NaCl (0.05%). All components were purchased from Sigma-Aldrich unless stated otherwise.

In this study, we used ASKA library (GFP -) (a complete set of *E. coli* K-12 ORF archive) that includes ~4400 ASKA clones[64]. This plasmid library collection was transformed into *E. coli* K12 BW25113 strain (see methods "Chemical-genetic screening"). Bacterial cultures were grown at 30°C unless noted otherwise.

3.2 Antimicrobial peptides (AMPs)

We used a wide variety of antimicrobial peptides (AMPs) which are diverse in their physicochemical properties and source of origin. Importantly, some of these AMPs have clinical relevance (Table 1). The following AMPs were used in this study: human beta-defensin-3 (HBD-3), protamine (PROA), PR-39, Peptide Glycine-Leucine Amide (PGLA), pexiganan (PEX), indolicidin (IND), bactenecin 5 (BAC5), R8, apidaecin IB (AP), rabbit 18-kDa cationic antimicrobial protein (CAP18), pleurocidin (PLEU), polymyxin B (PXB), LL-37 cathelicidin (LL37), tachyplesin II (TPII), cecropin P1 (CP1). AMPs were custom synthesized by ProteoGenix, except for PROA and PXB, which were purchased from Sigma-Aldrich. AMP solutions were prepared in sterile water and stored at -80°C until further use.

3.3 Plasmid DNA preparation and purification

Bacterial cells harbouring the ASKA plasmids were inoculated in a flask containing 10 ml of LB medium supplemented with chloramphenicol (20 µg/ml) and grown overnight. Cells were harvested by centrifugation at 6685 x g for 5 minutes. Plasmid DNA was isolated using innuPREP plasmid mini Kit (Analytik Jena AG) according to the manufacturer's instructions. The genomic DNA contamination was removed by digesting the plasmid DNA for overnight with Lambda exonuclease and exonuclease I (Fermentas) at 37°C. The digested plasmid DNA samples were purified with DNA Clean & Concentrator™ (Zymo) kit according to the manufacturer's instructions.

3.4 Chemical-genetic screening

We performed chemical-genetic screening to study the impact of the overexpression of each *E. coli* ORF on bacterial susceptibility to each of the 15 different AMPs. This high-throughput screening was carried out using ASKA plasmid library where each *E. coli* ORF is cloned into a high copy number expression plasmid (pCA24N-ORFGFP(-))[64]. This method applies a pooled fitness assay or competition experiment with deep sequencing readout. To this aim, ASKA library clones were grown in 96-well plates filled with LB medium. An equal aliquot of each clone of the library was pooled together and this pooled library was used for plasmid DNA isolation as described before[65]. The purified plasmid pool and the empty vector pCA24N (without an ORF), were transformed into *E. coli* BW25113 by electroporation. The strain harbouring empty vector serves as a negative control in the experiment. Both the pooled library and negative control strain were grown in MS medium supplemented with 20 µg/ml chloramphenicol. Cells were grown until the optical density reached OD600=1 and the protein expression was induced by 100 µM isopropyl-ß-D-thiogalactopyranoside (IPTG). After 1h induction, ~5 x 10^5 bacterial cells from the library were inoculated into each well of a 96-well microtiter plate containing a concentration gradient of an AMP in the MS medium supplemented with 20 µg/ml chloramphenicol and 100 µM IPTG. In parallel, the overexpression library and the negative control strain were grown in the absence of AMP but in the same growth condition as the AMP treated samples. To monitor the bacterial growth, the 96-well plates were incubated at 30°C in microplate reader (Biotek Synergy 2) for 24 h. After incubation time, we selected the wells in which the doubling time of the whole cell population was increased by 2-fold. From these wells, the cells were transferred into fresh 20 mL of MS medium supplemented with the corresponding AMP in a concentration that again resulted in a two-fold increase in doubling time. Following 12-15 generations of growth, the plasmid pool was isolated from both the ASKA pool and the negative control.

3.5 High-throughput sequencing of plasmid pool

To determine the relative abundance of each plasmid, the purified plasmid DNA samples were subjected to next-generation sequencing with SOLiD system (Life Technologies). DNA sequencing was carried out by István Nagy and his colleagues from Seqomics Ltd, Szeged. The plasmid DNA samples were fragmented and used for library preparation. Samples were sequenced using the SOLiD4 sequencer (Life Technologies). For each sample, we generated 20-25 million of 50 nucleotide long reads. CLC Bio Genomics Workbench 4.6 program was used

to analyze the quality values for each nucleotide. Negative control strain (*E. coli* BW25113 strain carrying the empty vector) was used to measure read counts originating from genomic DNA contamination during plasmid preparation (background). For each AMP treatment, we used two independent replicates in the screening. The experiment with negative control was also carried out twice. In the case of the untreated sample (in the absence of AMP), we had five independent replicates.

3.6 Data analysis and clustering of chemical-genetic profiles

Data analysis and clustering of chemical-genetic profiles were performed by our colleague Gergely Fekete. Raw sequence data processing and mapping onto *E. coli* ORFs were carried out as described previously[48]. We applied previously established protocols for data processing and normalization[66–68]. Following different steps of data normalization and transformation, a differential growth score (i.e. fold-change) was calculated for each gene as the ratio of the normalized relative read counts in treated and non-treated samples at the end of the competition assay. Fold-change values of biological replicates were averaged. In order to determine statistically significant fold-changes, we estimated the variance of biological replicate measurements as follows. Use of small sample sizes in estimating gene-specific variance can cause an unreliable outcome. Due to small sample sizes in the screen (n=2 for AMP treatments and n=5 for untreated competitions), we shared information across multiple genes and AMP treatments by calculating the standard deviation as a function of normalized read counts using lowess smoothing (i.e. local regression). This procedure is based on the observation that the variance depends on the mean. Similar procedures are commonly used in the gene expression literature[69]. Using this estimation of standard deviation, we applied z-tests to determine whether the treated and the non-treated samples differ significantly. Genes that showed at least 2-fold lower and higher relative abundance with a p-value<0.05 at the end of the competition upon AMP treatment were considered as sensitizing and resistance-enhancing genes, respectively.

We employed an ensemble clustering method to group the AMPs on the basis of their chemical-genetic profiles similarity[70]. This method calculates distance between chemical-genetic profiles of AMPs, and then generates multiple clustering based on perturbing the AMP chemical-genetic interaction data and the clustering parameters. As a next step, it combines the resulting clusters to obtain a consensus clustering which is robust and the best representative of multiple clustering[70]. The consensus matrix contains information about the frequency of AMPs

to be clustered together. Ensemble clustering methods are known to obtain a more robust clustering of data points than that produced from a single clustering result. The workflow was as follows. First, we removed genes that did not show AMP-specific interaction across treatments. Next, we employed distance metric and normalized variation of information to calculate distances between AMP chemical-genetic profiles, and using the calculated distance measure, we then generated 75,000 clusters of AMPs. Results of the 75,000 clusters were summarized in a consensus. Finally, using the hierarchical clustering and complete linkage we clustered this consensus matrix and plotted the result as a heatmap.

3.7 Chemical-genetic profiling of hypomorphic alleles

A total of 279 essential gene hypomorphs (with reduced protein expression) were constructed as described previously[71,72]. Construction and chemical-genetic profiling of the hypomorphic alleles was carried out by our collaborator Mohan Babu and his colleagues at University of Regina, Regina, Canada. Briefly, similar to mRNA perturbation by DAmP (*decreased abundance by mRNA perturbation)* alleles in yeast[73], we constructed hypomorphic mutation by introducing a kanamycin (Kan^R) marked C-terminal sequential peptide affinity fusion tag into each essential gene[74]. The tag perturbs the *3' end of the expressed mRNA* of the essential proteins, when combined with environmental/chemical stressors, or other mutations by destabilizing the transcript abundance. Previous studies have shown the importance of these hypomorphic alleles in studying gene-gene, and gene-environment or drug-gene interactions[71,75–77].

Similar to *E. coli* synthetic genetic array approach[76], our chemical-genetics screening method involves robotic pinning of each Kan^R marked single essential gene hypomorph arrayed in 384 colony format on Luria Broth (LB) medium onto the minimal medium containing AMPs. Each essential gene hypomorph was pinned onto a plate in quadruplicate, in two replicates, generating eight replicates in total for each hypomorph. The sub-inhibitory concentration was chosen based on 50% growth inhibition of wild-type cells using a serial dilution. In parallel, we also prepared two replicates of untreated control plates where essential gene hypomorphic strains were pinned onto minimal media without AMPs. After incubation at 32°C for 20 h, the plates (with and without AMPs) were digitally imaged and colony sizes were extracted from the imaged plates using an adapted version of the gitter toolbox[78]. SGAtools suite was used for the normalization of raw colony[53]. The normalized colony sizes from the AMP plate was subtracted from their corresponding colony screened without AMP to estimate the final hypomorphic-strain

fitness score (sensitive or resistant), which is as an average of all eight replicate measurements recorded for each hypomorphic allele. A z-score distribution based p-value was calculated for all interactions and those with p ≤0.05 were considered as significant interactions, as previously[77].

3.8 Calculating physicochemical properties of AMPs

For each AMP, different physicochemical properties (like amino acid frequency, isoelectric point, hydrophobicity, net charge) were calculated. These calculations were made by our colleague Ádám Györkei. An in-house perl script was used to count protein amino acid frequencies. Isoelectric point, hydrophobicity, hydrophobic moment and net charge was calculated with the peptides R package, version 2.462[17]. AMP length and molecular weight were calculated using the ExPasy Prot Param tool[79]. The alpha-helical content and the disordered structure of AMPs were calculated using PASTA 2.0 server[80].

3.9 Differentiating AMP clusters on the basis of physicochemical properties of AMPs

Ensemble clustering method grouped 15 AMPs into four main clusters, referred to as C1 – C4 (Figure 11A). AMPs in C1 and C2 clusters belong to membrane-targeting AMPs and share similarity in their physicochemical properties. Therefore, logistic regression framework was employed with two physicochemical properties to infer differences between C1 and C2 clusters AMPs. Model accuracy was determined using area under the receiver operating characteristic curve. For a global analysis of cluster properties, principal component analysis was applied to all the AMP properties with centering and scaling the data using the princomp R package. All the analysis and calculations were done in R version 3.5.0 in Rstudio version 1.1.447[81,82].

3.10 Calculating the overlap in resistance-enhancing and sensitivity-enhancing genes between AMP pairs

To calculate the overlap in resistance and sensitivity genes between AMP pairs, we used a modified version of the Jaccard index that takes into account measurement noise. For each AMP pair, we calculated the Jaccard index of overlap between the resistance gene sets and performed a correction by dividing this value by the average Jaccard index of overlap between replicate screens of the same AMPs. Thus, a corrected Jaccard index value of 1 between two AMPs indicates that the set of resistance genes overlap as much as that of two replicate

screens. Corrected Jaccard indices were calculated separately for resistance and sensitivity genes. Protein overexpressions associated with a fitness cost were identified using a previously published dataset[83]. In this dataset, those overexpression strains were deemed as having a fitness cost where the doubling time was at least two-fold higher than the doubling time of the strain harbouring the no-insert control of the pCA24N vector.

3.11 Enrichment analysis of collateral sensitivity-inducing genes

For each AMP pair, overrepresentation of collateral sensitivity-inducing genes was calculated over random expectation. Enrichment ratio (r) of collateral sensitivity-inducing genes for each AMP pair was calculated as follows:

$$r = x/e$$

where:

x - actual frequency of the genes showing collateral sensitivity interactions between AMP pair

e - expected frequency (based on marginal probability) of the genes showing collateral sensitivity interactions between AMP pair. Expected frequency (e) was calculated as follows:

$$e = R_{amp1} \times S_{amp2}$$

where:

R_{amp1} = frequency of resistance genes to AMP1 within all of the ~4400 genes

S_{amp2} = frequency of sensitive genes to AMP2 within all of the ~4400 genes

3.12 Gene ontology (GO) enrichment analysis of resistance-enhancing and sensitivity-enhancing genes

Biological Networks Gene Ontology tool (BiNGO)[84] was used to determine which Gene-ontology (GO) terms are significantly enriched in the resistance and sensitive gene sets. GO reference set was downloaded from EcoGene database[85]. The Benjamini-Hochberg FDR (FDR cutoff= 0.05) was used for multiple-testing correction[86].

Additionally, we calculated the enrichment of phospholipid and lipopolysaccharide related genes among those genes that showed collateral sensitivity between AMPs.

3.13 Minimum inhibitory concentration (MIC) measurement

Minimum inhibitory concentrations (MIC) were determined with a standard serial broth dilution technique with a minor modification[87]. Specifically, instead of a two-fold dilution series, smaller steps of AMP concentration were used (typically 1.2-fold) for the following reasons. First, two-fold dilutions were not suitable in capturing 90% growth inhibition because of steeper dose-response curves of AMPs. Second, gene overexpressions resulted in typically only small MIC changes. The protocol was as follows. A stock solution of AMP was diluted into the fresh minimal medium and 12-steps serial dilution were prepared in 96-well microtiter plates. For each AMP, we had 11 different concentrations (3 wells/AMP concentration/strain) in the 96-well plate. Three wells contained only medium to check the growth in the absence of AMP. Bacterial strains were grown overnight in MS medium supplemented with chloramphenicol. Overnight grown cultures were diluted 20 fold into fresh MS medium and grown further until the cell density reached OD_{600} ~1. To induce the protein expression, 100 µM of IPTG was added to the bacterial culture and incubated for 1 h at 30°C with continuous shaking at 300 rpm. Approximately half-million cells were inoculated into the wells of the 96-well microtiter plate with a 96-pin replicator and incubated at 30°C with continuous shaking at 300 r.p.m (3 replicates per strain per AMP concentration). In order to get background OD value of the medium, two rows in the 96-well plate were filled with MS medium only. After 24 h of incubation, OD_{600} values were measured in a microplate reader (Biotek Synergy 2). MIC was determined as the lowest concentration of AMP where the OD_{600} values were less than 0.05 after background normalization.

3.14 Measurement of membrane surface charge

To measure bacterial membrane surface charge, we performed a fluorescein isothiocyanate-labelled poly-L-lysine (FITC-PLL) (Sigma) binding assay. FITC-PLL is a polycationic molecule that is used to study the interaction between cationic peptides and anionic lipid membranes[48,88,89]. Bacterial cells were inoculated in MS medium and grown at 30°C for overnight. Overnight grown bacterial cultures were centrifuged and washed twice with 1X PBS buffer (pH 7.4). The washed cells were re-suspended in 1XPBS buffer to a final OD_{600} of 0.1. The bacterial suspension was incubated with 6.5 µg/ml of freshly prepared FITC-PLL for 10

minutes at room temperature. Cells were pelleted by centrifugation and the remaining amount of FITC-PLL in the supernatant was determined fluorometrically (excitation at 500 nm and emission at 530 nm) with or without bacterial exposure. The quantity of bound molecules was calculated from the difference between these values. The lower the amount of bound FITC-PLL, the less negatively charged the cell surface. For each bacterial strain, six biological replicates were used to measure the membrane surface charge.

3.15 Membrane potential measurement

BacLight™ Bacterial Membrane Potential Kit (Invitrogen) was used to measure transmembrane potential (Δψ). In this assay, a fluorescent membrane potential indicator dye ($DiOC_2$) exhibits green fluorescence in all bacterial cells and the fluorescence shifts to red in the cells that maintain a high membrane potential. The ratio of red/green fluorescence provides a measure of membrane potential. A previously described protocol was used to measure transmembrane potential[90]. Briefly, bacterial cells were inoculated into MS medium and incubated at 30°C for overnight. The overnight grown cultures were diluted into fresh MS medium and grown until log phase was reached. The grown cultures were diluted to 10^6 cells/mL in filtered PBS buffer. Aliquots of 500 µl of bacterial suspension were used for staining experiment. 5 µL of 3 mM DiOC2 was added to each sample tube and incubated for 20 minutes at room temperature in dark. Following incubation, the samples were analyzed using Fluorescence Activated Cell Sorter (BD Facscalibur) according to the instructions of the kit's manufacturer. The red/green fluorescence values were calculated relative to the control strain.

3.16 Membrane integrity measurement

To investigate the changes in membrane integrity of the *mlaD* overexpression and *mlaD* knockout strain, we tested their susceptibility to the amphipathic membrane-damaging agent bile acid. Bile acid stock solution (30%) was prepared in sterile water and then used to prepare a 12-step dilution series in a 96-well microtiter plate, each well containing 100 µl medium. The overnight cultures of the tested strains were diluted into fresh MS medium and grown to a cell density of OD_{600} = 1. In the case of the *mlaD* overexpression strain, the protein expression was induced by IPTG for 1h. Following the incubation, half-million cells were inoculated into the wells of the microtiter plate containing bile acid. Plates were incubated at 30°C with continuous shaking at 300 r.p.m. Following 24h of incubation, OD_{600} values were measured in a microplate

reader (Biotek Synergy 2). After background subtraction, the lowest inhibitory concentration of bile salt was determined for both strains in comparison to the corresponding control strains.

3.17 Growth curve measurement

To determine the difference in bacterial growth in the presence of an AMP, we performed growth curve analysis. Growth curve measurement for the overexpression strains was done by measuring OD_{600} of the liquid bacterial cultures at different time points in a standard 96-well plate containing a 12-step dilution series of the tested AMP in MS medium. Overexpression strains were grown overnight in MS medium supplemented with chloramphenicol. Overnight cultures were diluted 20-fold into fresh MS medium supplemented with chloramphenicol and grown until the cell density reached OD_{600} = 1. Cells were induced by IPTG for 1 h. After the incubation time, half-million cells were inoculated into each well of a 96-well microtiter plate containing a concentration gradient of an AMP in the MS medium supplemented with 20 µg/ml chloramphenicol and 100 µM IPTG (3 wells/AMP concentration/strain). Plates were incubated in a microplate reader (Biotek Synergy 2) for continuous growth monitoring at 30°C for 24 h. The recorded OD_{600} values at different time points were used to prepare growth curve.

3.18 Construction of *mlaD* mutant

We constructed *mlaD* knockout mutant of *E. coli* BW25113 by removing the kanamycin resistance cassette present in the position of the gene in *mlaD* knockout strain from KEIO collection[91]. Kanamycin resistance cassette was removed using plasmid borne (pFT-A) expression of FLP recombinase[92]. We verified the excision of kanamycin cassette using polymerase chain reaction. (PCR) The following primers were used in the PCR, mlaD_del_ver_Fw (5'- TCACGGTGACGTGGATTTC) and mlaD_del_ver_Rev (5'- GCCTCGTCCATCAGCTTATAC).

4. Results

4.1 Generating chemical-genetic interaction profiles

We performed a genome-wide overexpression screen to examine the effect of overexpression of each of 4,400 *E. coli* genes on bacterial susceptibility against a set of 15 AMPs. The AMPs used in this study are diverse in their physicochemical properties, mechanism of action and importantly some of them have clinical relevance (Table 1).

Table 1. List of AMPs used in this study, their abbreviation, described mode of action and clinical relevance (for details and references, see Supplementary Table 2).

Name of AMP	Abbreviation	Mode of action	Clinical relevance
Apidaecin IB	AP	Inhibits protein biosynthesis by targeting ribosomes, inhibits DnaK, GroEL/GroES, FtsH	Yes
Bactenecin 5	BAC5	Inhibits protein and RNA synthesis	n.a.
CAP18	CAP18	Disrupts cell membrane	Yes
Cecropin P1	CP1	Disrupts cell membrane	n.a.
Human beta-defensin-3	HBD-3	Disrupts cell membrane, inhibits lipid II in peptidoglycan biosynthesis	n.a.
Indolicidin	IND	Inhibits DNA and protein synthesis, disrupts cell membrane, inhibits septum formation	Yes
LL-37 human cathelicidin	LL37	Disrupts cell membrane, induces ROS formation	Yes
Peptide glycine-leucine amide	PGLA	Disrupts cell membrane	n.a.
Pexiganan	PEX	Disrupts cell membrane	Yes
Pleurocidin	PLEU	Disrupts cell membrane, induces ROS formation, inhibits protein and DNA synthesis	n.a.
Polymyxin B	PXB	Disrupts cell membrane, induces ROS formation	Yes
PR-39	PR39	Inhibits protein and DNA synthesis	n.a.
Protamine	PROA	Affects cellular respiration, affects glycolysis, disrupts cell envelope	n.a.
R8	R8	n.a.	n.a.
Tachyplesin II	TPII	Disrupts cell membrane	n.a.

n.a. – no data available

We used a sensitive competition assay to monitor growth of a pooled plasmid library overexpressing all *E. coli* ORFs. *E. coli* cells carrying the pooled plasmid collection were grown in the presence and absence of one of the 15 AMPs. (Figure 8A). Following about 12 generations of growth, the plasmid pool was isolated and subjected to deep sequencing to determine the abundance of each plasmid (for details see Methods). If the relative abundance of a plasmid was at least 2-fold lower in the presence of an AMP than in its absence, the specific growth defect in the AMP-treated sample was considered sensitivity interaction. In a similar vein, an improved growth measured by at least 2-fold higher relative abundance in the presence of the AMP was considered as a resistant interaction (Figure 8).

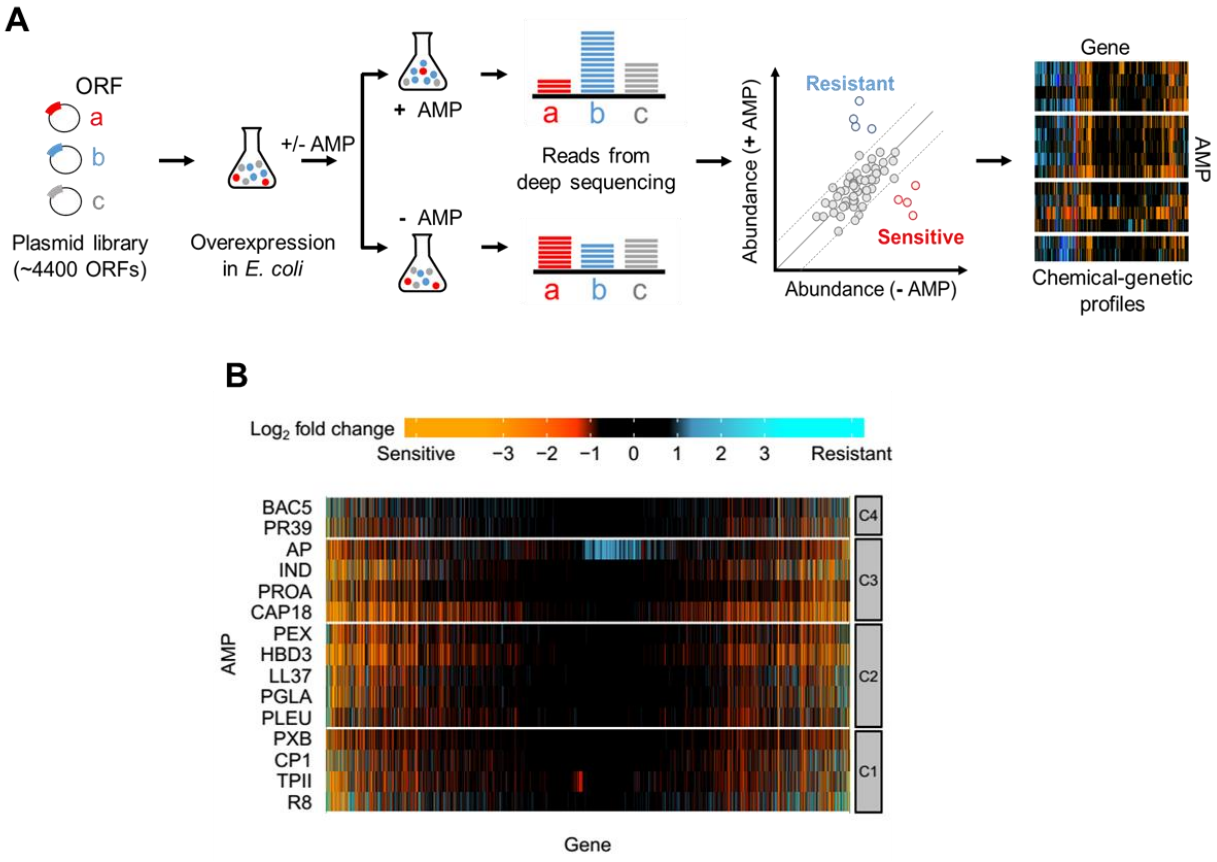

Figure 8. Chemical-genetic screening (A) Schematic overview of the chemical-genetic approach. The chemical-genetic interactions of all ~4400 single gene-overexpressions and 15 different AMPs were measured using a sensitive competition assay (see Methods). **(B)** Heatmap shows the chemical-genetic interaction scores. Resistant and sensitive chemical-genetic interactions are represented by blue and red, respectively (n = 66,615). Groups C1-C4 refer to AMP clusters defined in Figure 11A.

Next, to address the accuracy of our workflow, we applied three different approaches. First, we examined the reproducibility of chemical-genetic profiles. To do so, we tested correlation of chemical-genetic interaction scores between replicates. We found that the overall correlation was good (r = 0.63 from Pearson's correlation, Figure 9) and was in agreement with previous studies[49,93], showing reproducibility of chemical-genetic interactions.

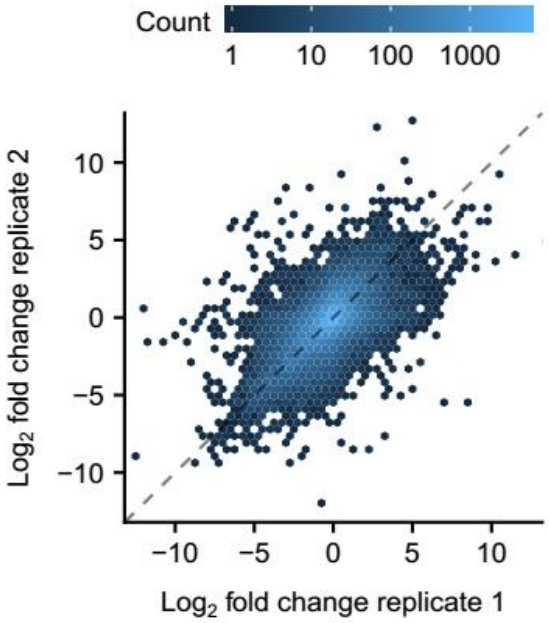

Figure 9. A density scatter plot showing the overall correlation of replicate measures of the chemical-genetic scores. Pearson's rho (r) quantifies the overall reproducibility of the procedure ($p = 2.2*10^{-16}$, r = 0.63 from Pearson correlation, n=53292).

Second, we randomly selected 19 overexpression strains that showed diverse chemical-genetic interactions with multiple AMPs in the screen and did not influence bacterial growth in the absence of AMPs. For these 19 strains, we determined minimum inhibitory concentrations (MIC) of the interacting AMPs. In total, we performed 92 measurements representing 4-5 AMPs per strain on average. In total, 83% cases showed a MIC difference in the expected direction upon over-expression (Figure 10), demonstrating that the majority of the chemical-genetic interactions can be confirmed by an independent experiment.

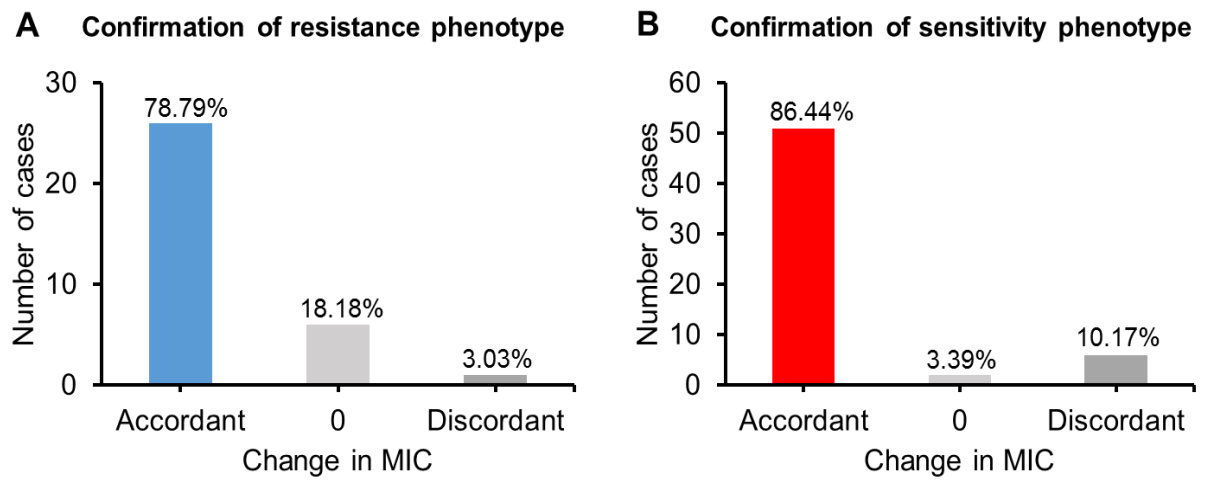

Figure 10. Validation of the chemical-genetic interactions. We randomly selected 19 overexpression strains and measured the minimum inhibitory concentration (MIC) of the corresponding AMPs for these strains. In total 92 MIC measurements were carried out. **(A)** In the case of resistant chemical-genetic interactions, 26 out of 33 interactions (78.79% true positive) were confirmed by the MIC measurements, while a single case showed an opposite effect. **(B)** Out of 59 sensitive chemical-genetic interactions, 51 (86.44% true positive) showed the expected MIC change. Although a MIC change is not necessarily expected upon a chemical-genetic interaction, we could confirm 83% of the observed chemical-genetic interactions with this approach. The chemogenomic screens are performed at sublethal drug concentration and thus they are not expected to directly correlate with the extent of MIC changes upon gene overexpression/deletion. Therefore, we focused on the presence and absence of chemical-genetic interactions.

Third, we compared the chemical-genetic profiles with literature curated list of resistance determinants in *E. coli*. To this end, we collected those genes that provide resistance or sensitivity to AMPs when overexpressed in *E. coli*. We found that 70 % of the 13 cases were in agreement with our chemical-genetic screen (Table 2).

Table 2. Literature curated examples of *E. coli* gene overexpression as a confirmation of our chemical-genetic screening.

Gene	AMP	Overexpression phenotype	
		Literature	Chemical-genetic profile
ptrB	BAC5	Resistance[94]	Confirmed
	PR39	Resistance[94]	Confirmed
marA	PXB	Resistance[95]	Confirmed
	LL37	Resistance[95]	X
ompT	PROA	Resistance[96]	Confirmed
	LL37	Resistance[34]	Confirmed
arnT	PXB	Resistance[97]	X
nlpE	PROA	Resistance[98]	Confirmed
eptA	PXB	Resistance[33]	Confirmed
pmrD	PXB	Resistance[99]	X
sbmA	PR39	Sensitivity[100]	Confirmed
waaY	CAP18	Sensitivity[48]	Confirmed
prfA	AP	Resistance[101]	X

Taken together, these results show the high sensitivity of our workflow in determining chemical-genetic interactions between AMPs and gene overexpression.

4.2 Chemical-genetic profiles group AMPs with similar mechanisms of action and physicochemical properties

We next tested whether AMPs with similar mechanistic and physicochemical properties cluster together based on their chemical-genetic profiles. To address this question, we collected experimentally established mechanisms of action from the literature and calculated different physicochemical properties (see Methods) of AMPs used in this study. Then, we performed consensus clustering analysis using the chemical-genetic interaction profiles of AMPs. This analysis grouped the AMPs into four different clusters (referred to as C1-C4) (Figure 11A).

Mostly AMPs that have been shown to target bacterial membrane (create pores) belongs to cluster C1 and C2 whereas cluster C3 and C4 contain intracellular targeting AMPs (Figure 11A). We compared the collected physicochemical properties and mechanisms of action the AMPs in the obtained clusters. We found that membrane-targeting (C1and C2) and intracellular-targeting AMPs (C3 and C4) can be differentiated based on their physicochemical properties (Figure 11B, Figure 12).

Specifically, AMPs in cluster C1 and C2 have a lower isoelectric point and proline content, they show higher propensity to form secondary structures and contain more hydrophobic residues than the rest of peptides (Figure 11B). These properties allow them to

integrate into the bacterial lipid membrane and to create pores[14,102]. Although AMPs in both C1 and C2 clusters are membrane targeting, they can be differentiated when multiple physicochemical properties are considered jointly (Supplementary Figure 1).

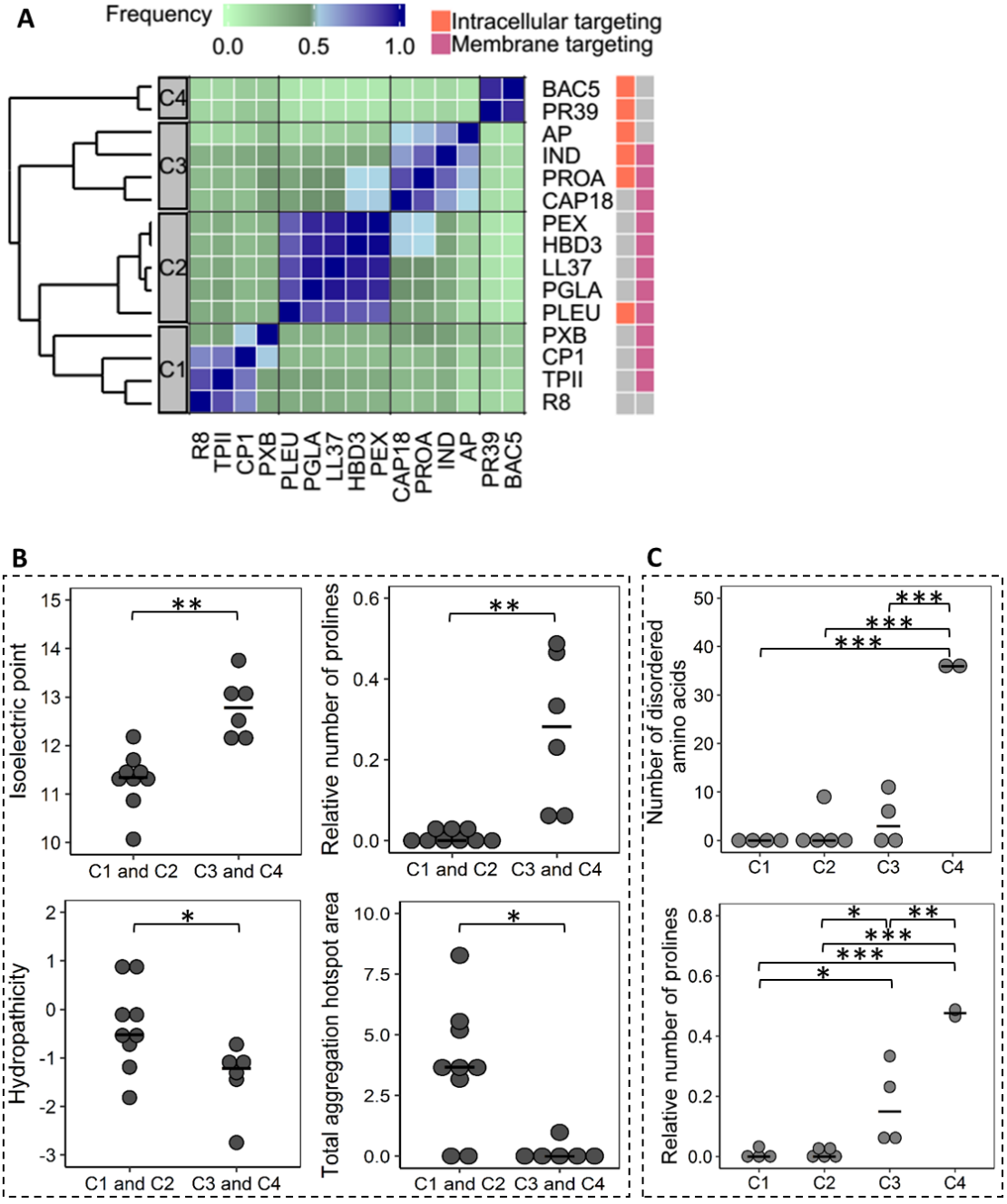

Figure 11. Chemical-genetic profiling differentiates membrane-targeting and intracellular-targeting AMPs with distinct physicochemical properties. (A) Heatmap shows the

ensemble clustering of the AMPs based on their chemical-genetic profiles (see Methods). For each AMP pair, the color code represents the frequency of being closest neighbours across the ensemble of clusters. C1, C2, C3, and C4 represent four major clusters. Membrane-targeting and intracellular-targeting AMP are labelled with pink and orange color, respectively. Grey color indicates that the mode of action of the corresponding AMP is unknown. **(B)** Most important physicochemical properties that differentiated AMPs in cluster C1 and C2 (n=9) from AMPs in cluster C3 and C4 (n=6) ($p < 0.05$, two-sided Mann–Whitney U test). **(C)** Physicochemical properties that distinguished the clusters when the 4 main AMP clusters were considered separately ($p<0.05$ ANOVA, Tukey post hoc test, n=15). Significant differences are marked with asterisks indicating p-values as follows: *** <0.001, ** < 0.01, * < 0.05. Central horizontal bars represent median values.

Unlike membrane targeting AMPs in C1 and C2 clusters, intracellular targeting AMPs in C3 and C4 contain some unique physicochemical properties. AMPs in cluster C4 have higher number of consecutive prolines and therefore show higher propensity to structural disorder (Figure 11C). Importantly, higher proline/arginine content and structural disorder are important characteristics of intracellular targeting AMPs[103].

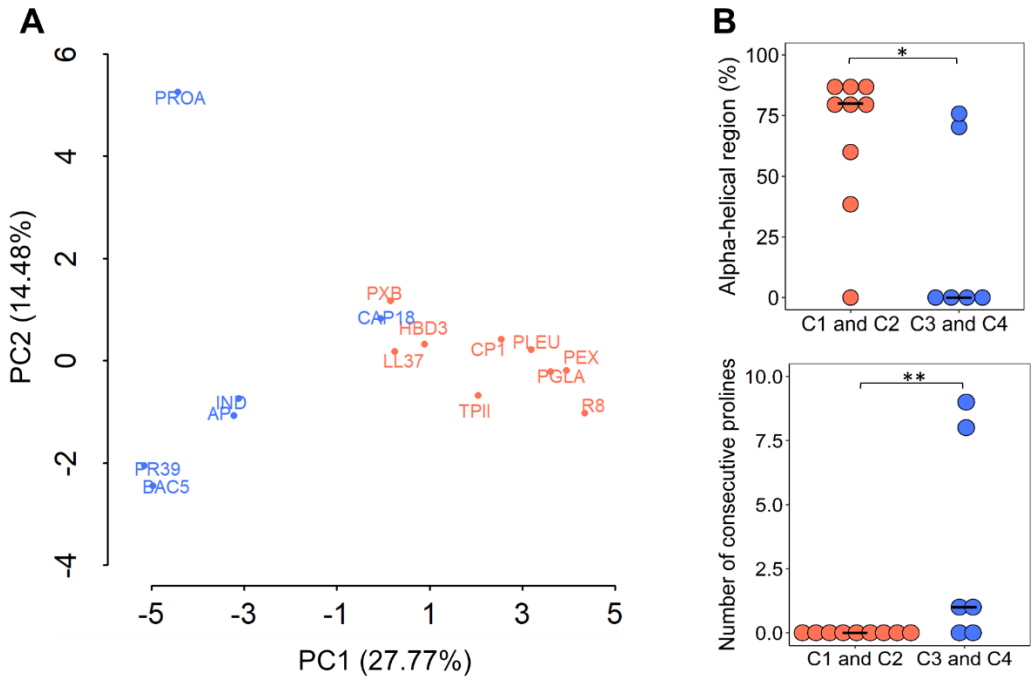

Figure 12. Membrane-targeting and intracellular-targeting AMPs showed different physicochemical properties. (A) Principle component analysis (PCA) of the physicochemical properties differentiated AMPs in C1-C2 clusters (orange) from AMPs in C3-C4 clusters (blue) (P = 4.128*10^{-5}, logistic regression, n=15). **(B)** Two important physicochemical properties that differentiate membrane-targeting AMPs (orange, C1 and C2) from intracellular-targeting AMPs (blue, C3 and C4). *P*-values are 0.0264 and 0.0080, from two-sided Mann–Whitney U test for alpha-helical region content and number of consecutive prolines respectively. Central horizontal bars represent median values.

Notably, AMPs in C3 cluster are relatively diverse in physicochemical properties as compared to the rest of the clusters. These AMPs shared physicochemical similarities with both the membrane targeting and intracellular targeting AMPs. For example, indolicidin (IND) and protamine (PROA) in cluster C3 are known to target bacterial membrane and intracellular processes, as well (Table 1). CAP18 which is considered as a membrane-targeting AMP showed high similarity with PROA (Figure 11A). This indicates that CAP18 might also possess intracellular targeting activity as PROA. Future study should provide deeper insights on mode of action of CAP18.

Taken together, these results suggest that similarity in chemical-genetic profiles reflects similarity in broad mechanisms of action and physicochemical properties of AMPs. Therefore, chemical-genetic profiles can capture subtle differences in how these AMPs interact with the bacterial cell.

4.3 A large and functionally diverse set of genes modulate bacterial susceptibility to AMPs

Our results show that *E. coli* has a large repertoire of genes that influence bacterial susceptibility to AMPs. In particular, we found between 59 – 553 resistance-enhancing and 260 – 1404 sensitivity-enhancing genes per AMP (Figure 13A).

These results substantially broaden the scope of resistance determinants as previously reported resistance genes in *E. coli* constitute only ~0.6 % of the genes identified in our chemical-genetic profiling. Importantly, the identified AMP susceptibility modulating genes belong to diverse functional categories including previously known resistance mechanism like cell membrane biogenesis, lipid transport, translation and ribosome biogenesis (Figure 13B). In the case of AMP susceptibility enhancing genes, cell envelope related functions were

significantly enriched across multiple AMPs (including membrane targeting and intracellular targeting) showing that the majority of the interactions did not show an obvious functional connection with known mechanism of action of AMPs (Supplementary Table 3).

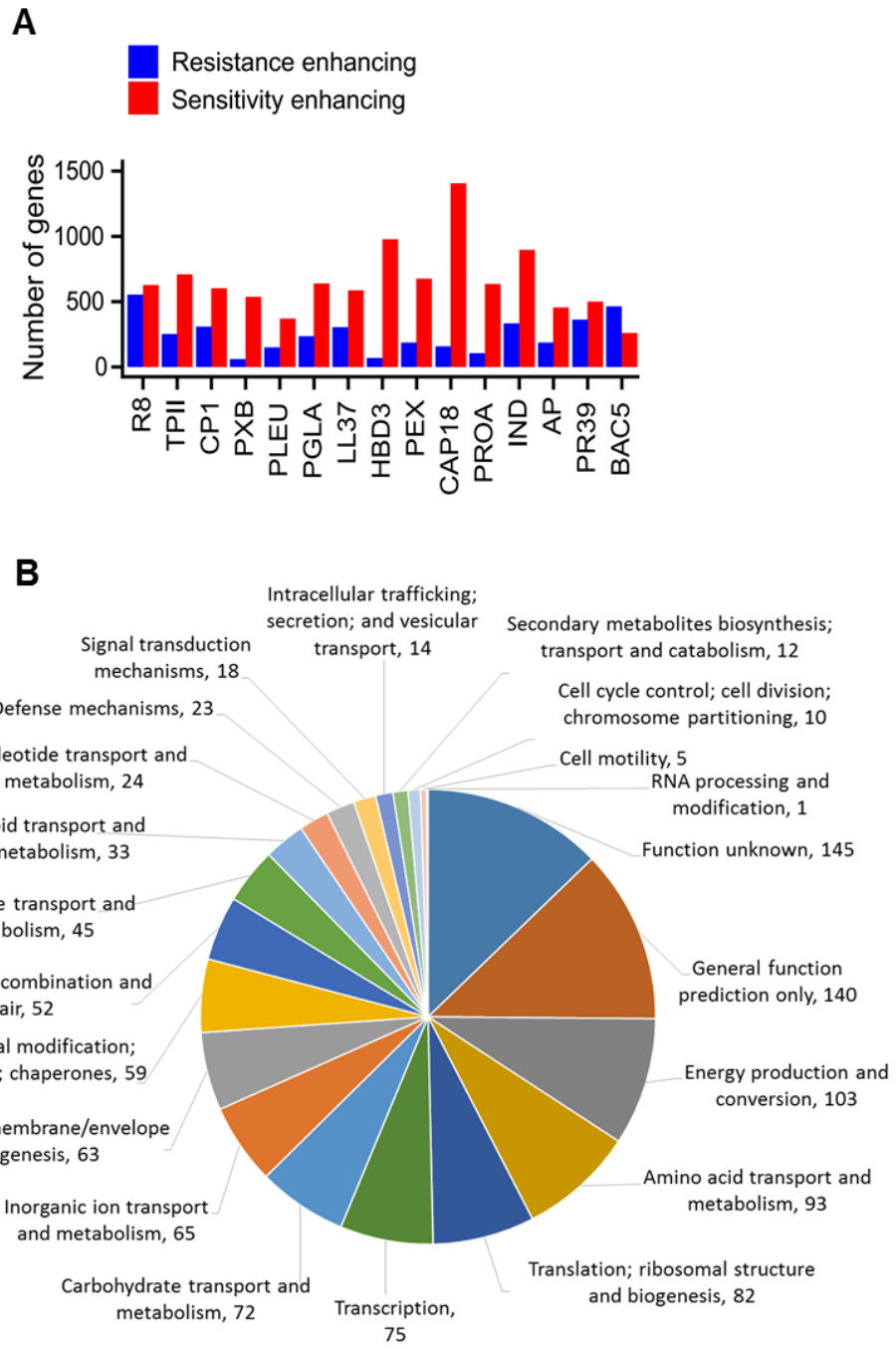

Figure 13. *E. coli* genome harbours a large diversity of resistance determinants. (A) Number of genes enhancing resistance and sensitivity for each AMP. **(B)** Distribution of Clusters of Orthologous Groups (COG) categories among the genes that show resistance to at least one AMP in the chemical-genetic screen. Value with each COG category shows total number of genes that belong to corresponding COG category.

Next, we wondered whether these resistance determinants are functionally diverse across different AMPs. To address this, we calculated the overlap between resistance-enhancing and sensitivity-enhancing gene set across AMPs. A normalized Jaccard similarity index was employed to calculate the overlap in gene sets between AMP pairs (see Method). We found that typically ~31% and 63% of the resistance-enhancing and sensitivity-enhancing genes overlapped between AMP pairs (Figure 14A).

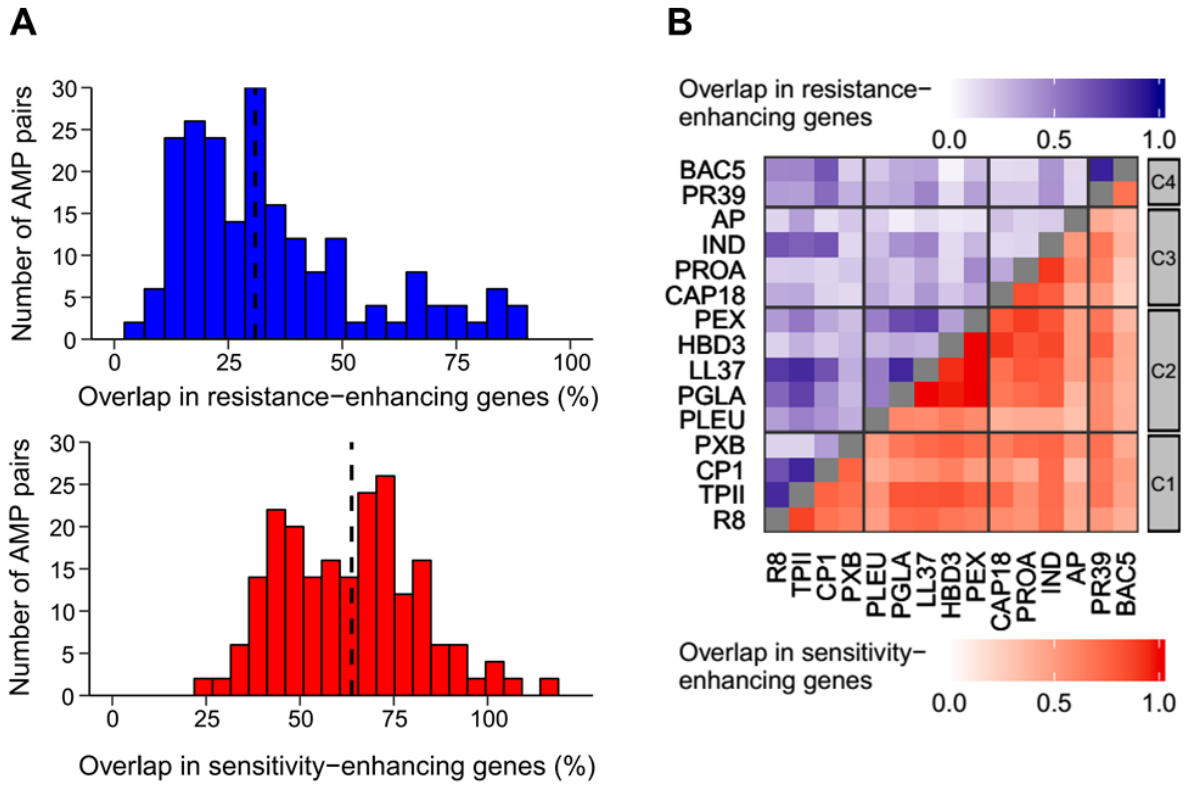

Figure 14. Resistance-enhancing genes overlap only to a limited extent between AMPs. (A) Distributions of overlaps in the resistance (blue) and sensitive (red) chemical-genetic interactions for all possible AMP pairs. Dashed line represents median value. **(B)** Heatmap

shows the Jaccard similarity-index calculated for resistance- and sensitivity-enhancing genes 0between AMPs. The darker the color the highest similarity between AMPs.

The low overlap in resistance-enhancing genes indicates substantial variation in the latent resistome across AMPs. Notably, resistance modulating genes varied greatly even between AMPs that group in the same chemical-genetic cluster, for example, AMPs in cluster C3 (Figure 14B). This variation could reflect subtle differences in the mechanism of action across AMPs in C3 cluster as these AMPs differ in their physicochemical properties and cellular targets (Table 1). Interestingly, the overlap in resistance-enhancing genes was significantly lower between AMPs with different modes of action (i.e. between membrane- (C1, C2) and intracellular-targeting (C3, C4) AMPs) (Figure 15).

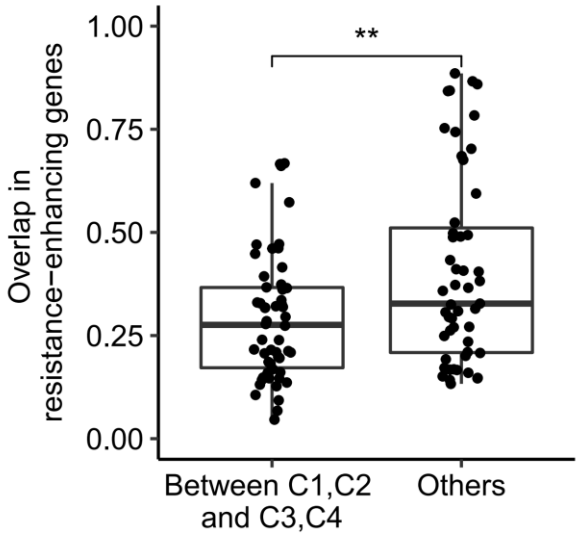

Figure 15. The overlaps in the latent resistomes (genes enhancing resistance upon overexpression) between AMP pairs belonging to different chemical-genetic clusters. Significant difference: ** *P* = 0.0045 from two-tailed unpaired t-test, n = 54 and n = 51 for between C1, C2 and C3, C4, and others, respectively.

Since protein overexpression may induce fitness cost, there is a considerable risk of having non-specific chemical-genetic interactions. Therefore, we examined whether the above results could be affected by potential non-specific chemical-genetic interactions caused by the overexpression associated fitness cost[83]. To this end, *E. coli* genes were divided into two

groups on the basis of presence or absence of overexpression associated fitness defect. A previously published dataset was used to define the fitness defect induced by protein overexpression. Next, we tested the extent of overlap in resistance-enhancing and sensitivity-enhancing genes in both the groups. Notably, the extent of overlap remained similar in both groups, validating that our results are not distorted by overexpression associated fitness defect (Figure 16).

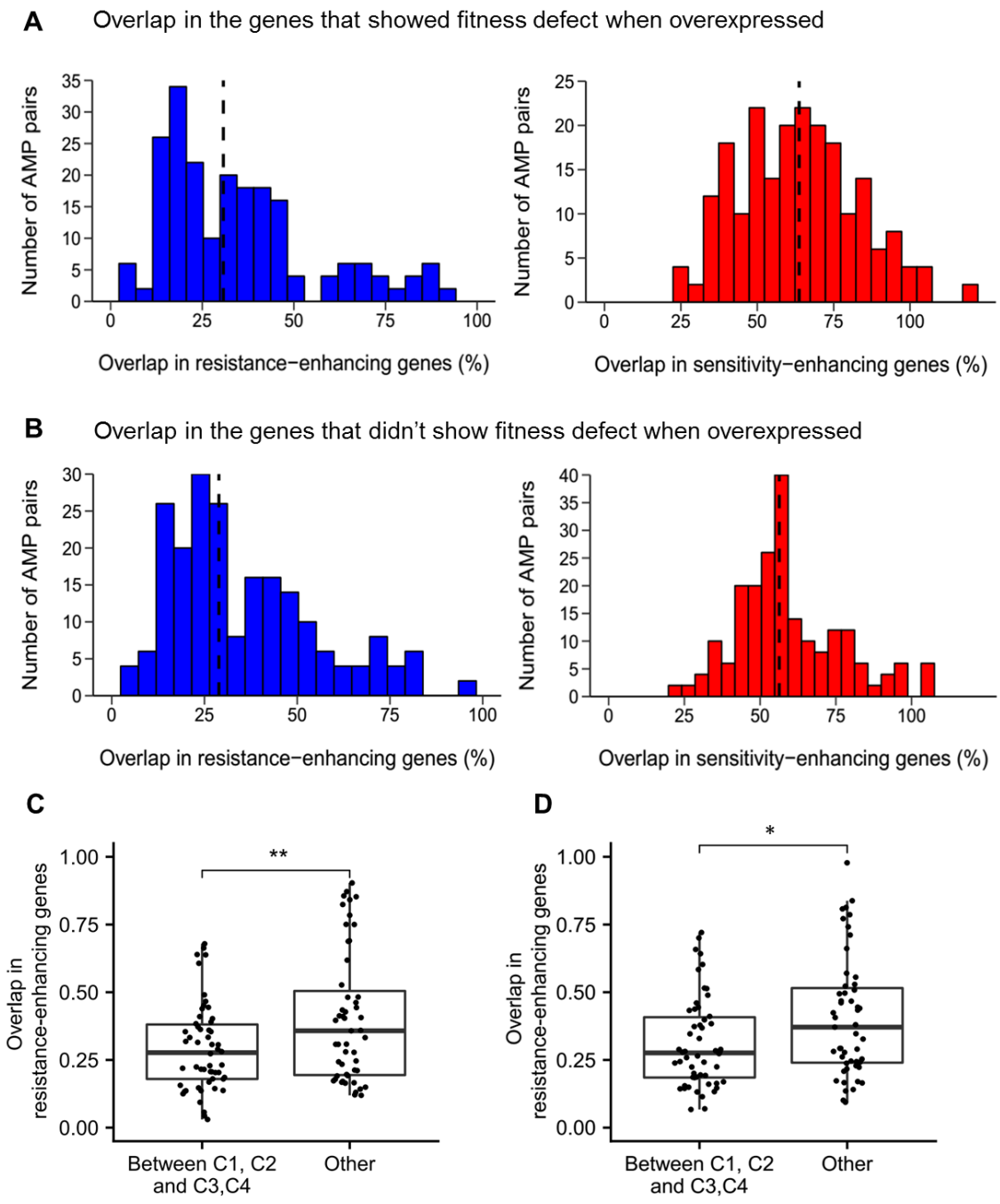

Figure 16. Distributions of overlaps in the chemical-genetic interactions for the resistant-enhancing (blue) and sensitivity-enhancing (red) genes for all possible AMP pairs (*n* = 105 AMP pairs) when the effect of the gene overexpression on growth rate was taken into consideration. (A) Histograms show distribution of overlaps in the genes that have been shown to cause fitness defect when overexpressed (median = 30.76 and 63.7 for resistance- and sensitivity-enhancing genes, respectively), and **(B)** those genes that do not cause fitness defect (median = 28.88 and 56.32 for resistance- and sensitivity-enhancing genes, respectively). A previously published dataset was used to determine the effect of gene overexpression on cell growth[83] (see Method). Dashed line represents median value. **(C)** The overlap in the resistance-enhancing genes that cause fitness defect when overexpressed (significant difference: ** P = 0.0071 from two-tailed unpaired *t*-test, n = 54 and n = 51 for between C1, C2 and C3, C4, and others, respectively), and **(D)** those that do not cause fitness defect genes between AMP pairs (significant difference: * P = 0.015 from two-tailed unpaired *t*-test, n = 54 and n = 51 for between C1, C2 and C3, C4, and others, respectively).

In sum, our results reveal functionally diverse gene sets across AMPs and reflect on mechanistic differences between these AMPs.

4.4 Partial depletion of essential genes reveals the intrinsic AMP resistome

Genome-wide deletion mutant screening, which is a complementary approach of overexpression screening identifies different aspects of resistance mechanisms[104]. Resistance upon gene overexpression informs on latent resistome while sensitivity upon gene depletion reveals intrinsic resistome[39].

We wondered how the reduced gene dosage shapes AMP susceptibility and differentiates the AMPs. To this end, we carried out chemical-genetic screening with the hypomorphic alleles (partially depleted essential genes) of 279 essential genes of *Escherichia coli.* For this screening, we selected two membrane-targeting (Pexiganan (PEX) and LL37 from C2) and two primarily intracellularly-targeting (BAC5 and PR39 from C4) AMPs. Using a well-established high-density agar plate assay[72,75,105], we generated chemical-genetic interaction profiles with the hypomorphic alleles of the essential genes.

We found that 75% of tested hypomorphic alleles show chemical-genetic interaction with at least one AMPs. We found that overlap in the intrinsic resistomes between AMPs with similar

modes of action was considerably high. For example, resistance determinants of the membrane-targeting (PEX and LL37) and intracellular-targeting (BAC5 and PR39) AMPs overlapped to 87% and 86%, respectively (Figure 17A). In contrast, the resistance determinants of these two groups of AMPs overlapped only to 59% on average (Figure 17A). Next, we sought to compare the overlap pattern of the essential genes from the overexpression screen for these 4 AMPs. Interestingly, we found a similar pattern as hypomorphic alleles results showing high overlap between AMPs with similar modes of action (Figure 17B).

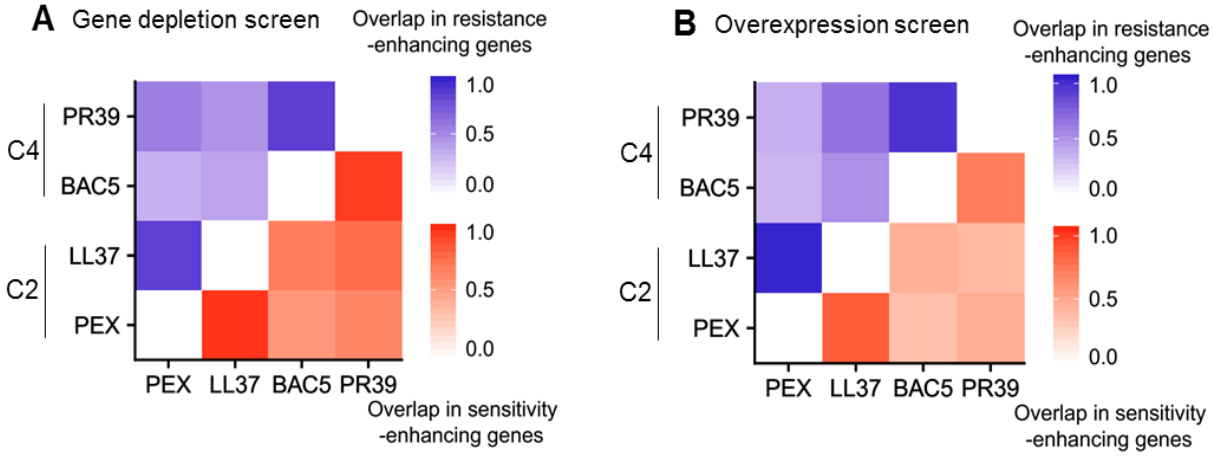

Figure 17. Overlap in the resistance- and sensitivity-enhancing genes from (A) hypomorphic alleles screening and (B) overexpression screening show similar pattern. Heatmap depicts Jaccard similarity-index calculated for resistance- (blue) and sensitivity-enhancing genes (red) between AMPs

Additionally, we tested whether the chemical-genetic interactions are unique to AMPs or they arise due to sick phenotype of strains partially depleted in essential genes (hypomorphic alleles). To this end, we generated chemical-genetic profiles of hypomorphic alleles in response to four small-molecule antibiotics with distinct modes of action. We found that antibiotics and AMPs have very distinct chemical-genetic-genetic profiles which suggest that the obtained chemical-genetic interactions are not due to sick phenotype of the strains (Figure 18).

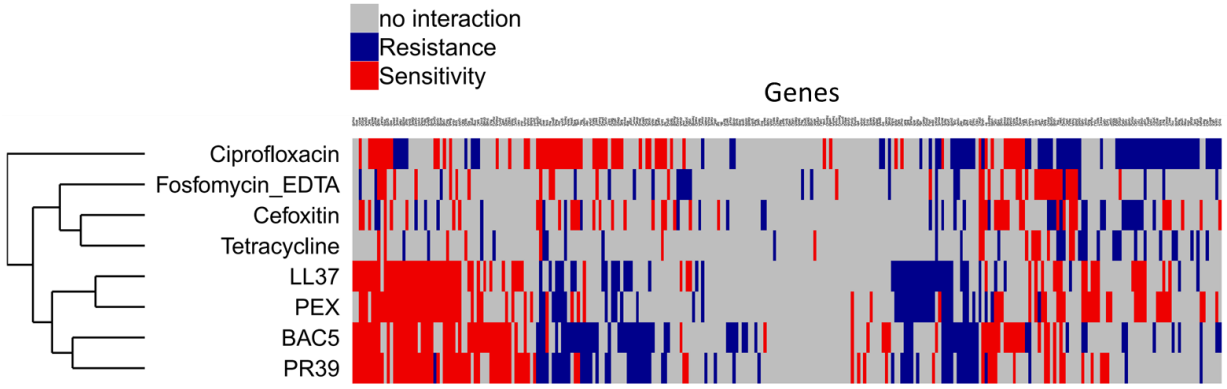

Figure 18. Antibiotics and AMPs have distinct chemical-genetic interaction profiles. Heatmap and dendrogram (Ward's method with Euclidean distances) show chemical-genetic interaction profiles across hypomorphic alleles of all essential *E. coli* genes in response to four antibiotics (Ciprofloxacin, fosfomycin, cefoxitin and tetracycline) of different modes of action and four AMPs (LL37, PEX, BAC5 and PR39). The four tested AMPs cluster together indicating that the majority of the chemical-genetic interactions are specific to AMPs and not shared with antibiotics.

It has been shown that comparison of overexpression and gene depletion screening can advise on possible drug targets[39,54]. In particular, genes that increase bacterial resistance upon overexpression and confer sensitivity when depleted may directly affect the bacterial susceptibility against drugs[54].

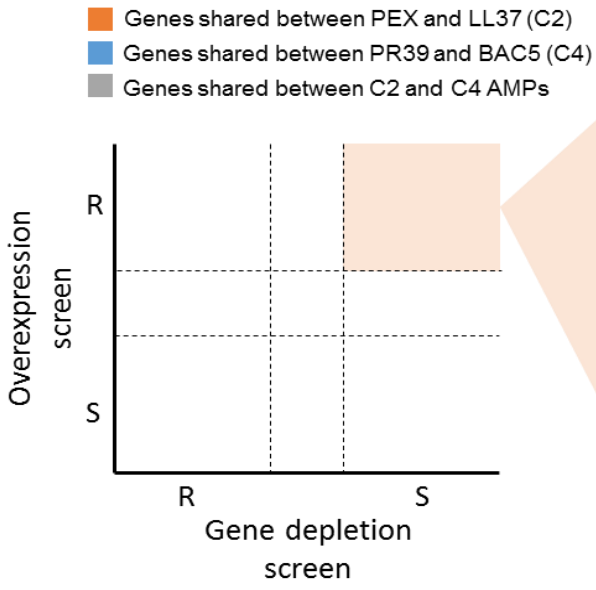

C2		C4	
PEX	LL37	PR39	BAC5
cca	*cca*	*lpxA*	*lpxA*
argS	*ispF*	*acpS*	*acpS*
grpE	*grpE*	*folA*	*grpE*
ribA	*ribA*	*ubiA*	*ubiA*
ribC	*ribC*	*nusA*	*eno*
rpoH	*rpoH*	*pth*	*fbaA*
rpoB	*accB*		*rfaK*
rpsE	*rpsE*		*ispF*
fbaA	*infA*		*rpsM*
rplC	*frr*		*ydfB*
	ssb		*rplB*
	rplW		*frr*
	cysS		
	rpsN		
	rpmD		

Figure 19. Schematic figure showing sets of essential genes that simultaneously enhance AMP resistance when overexpressed and sensitivity when depleted. Color code is explained in the figure.

By comparing the overexpression and hypomorphic (gene depletion) screening data we found dozens of essential genes that showed such properties (Figure 19). Remarkably, *folA* (dihydrofolate reductase), a known target of PR39 peptide[106], was among the set of 6 genes that simultaneously conferred resistance when overexpressed and sensitivity when depleted in the presence of PR39 (Figure 19). Together, these findings reflect differences in the resistance determinants between AMPs, and showed that mode of action of AMPs shapes both the intrinsic and the latent AMP resistomes.

4.5 Collateral sensitivity interactions are frequent between functionally dissimilar AMPs

We demonstrated that there is low overlap in resistance determinants between AMPs, and the mode of action can have a strong influence on difference in resistance determinants across AMPs. Therefore, we hypothesized that some of the genes might show collateral sensitivity interactions (i.e. increase resistance to one AMP while simultaneously sensitizing to another one) between AMPs. Interestingly, we found multiple genes showing collateral sensitivity interactions between AMPs. For example, we identified 643 genes that confer resistance to 2 or more AMPs while increasing sensitivity to at least 2 other AMPs upon overexpression, and these interactions are overrepresented among plasma membrane proteins (Figure 20).

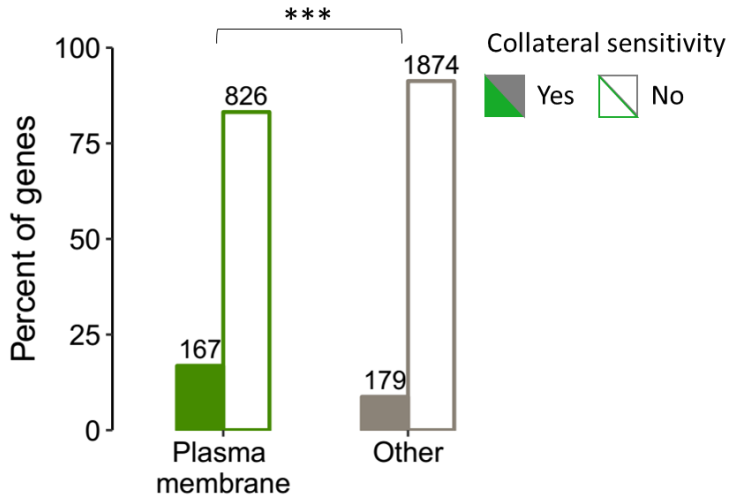

Figure 20. Collateral sensitivity interactions (resistance to at least two AMPs while sensitivity to at least 2 other AMPs) are significantly overrepresented among proteins localized in the plasma membrane compared to other localizations (*** *P* = 1.634e-10, two-sided Fisher's exact test).

Furthermore, we systematically examined the occurrence of collateral sensitivity inducing genes between each AMP pair (Figure 21A). The obtained results allowed us to identify the following patterns. First, the genes inducing collateral sensitivity between AMPs are widespread and such genes are typically underrepresented (35% compared to random expectation) between AMPs that group together in the same cluster (i.e. within cluster) (Figure 21B). Second, for some AMPs, collateral sensitivity interactions were very frequent, for example, intracellular-targeting AMPs (PR39, BAC5, PROA) and a membrane-targeting AMP (CP1) (Figure 21A). Third, collateral sensitivity inducing genes are relatively overrepresented between AMP clusters. In particular, we found overrepresentation of these genes between C1, C2 (membrane targeting) and C3, C4 (intracellular targeting) AMP clusters (Figure 21B).

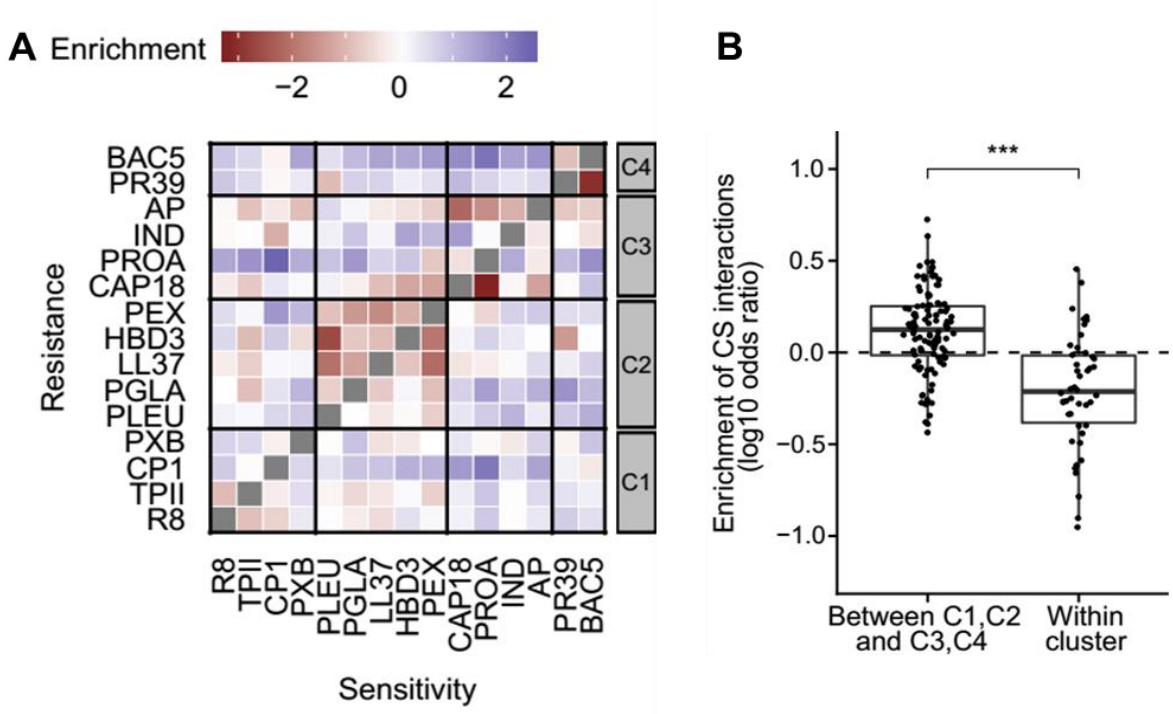

Figure 21. Genes inducing collateral sensitivity interactions between AMPs are widespread. (A) Heatmap showing the overrepresentation of collateral sensitivity-inducing genes for each AMP pairs. **(B)** Collateral sensitivity effects were especially pronounced between

membrane-targeting and intracellular-targeting AMPs as compared to within cluster (P = 2.1*10^{-07} from two-tailed unpaired t-test test). Y-axis shows odds ratio for occurrence of collateral sensitivity interactions between AMP pairs.

Interestingly, when we analyzed hypomorph screening data, the same pattern emerged showing that majority of the collateral sensitivity interactions were found between proline-rich AMPs in cluster C4 (BAC5, PR39) and membrane-targeting AMPs (LL37, PEX) (Figure 22). However, the enrichment of collateral sensitivity interactions between these two groups of AMPs was not statistically significant, the trend remains same as the overexpression screen (Figure 21B and Figure 22B). Further analysis of collateral sensitivity-inducing hypomorphic alleles showed that these alleles were significantly enriched in functions related to ribosome assembly (Figure 23).

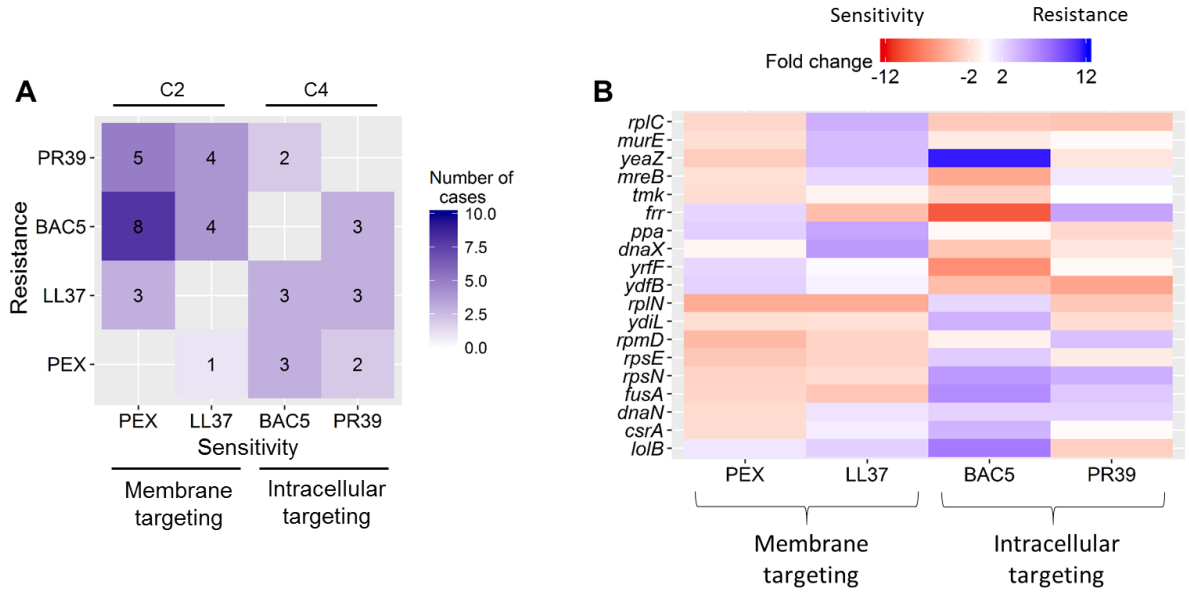

Figure 22. Hypomorphic alleles induce collateral sensitivity between intracellularly-targeting and membrane-targeting AMPs. (A) Heatmap represents number of hypomorphic alleles (values in square) that show collateral sensitivity between each pair of AMPs. **(B)** Chemical-genetic interactions of the collateral sensitivity-inducing hypomorphic alleles.

Overall, these results suggest that collateral sensitivity interaction between AMPs are frequent and more pronounced between membrane- and intracellular-targeting AMPs.

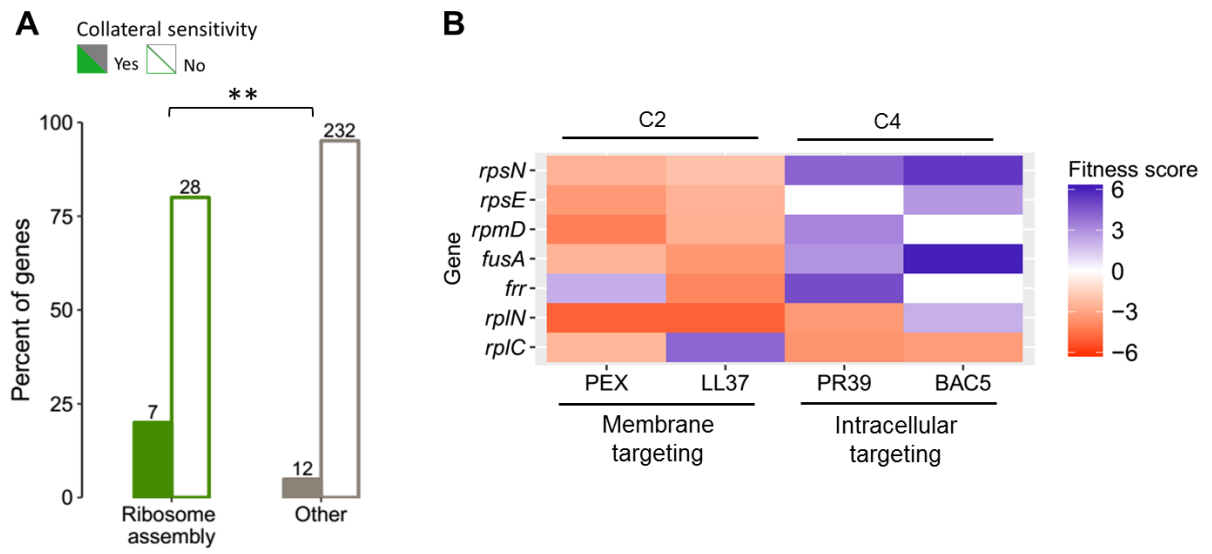

Figure 23. Hypomorphic alleles involved in ribosome assembly showed frequent collateral sensitivity interactions. (A) Hypomorphic alleles showing collateral sensitivity interactions were significantly enriched in function related to ribosome assembly (P = 0.004, two-sided Fisher's exact test). **(B)** Heatmap depicting fitness scores of the genes enriched in ribosome assembly function. Blue and red color represent resistance and sensitivity interactions, respectively.

4.6 Perturbed phospholipid trafficking as a mechanism underlying the collateral sensitivity interactions between AMPs

What could be the underlying molecular mechanism of the observed collateral sensitivity interactions between membrane targeting and intracellular targeting AMPs? To address this, we selected those genes that show collateral sensitivity interactions with multiple AMPs when they were overexpressed. We found 14 genes showing resistance to at least four membrane targeting (C1 and C2) and collateral sensitivity to multiple intracellular targeting AMPs (C3 and C4) (Figure 24). We found that genes related to membrane phospholipid (PL) and lipopolysaccharide (LPS) composition were significantly enriched among these 14 genes (Figure 24B). This trend is exemplified by MlaD that showed resistance to at least four membrane-targeting peptides and at the same time, it increased susceptibility to multiple intracellular-targeting AMPs (Figure 24A).

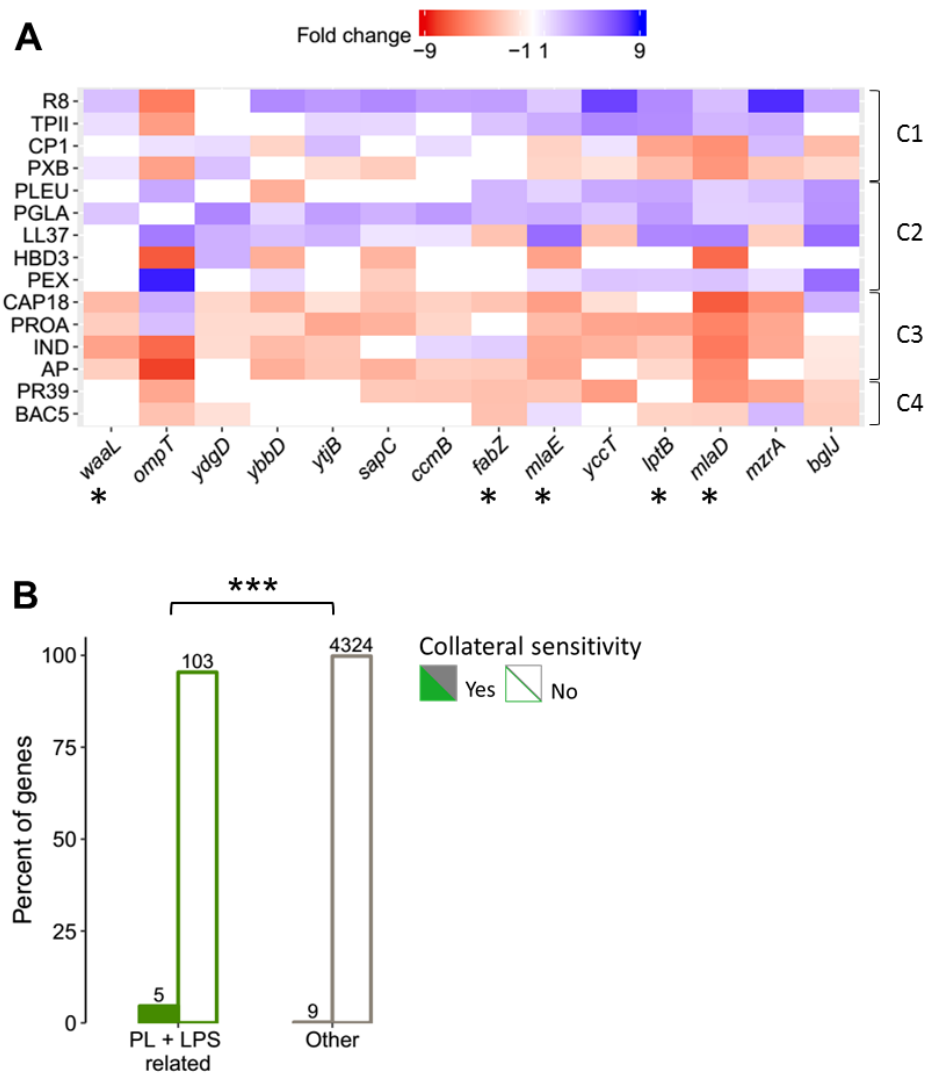

Figure 24. Phospholipid (PL) and lipopolysaccharide (LPS)-related genes frequently show collateral sensitivity interactions to multiple AMPs. Heatmap represents the chemical-genetic signatures of 14 genes (from overexpression screen) showing resistance (blue) to at least 4 membrane-targeting AMPs (C1 and C2) while at the same time sensitivity (red) to at least 4 intracellular-targeting AMPs (C3 and C4). Genes marked with asterisk have functions related to PL and LPS composition of the bacterial membranes. **(B)** The 14 genes that showed collateral sensitivity interaction to multiple AMPs, were significantly enriched in functions related to PL and LPS composition of the bacterial membranes (P = 1.3*10^{-5} from two-sided Fisher's exact test).

MlaD is a member of phospholipid transport system (Mla pathway) in Gram-negative bacteria[107]. The same trend was observed for MlaE as well that is also a component of Mla pathway (Figure 24A).

In particular, we focused on MlaD for two reasons. First, MlaD overexpression results in frequent collateral sensitivity interactions towards multiple AMPs. Second, several studies have demonstrated that Mla pathway plays an important role in bacterial pathogenesis, virulence and antibiotic resistance[108–110].

We next deciphered the mechanism underlying collateral sensitivity interactions of the *mlaD* overexpression. It is known that overexpression of a component of a protein complex may cause loss of function phenotype[111,112]. Since MlaD is part of a protein complex, so, we first tested whether overexpression of *mlaD* has a loss of function or gain of function phenotype. We tested susceptibility profiles of *mlaD* overexpression and *mlaD* deletion mutant across selected AMPs based on chemical-genetic signatures. We found that both type of mutants showed resistance to membrane-targeting AMPs and sensitivity to intracellular-targeting AMPs (Figure 25).

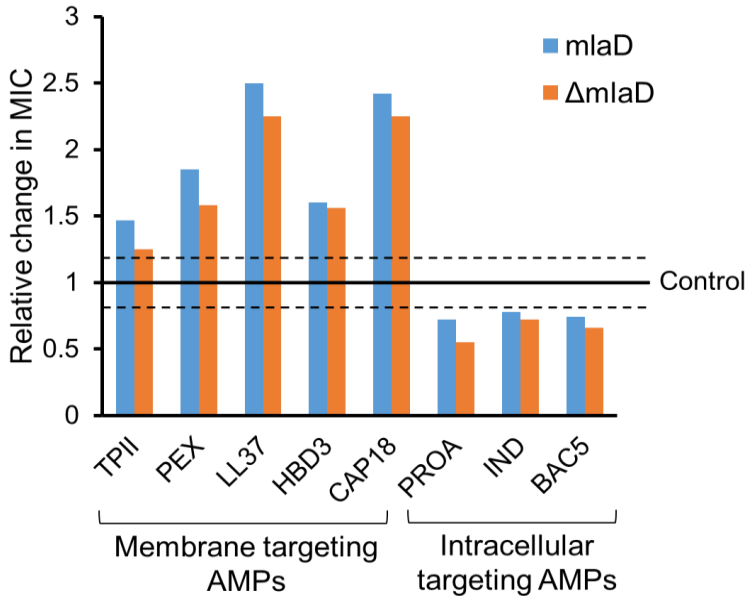

Figure 25. Depletion of *mlaD* showed resistance to membrane-targeting AMPs and sensitivity to intracellular-targeting AMPs. Relative change in MIC was calculated by comparing the MIC to corresponding controls (see Supplementary Figure 2 and 3). Dashed

lines represent previously defined cut-offs for resistance (≥1.2 x MIC of the control) and sensitivity (≤0.8 x MIC of the control)[48].

These results demonstrated that overexpression perturbs *mlaD* function and resulted in loss of function phenotype (Figure 25).

As an additional confirmation, we also tested the susceptibility of *mlaD* mutants towards bile salt. It has been demonstrated that deletion of any component of Mla-pathway cause accumulation of phospholipids in the outer membrane and makes bacteria more sensitive to bile salt[107]. As expected, we found that both the mutants showed increased sensitivity to bile salt (Figure 26).

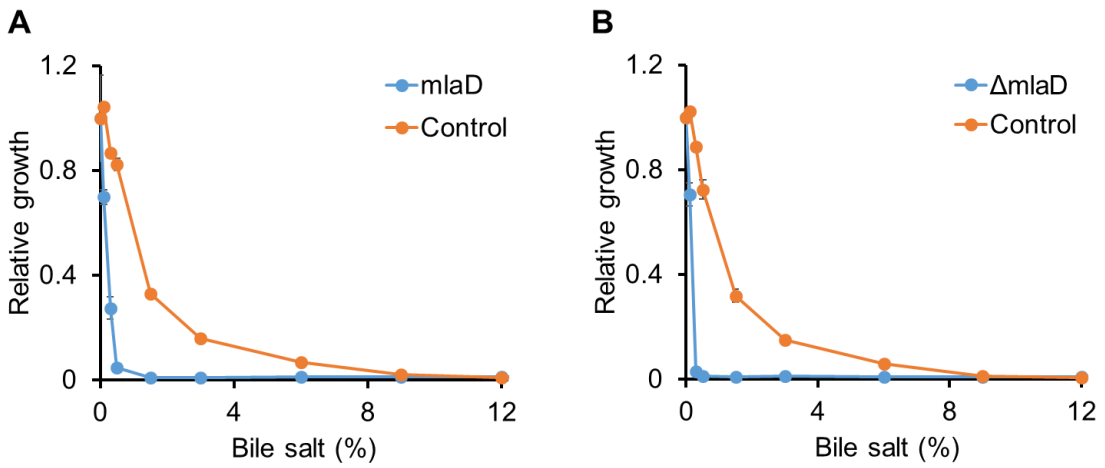

Figure 26: *mlaD* overexpression and *mlaD* knockout mutant show sensitivity to bile acid. Both the *mlaD* overexpression **(A)** and the knockout strain **(B)** show sensitivity to bile acid. The blue line represents the *mlaD* overexpression strain and knockout mutant while the orange line represents corresponding control.

Why does the deletion of *mlaD* cause resistance to membrane-targeting (pore-formers) and sensitivity to intracellular-targeting AMPs? We hypothesized that deletion of *mlaD* increases bacterial resistance to membrane-targeting AMPs by decreasing the negative surface charge on bacterial membrane. We expected this because of the following reasons. First, membrane surface charge is a major factor that contributes to bacterial resistance to membrane-targeting AMPs[8]. Second, it is known that depletion of Mla pathway function influences membrane

composition by accumulating phospholipids in the outer leaflet of outer membrane[107] and altered membrane composition can change net negative surface charge of the membrane[8,27]. Third, accumulation of phospholipids in the outer membrane changes membrane fluidity that could affect pore formation by AMPs[113]. On the other hand, perturbation in membrane composition can influence membrane properties like permeability, membrane potential[114]. Since, some intracellular targeting AMPs (like PROA, IND, BAC5) use membrane potential to translocate themselves inside the bacterial cell[115,116], we hypothesized that this effect could be the underlying mechanism of collateral sensitivity interactions. Considering these effects, we measured negative surface charge and membrane potential of both the *mlaD* overexpression and deletion strain. As expected, both the strains showed decreased negative surface charge and increased membrane potential (Figure 27).

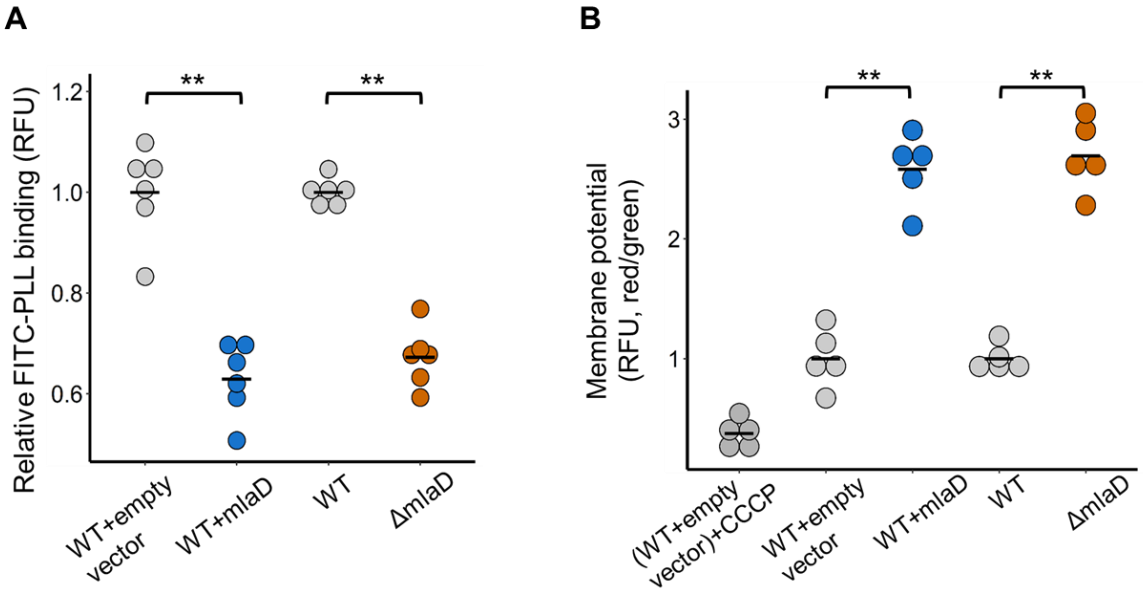

Figure 27. Deletion of *mlaD* decreased negative surface charge on membrane and increased membrane potential. (A) Both *mlaD* overexpression and deletion strain showed decreased net negative surface charge of the bacterial cell. ** indicates significant difference *P* = 0.0021, two-sided Mann–Whitney U test, six biological replicates for each genotype. Charge measurement was done using FITC-labelled poly-L-lysine (FITC-PLL) assay where surface charge is proportional with the binding of FITC-PLL (see Methods). **(B)** Both *mlaD* overexpression and deletion strains showed increased membrane potential (*P* = 0.0079, two-sided Mann–Whitney U test, five biological replicates for each genotype). Relative membrane potential was measured by determining relative fluorescence (RFU) using a carbocyanine dye

DiOC2(3) assay (see Methods). Red/green ratios were calculated using population mean fluorescence intensities.

Altogether, our results showed that depletion of functional *mlaD* decreased negative surface charge on bacterial membrane. Decreased negative surface charge results in weaker electrostatic interactions between bacterial membrane and membrane-targeting AMPs and therefore confers resistance against membrane-targeting AMPs. At the same time, depletion of functional *mlaD* increased the membrane potential that helps in translocation of intracellular targeting AMPs inside the bacterial cell (Figure 28).

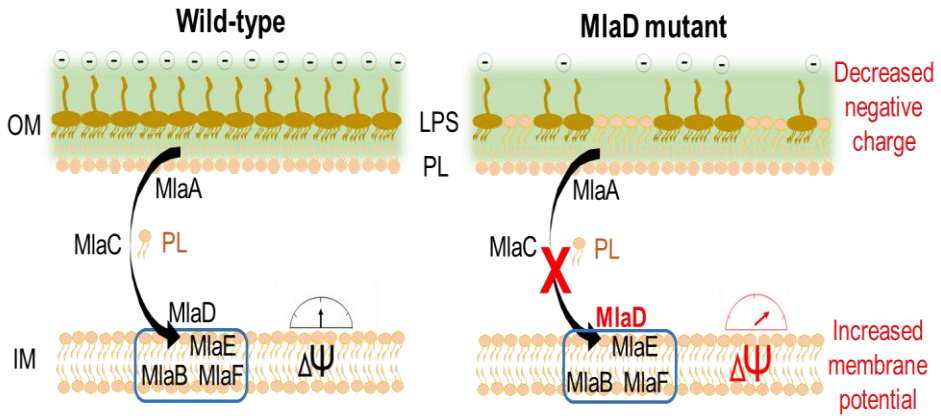

Figure 28. Schematic representation of the proposed molecular mechanism of the antagonistic mutational effects of *mlaD.* Depletion of functional *mlaD* perturbs Mla pathway, causing accumulation of phospholipids in the outer membrane. This perturbation results in decreased net negative surface charge which causes weaker electrostatic interaction between the bacterial membrane and the AMPs, and therefore providing resistance to membrane-targeting AMPs. At the same time, this mutation also increases membrane potential which drives the cellular uptake of certain intracellular-targeting peptides. Abbreviations: OM - outer membrane, IM - inner membrane, PL - phospholipid, LPS - lipopolysaccharide, Δψ - membrane potential.

Furthermore, we examined how general is the identified molecular mechanism of collateral sensitivity interactions between AMPs. To this end, we randomly selected three overexpression mutants that are not related to phospholipid transport system (Mla-pathway) and showed resistance to membrane targeting AMPs and sensitivity to intracellular targeting AMPs

in the chemical-genetic screen. First, we verified the overexpression phenotype of these strain by measuring their susceptibility to membrane- and intracellular-targeting AMPs, and then, we measured the negative surface charge and membrane potential.

A

Gene	Description
rpoH	RNA polymerase, sigma 32 (sigma H) factor
ytjB	Probably inner membrane protein. This gene has a function related to lipoate utilization.
murA	UDP-N-acetylglucosamine 1-carboxyvinyltransferase. This gene is involved in assembly of peptidoglycan.

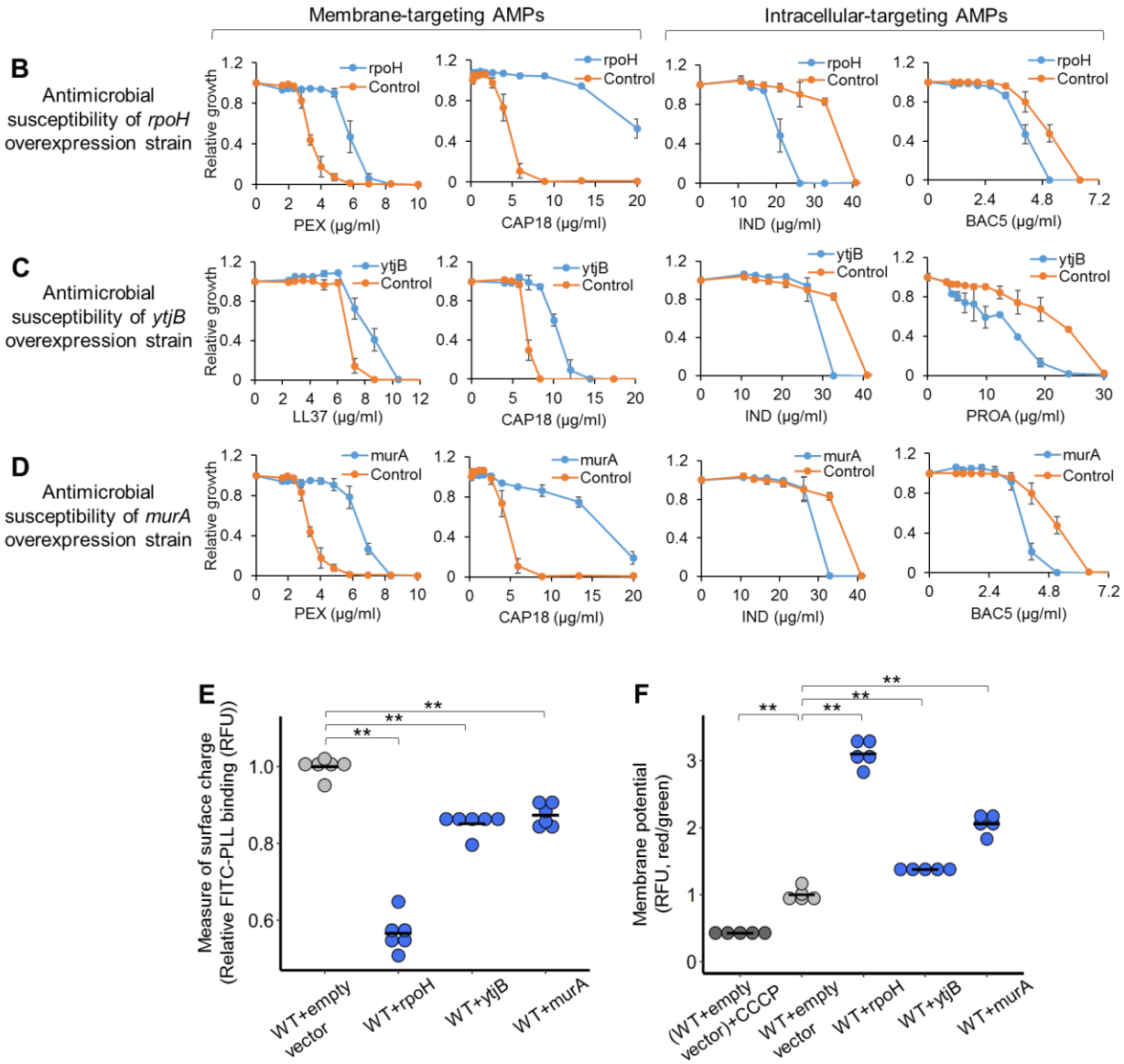

Figure 29. Antimicrobial susceptibility of *rpoH*, *ytjB* and *murA* overexpression strains to membrane- and intracellular-targeting AMPs. (A) The top panel describes the function of the tested genes. **(B,C,D)** *rpoH*, *ytjB* and *murA* overexpression strains showed resistance to membrane-targeting and sensitivity to intracellular-targeting AMPs. The bacterial susceptibility to AMPs was tested by MIC determination. Growth is shown relative to growth in the absence of the corresponding AMP. Error bars indicate the standard errors based on three biological replicates. **(E)** Decreased net negative surface charge of the *rpoH*, *ytjB* and *murA* overexpression strains. Significant differences: ** $P = 0.0021$, $P = 0.0021$ and $P = 0.0021$ for WT+empty vector vs WT+*rpoH* overexpression, WT+empty vector vs WT+*ytjB* overexpression, WT+empty vector vs WT+*murA* overexpression strain respectively, from two-sided Mann–Whitney U test, $n = 6$ biological replicates for each genotype. Charge measurement was done using FITC-labelled poly-L-lysine (FITC-PLL) assay where the fluorescence signal is proportional to the binding of the FITC-PLL molecules. A lower binding of FITC-PLL indicates a less net negative surface charge of the outer bacterial membrane (see Methods). (**F)** Increased membrane potential of *rpoH*, *ytjB* and *murA* overexpression strains. Significant differences: ** $P = 0.0079$, $P = 0.0079$, $P = 0.0079$ and $P = 0.0079$ for WT+empty vector CCCP control vs WT+empty vector, WT+empty vector vs WT+*rpoH* overexpression, WT+empty vector vs WT+*ytjB* overexpression, and WT+empty vector vs WT+*murA* overexpression strains, respectively, from two-sided Mann–Whitney U test, $n = 5$ biological replicates for each genotype. Relative membrane potential was measured by determining relative fluorescence (RFU) using a carbocyanine dye DiOC2(3) assay (see Methods). Red/green ratios were calculated using population mean fluorescence intensities. WT *E. coli* carrying the empty vector treated with cyanide-m-chlorophenylhydrazone (CCCP, a chemical inhibitor of proton motive force) was used as an experimental control for diminished membrane potential.

Consistent with previous results with MlaD, all three strains showed a decreased negative surface charge and an increased membrane potential (Figure 29).

4.7 Chemical-genetic profiles inform on cross-resistance spectra of AMPs

Due to the differences in the modes of action of AMPs, the interacting gene sets in the chemical-genetic profiles largely differed from AMP to AMP. Since bacterial susceptibility can be defined by different gene sets for AMPs with distinct modes of action, we hypothesized that chemical-genetic profiles that differentiate these AMPs can advise on the cross-resistance spectrum. To test our hypothesis, we used our recently published dataset of antimicrobial

susceptibility profiles of AMP-evolved lines (NCOMMS-19-06281A, under revision)[117]. In this published study, an adaptive laboratory evolution was carried out against a set of diverse AMPs and measured susceptibility of AMP-evolved lines against 7 different AMPs (mostly membrane-targeting AMPs) out of 15 AMPs that we studied in our screening. In order to have representative AMPs from all four chemical-genetic clusters in our study, we extended this dataset by determining susceptibility profile of the AMP-evolved lines against 4 more AMPs including intracellular- and dual-targeting AMPs from cluster C4 and C3.

The resulting dataset provides a comprehensive view on cross-resistance and collateral sensitivity interactions between AMPs. By integrating this comprehensive dataset with chemical-genetic profiles of AMPs, we identified the following interesting patterns. First, cross-resistance interactions at 2-fold MIC increase were significantly overrepresented between exclusively membrane-targeting AMPs or between exclusively intracellular-targeting AMPs (Figure 30).

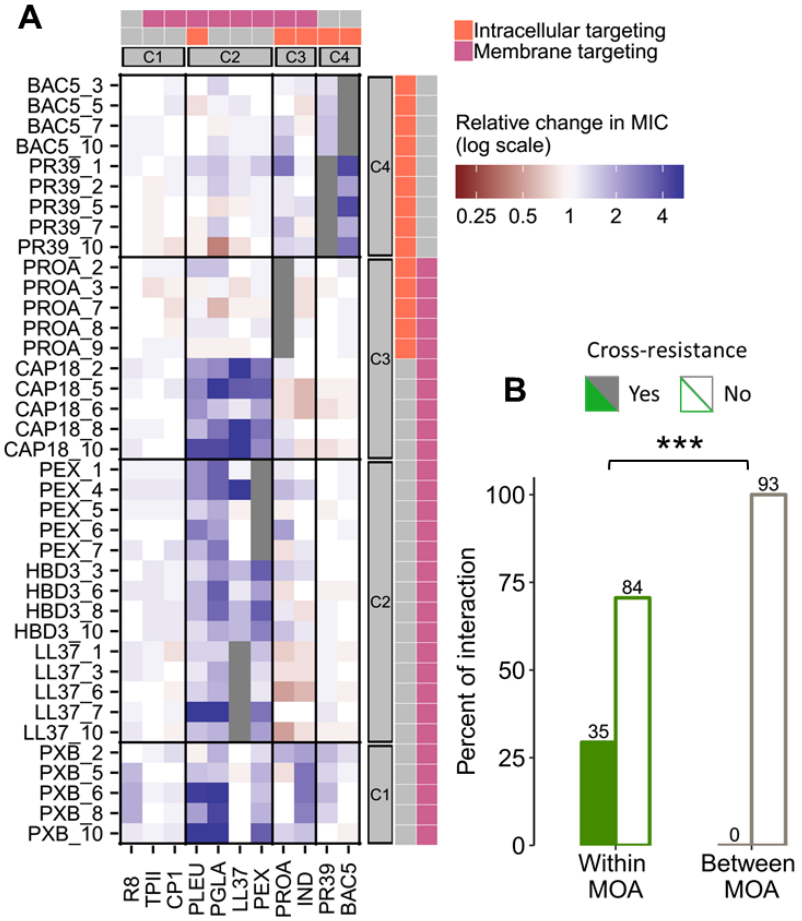

Figure 30. Chemical-genetic profiles inform on cross-resistance spectra of AMP-evolved lines. (A) Heatmap showing cross-resistance spectra of AMP-evolved lines (rows) towards a set of AMPs (columns). Relative change in MIC was determined for each evolved line by comparing its MIC to the ancestral cell line (control). **(B)** Cross-resistance interactions are significantly overrepresented between exclusively membrane-targeting AMPs or exclusively intracellular-targeting AMPs (i.e. within MOA) as compared to AMP pairs from the two groups (i.e. Between MOA). Significant difference: *** $P = 1.333*10^{-10}$ from two-sided Fisher's exact test, $n = 119$ and 93 for within MOA and between MOA, respectively.

Notably, collateral sensitivity interactions (at ≥20% decrease in MIC) were significantly overrepresented between membrane-targeting and intracellular-targeting AMPs (Figure 31). This result is consistent with the observed pattern of collateral sensitivity from overexpression screen (Figure 21B).

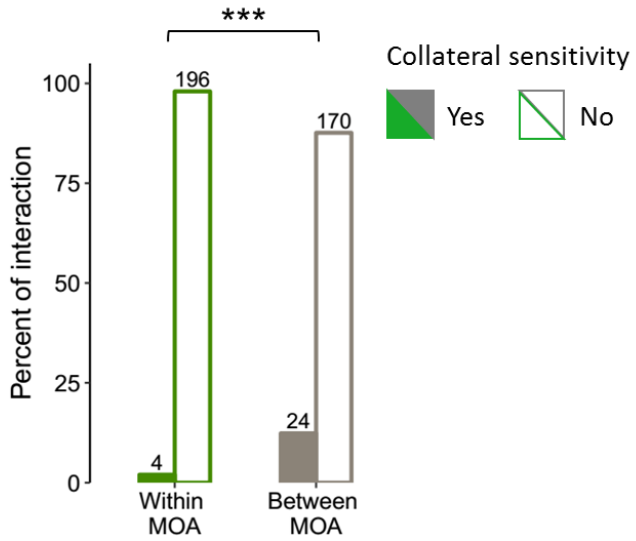

Figure 31. Collateral-sensitivity interactions (at ≥20% decrease in MIC) were significantly overrepresented between membrane-targeting and intracellular-targeting AMPs (i.e. between MOA). Significant difference: *** $P = 4.83*10^{-5}$ from two-sided Fisher's exact test, $n = 200$ and 194 for within MOA and between MOA, respectively.

Second, even membrane-targeting AMPs (cluster C1 and C2) differed in cross-resistance interactions. We found that lineages adapted to AMPs from C2 cluster do not show cross-resistance to AMP from C1 cluster (Figure 32C). These results are in agreement with

chemical-genetic clustering as AMPs in C1 cluster differ their chemical-genetic profiles from AMPs in C2 cluster (Figure 11A). In a similar vein, lineages adapted to AMP from C4 cluster (intracellular-targeting AMPs) showed frequent cross-resistance to AMPs from the same cluster but not to other intracellular targeting AMPs from C3 cluster (Figure 32B). Third, confirming the diverse nature (i.e. both membrane-targeting and intracellular-targeting) of AMPs in C3 cluster (Figure 11A), we found no cross-resistance between AMPs from this cluster (Figure 30).

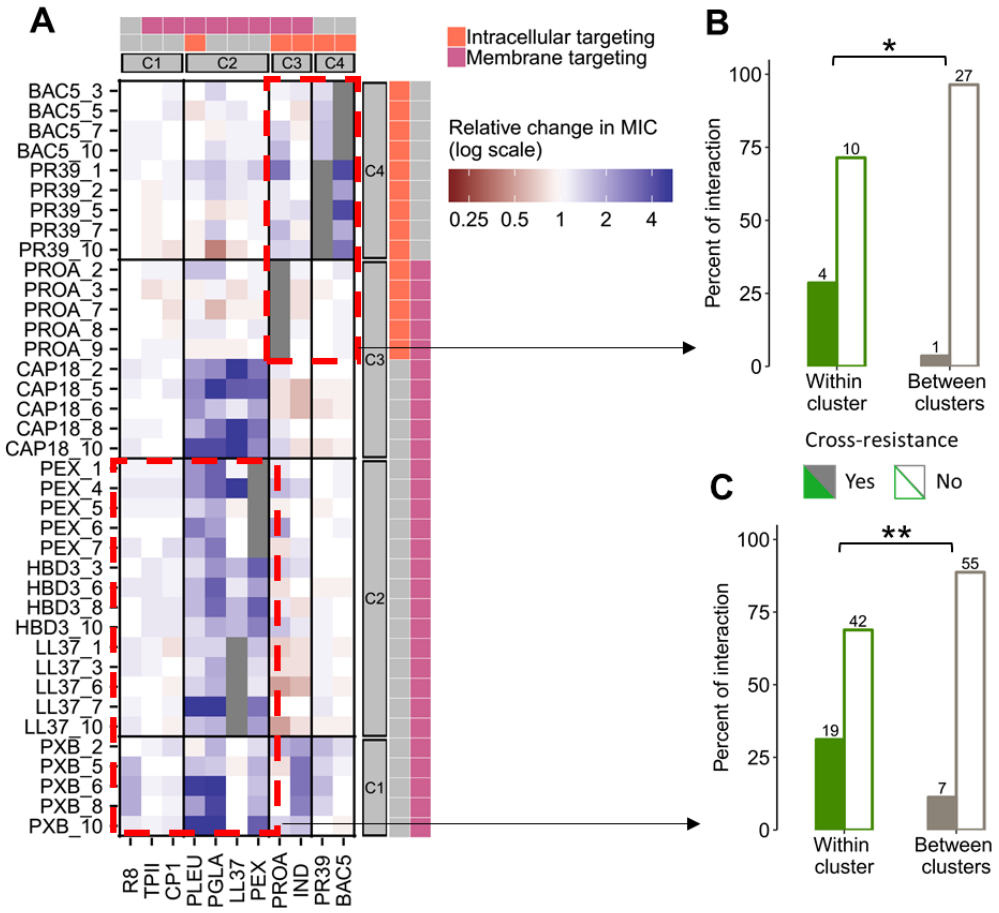

Figure 32. Chemical-genetic clustering provided insights into the cross-resistance patterns between AMPs. (A) Heatmap shows cross-resistance spectra of AMP-evolved lines (rows) towards a set of 11 AMPs (columns). **(B)** Enrichment of cross-resistance interactions between intracellular-targeting AMPs (C3 and C4 cluster) (Significant difference: * P = 0.0353 from two-sided Fisher's exact test, n = 14 and 28 for within cluster and between clusters, respectively). CAP18-adapted lines were not included in the analysis because CAP18 is known as a membrane-targeting AMP in the literature. **(C)** Enrichment of cross-resistance interactions between membrane-targeting AMPs (C1 and C2 cluster) (Significant difference: ** P = 0.0082

from two-sided Fisher's exact test, n = 61 and 62 for within cluster and between clusters, respectively).

Altogether, these results demonstrate that chemical-genetic profiles capture subtle differences in resistance determinants between AMPs with similar broad modes of action, and therefore inform on cross-resistance patterns between AMPs.

5. Discussion

Development of antibiotic resistance in bacteria has become a serious threat to public health, and a new class of antibiotics is needed to treat resistant bacteria. AMPs are molecules of host-defense system and have been proposed as the basis for a novel class of anti-infectives[7,13]. Considerable efforts have been allocated for developing AMP-based therapeutic strategies against pathogens[7,18,118]. Despite the clinical importance of AMPs, the vital concern is that therapeutic use of AMPs holds the risk of cross-resistance to our own immunity peptides[61,62,119]. Our knowledge on the potential for cross-resistance between AMPs remains extremely limited owing to a lack of comprehensive studies on the genetic determinants of resistance to different AMPs. To address this issue, we applied a high-throughput chemical-genetic approach which uncovered the gene sets shaping bacterial resistance to a comprehensive set of AMPs (Figure 8) and the following conclusions were reached.

First, the resulting chemical-genetic profiles grouped the AMPs according to their mode of actions (Figure 11). We found that similarity in chemical-genetic profiles informs on similarity in functional and physicochemical properties of AMPs (Figure 11, and 12). In particular, membrane-targeting AMPs that have unique physicochemical properties (contributing to membrane disruption) clustered separately from intracellular-targeting AMPs (Figure 12). Therefore, chemical-genetic profiles can capture subtle differences in bactericidal effects across AMPs. Previous studies on antibiotics have demonstrated the importance of chemical-genetics in differentiating antibiotics on the basis of their mode of action and cellular targets[40,49]. Antibiotics with similar chemical-genetic profiles are likely to share mechanism of action[49]. Chemical-genetics data are good source to get insights into a variety of processes like mode of action of drugs and their cellular targets and bacterial resistance mechanisms[40,51].

Second, we found that a large number of functionally diverse genes influenced AMP resistance in bacteria (Figure 13). These results substantially broaden the scope AMP resistance modulating genes, as a small fraction of resistance genes has been reported previously. Majority of the reported resistance genes belong to a common mechanism of AMP resistance, i.e., membrane surface modification[27]. Importantly, genes related to cell envelope function were significantly overrepresented among AMPs susceptibility modulating genes (Supplementary Table 3). Furthermore, we found that resistance-enhancing genes substantially

differ across the AMPs with different modes of action (Figure 14). Although generalizations about mechanism of action of membrane-targeting AMPs are common in the literature[8,27], we found that even membrane-targeting AMPs grouped into two different clusters showing the difference in their chemical-genetic profiles. The differences in the chemical-genetic profiles were prominent between AMPs with different modes of action. In particular, resistance-enhancing genes showed significantly low overlap between membrane (C1 and C2)- and intracellular-targeting AMPs (C3 and C4) (Figure 15). These results reveal that AMPs differ considerably in their resistance determinants and these differences are shaped by mechanistic action of AMPs. Our knowledge on mechanistic differences between AMPs is limited, therefore these results can be further used to understand how different AMPs interact with bacteria and exert their antimicrobial activity.

Third, the observed limited overlap in resistance determinants across AMPs advised on collateral sensitivity interactions (negative trade-offs) between AMPs with different modes of action. We found that collateral sensitivity interactions were widespread between AMPs (Figure 21). In particular, collateral sensitivity interactions were frequent between membrane-targeting and intracellular-targeting AMPs (Figure 21B). By studying four overexpression mutants, we uncovered the molecular mechanism underlying collateral sensitivity interactions between membrane-targeting and intracellular-targeting AMPs (Figure 28 and 29). Our results provide important insights into why host-defense peptides have remained effective against bacteria in spite of long term co-evolution. One possible explanation is that host-defense system deploys multiple defense molecules against pathogens and due to negative trade-offs between these molecules, evolution of bacterial resistance can be limited.

Recent studies have focused on collateral sensitivity interactions between antibiotics using experimental evolution approach[44,45,90]. In these studies, susceptibility of antibiotic-evolved lines was tested against a set of AMPs to find whether the resistant bacteria show resistance or sensitivity to other antibiotics. With this approach, we can test only a limited number of resistance mutations whereas chemical-genetics measure contribution of every single gene to bacterial susceptibility against different drugs. As collateral sensitivity emerges as an important concept in the field of multi-drug therapeutics[47,90], these findings could be useful to design effective therapeutic strategies. Combination of those AMPs that have different physicochemical properties and mode of action, may be useful in designing a potential combination therapy. For example, combinations of membrane-targeting and intracellular-targeting AMPs (in particular,

proline/arginine-rich AMPs) could be effective because i) collateral sensitivity interactions are frequent between membrane-targeting and proline/arginine-rich AMPs (Figure 21B), ii) bacteria adapted to human AMPs did not show cross-resistance to proline/arginine-rich AMPs (Figure 30A).

Fourth, by integrating experimental evolution results from our recently published study, we showed that chemical-genetic profiles informed on cross-resistance interactions between AMPs. Since most of the studies on cross-resistance have focused on only membrane-targeting AMPs, our understanding of cross-resistance between functionally diverse AMPs remains limited. Performing a systematic analysis on cross-resistance between functionally diverse AMPs. We demonstrated that cross-resistance interactions frequently occurred between AMPs that show similarity in their mode of action and chemical-genetic profiles (Figure 30). Furthermore, our chemical-genetic clustering illustrated the differences between cross-resistance patterns that cannot be explained by the mode of action of AMPs. For example, lineages adapted to AMPs from C2 cluster (membrane-targeting AMPs) showed cross-resistance to C2 AMPs but rarely showed cross-resistance to AMPs from C1 cluster (membrane-targeting AMPs). AMPs from both the clusters are known as membrane targeting AMPs but they differ from each other in their chemical-genetic profiles and cross-resistance interactions (Figure 11 and Figure 32). These difference can be used to predict cross-resistance between clinically relevant and human AMPs. For example, we found that lineages adapted to human beta-defensin-3 (belongs to C2 cluster) frequently showed cross-resistance to other clinically relevant and human AMPs like LL37 (human cathelicidin) and pexiganan (under clinical phase 3) present in C2 cluster. A previous study has also demonstrated cross-resistance between pexiganan and human-neutrophil-defensin-1 (hNP-1) in *Staphylococcus aureus*[120]*.* These results suggest that understanding of the differences in resistance determinants between AMPs can help in choosing AMPs with limited cross-resistance to human AMPs.

Taken together, our findings have important implications in developing AMP-based therapies. Our results demonstrated that AMPs with different physicochemical properties and mode of action vary substantially in their resistance determinants. As a consequence, cross-resistance interactions were frequent between AMPs with a similar mode of action. On the other hand, collateral sensitivity interactions were pronounced between AMPs with different modes of action. Therefore, while selecting therapeutic AMPs, the differences in AMP resistance determinants and mode of action should be considered to avoid risk of cross-resistance to human immunity peptides. Our results suggest that proline/arginine-rich AMPs could be

potential AMP candidates in this respect as lineages adapted to human AMPs didn't show cross-resistance to proline/arginine-rich AMPs. Moreover, collateral sensitivity interactions are frequent for these AMPs. Notably, several reports have highlighted the importance of proline/arginine-rich AMPs as the lead molecules for the development of AMP-based therapy[118]. We believe that, in future, the chemical-genetic map could inform on how to choose therapeutic AMPs with minimal cross-resistance to human immunity peptides.

6. Conclusion

Despite the clinical importance of AMPs, the vital concern is that therapeutic application of AMPs may induce cross-resistance to our own immunity peptides[61,62,119]. Thus, finding an approach which differentiates resistance determinants between different AMPs and advises on possible cross-resistance between therapeutic and host AMPs would be prerequisite for the development of AMP-based therapies. To this end, we systematically determined the chemical-genetic interactions of ~4400 single-gene overexpression strains and 15 diverse AMPs. This comprehensive compendium revealed multiple and functionally diverse genes that modulate bacterial susceptibility to different AMPs. AMPs differ considerably in their resistance determinants and resistance-enhancing genes overlap only to a limited extent between AMPs. We found that chemical-genetic profiles clustered the AMPs according to their mechanistic property and revealed distinct and often antagonistic mutational effects between membrane-targeting and intracellular-targeting AMPs. Finally, by analyzing the cross-resistance spectra of AMP-adapted lines we showed that cross-resistance rarely occurs between AMPs with distinct modes of action or distinct chemical-genetic clusters.

In conclusion, our work demonstrates that chemical-genetic profiles capture subtle differences in resistance determinants between AMPs, and therefore inform on collateral sensitivity and cross-resistance patterns between AMPs. These findings can be used to avoid those AMPs in clinical settings that are more likely to cause cross-resistance to human immunity peptides.

7. Personal contribution

The results presented in this PhD dissertation originated from the work I carried out in the Csaba Pal lab, laboratory of microbial experimental evolution at the Institute of Biochemistry, MTA-BRC, Szeged. I performed majority of the experiments, such as chemical-genetic screening, validation of chemical-genetic workflow, determination of minimum inhibitory concentration of AMPs, biochemical assays (membrane surface charge and membrane potential measurement, membrane integrity assay etc.), growth rate measurements. Preparation of plasmid DNA samples for deep sequencing was done jointly with my colleague Móni Számel. Deep sequencing was carried out by István Nagy and his colleagues from Seqomics Ltd, Szeged. Overexpression screen data normalization and analysis (such as clustering of chemical-genetic profiles, overlap in chemical-genetic profiles between AMPs) was performed by our colleague Gergely Fekete from Balázs Papp lab, laboratory of computational systems biology at MTA-BRC, Szeged. I have contributed significantly in data analysis and statistical evaluation part as well. In particular, I had performed the downstream analysis including gene ontology enrichment, calculating collateral sensitivity-inducing genes and their enrichment analysis. Construction of hypomorphic alleles and chemical-genetic screening was performed by our collaborator Mohan Babu and his colleagues at University of Regina, Regina, Canada. I analyzed the obtained hypomorphic alleles data to calculated the Jaccard similarity index and collateral sensitivity interactions for each AMP pair.

8. Acknowledgement

My PhD journey has been truly an amazing experience for me, and I would like to thank many people for their support and guidance during this journey.

First and foremost, I want to thank my supervisor Csaba Pál for his encouraging attitude and scientific guidance throughout my PhD study. I would like to express my sincere gratitude to him for his tremendous academic support and insightful discussions to make my PhD experience productive. It has been really a great experience working with Csaba. Thanks for the opportunity!

Similar, profound gratitude goes to Balázs Papp for his thoughtful inputs and guidance during my PhD. I really appreciate his support and constructive suggestions which have contributed greatly to the improvement of my research project.

I would also wish to express my gratitude to my co-supervisor Bálint Kintses for his constant guidance and extended discussions. His friendly supervision and expert advice have been invaluable throughout all stages of the project.

I'm very thankful to Orsolya Méhi, Móni Számel and Gergely Fekete for their great help and support. I'm thankful to all the members of "Antimicrobial Resistome Research Unit" for their support and fun time. You guys have been a source of friendships and valuable advice.

I also express my gratitude to all my colleagues for their help and their contribution to my personal and professional time at BRC. I thank Zoltán Farkas, Ádám Györkei, Lejla Daruka, Bálint Csörgő, Viktória Lázár, Réka Spohn, Ana Martins, Ákos Nyerges, Gábor Apjok, Petra Éva Szili, Dorottya Kalapis, Vidovics Petra Fanni, Eszter Ari, Károly Kovács, Roland Tengölics, Gábor Grézal.

Many thanks to Andreea Daraba and Andrea Tóth for their immense technical assistance and for helping with the lab administration work.

I thank Kotogány Edit for her help while doing flow cytometry measurements.

I would also like to thank István Nagy and the team of SeqOmics Ltd. for helping us with the DNA sequencing.

I am especially thankful to our collaborator Dr. Mohan Babu and his colleagues, Ali Hosseinnia, Alla Gagarinova, Sunyoung Kim and Sadhna Phanse for their excellent work with hypomorphic alleles screening and for providing the valuable dataset.

I would also like to thank all my friends in Hungary who made my time enjoyable in large part. I thank Amna Shahid, Imran Baba, Dhirendra K. Singh and Rantidev Shukla.

Furthermore, I wish to thank my thesis reviewer for constructive comments and suggestions.

Last but not least, I am deeply thankful to my family members for their love and support.

Thank you all, it’s been an absolute pleasure working with you guys.

9. References

1. Haney, E. F., Mansour, S. C. & Hancock, R. E. W. Antimicrobial Peptides: An Introduction. *Methods Mol. Biol.* **1548**, 3–22 (2017).
2. Brogden, K. A. Antimicrobial peptides: Pore formers or metabolic inhibitors in bacteria? *Nat. Rev. Microbiol.* **3**, 238–250 (2005).
3. Zasloff, M. Antimicrobial peptides of multicellular organisms. *Nature* **415**, 389–95 (2002).
4. Phoenix, D. A., Dennison, S. R. & Harris, F. Antimicrobial Peptides: Their History, Evolution, and Functional Promiscuity. in *Antimicrobial Peptides* (2013). doi:10.1002/9783527652853.ch1
5. Bensch, K. W., Raida, M., Mägert, H. J., Schulz-Knappe, P. & Forssmann, W. G. hBD-1: a novel β-defensin from human plasma. *FEBS Lett.* (1995). doi:10.1016/0014-5793(95)00687-5
6. Galloo, R. L. *et al.* Identification of CRAMP, a cathelin-related antimicrobial peptide expressed in the embryonic and adult mouse. *J. Biol. Chem.* (1997). doi:10.1074/jbc.272.20.13088
7. Hancock, R. E. W. & Sahl, H.-G. Antimicrobial and host-defense peptides as new anti-infective therapeutic strategies. *Nat. Biotechnol.* **24**, 1551–1557 (2006).
8. Yeaman, M. R. Mechanisms of Antimicrobial Peptide Action and Resistance. *Pharmacol. Rev.* **55**, 27–55 (2003).
9. Park, C. B., Kim, H. S. & Kim, S. C. Mechanism of action of the antimicrobial peptide buforin II: Buforin II kills microorganisms by penetrating the cell membrane and inhibiting cellular functions. *Biochem. Biophys. Res. Commun.* (1998). doi:10.1006/bbrc.1998.8159
10. Le, C.-F., Fang, C.-M. & Sekaran, S. D. Intracellular Targeting Mechanisms by Antimicrobial Peptides. *Antimicrob. Agents Chemother.* **61**, (2017).
11. Diamond, G., Beckloff, N., Weinberg, A. & Kisich, K. The Roles of Antimicrobial Peptides in Innate Host Defense. *Curr. Pharm. Des.* (2009). doi:10.2174/138161209788682325
12. Felício, M. R., Silva, O. N., Gonçalves, S., Santos, N. C. & Franco, O. L. Peptides with Dual Antimicrobial and Anticancer Activities. *Front. Chem.* (2017). doi:10.3389/fchem.2017.00005
13. Mahlapuu, M., Håkansson, J., Ringstad, L. & Björn, C. Antimicrobial Peptides: An Emerging Category of Therapeutic Agents. *Front. Cell. Infect. Microbiol.* **6**, 194 (2016).
14. Torrent, M., Andreu, D., Nogués, V. M. & Boix, E. Connecting Peptide Physicochemical and Antimicrobial Properties by a Rational Prediction Model. *PLoS One* **6**, e16968

(2011).

15. Bahar, A. & Ren, D. Antimicrobial Peptides. *Pharmaceuticals* **6**, 1543–1575 (2013).
16. Dathe, M. *et al.* Hydrophobicity, hydrophobic moment and angle subtended by charged residues modulate antibacterial and haemolytic activity of amphipathic helical peptides. *FEBS Lett.* (1997). doi:10.1016/S0014-5793(97)00055-0
17. Osorio, D., Rondòn-Villarreal, P., Torres, R., Rondon-Villarreal, P. & Torres, R. Peptides : A Package for Data Mining of Antimicrobial Peptides. *R J.* (2012). doi:10.1080/07294360701658781
18. Findlay, B., Zhanel, G. G. & Schweizer, F. Cationic amphiphiles, a new generation of antimicrobials inspired by the natural antimicrobial peptide scaffold. *Antimicrobial Agents and Chemotherapy* (2010). doi:10.1128/AAC.00530-10
19. Li, J. *et al.* Membrane active antimicrobial peptides: Translating mechanistic insights to design. *Frontiers in Neuroscience* (2017). doi:10.3389/fnins.2017.00073
20. Pieta, P., Mirza, J. & Lipkowski, J. Direct visualization of the alamethicin pore formed in a planar phospholipid matrix. *Proc. Natl. Acad. Sci.* (2012). doi:10.1073/pnas.1201559110
21. Scheit, K. H., Reddy, E. S. P. & Bhargava, P. M. Seminalplasmin is a potent inhibitor of E.coli RNA polymerase in vitro [18]. *Nature* (1979). doi:10.1038/279728a0
22. Chitnis, S. N., Prasad, K. S. N. & Bhargava, P. M. Isolation and Characterization of Autolysis-Defective Mutants of Escherichia Coli that are Resistant to the Lytic Activity of Seminalplasmin. *J. Gen. Microbiol.* (2009). doi:10.1099/00221287-136-3-463
23. Chitnis, S. N., Prasad, K. N. & Bhargava, P. M. Bacteriolytic Activity of Seminalplasmin. *Microbiology* (2009). doi:10.1099/00221287-133-5-1265
24. G., R. *et al.* Functional characterization of SbmA, a bacterial inner membrane transporter required for importing the antimicrobial peptide Bac7(1-35). *J. Bacteriol.* (2013). doi:10.1128/JB.00818-13
25. Eswarappa, S. M., Panguluri, K. K., Hensel, M. & Chakravortty, D. The yejABEF operon of Salmonella confers resistance to antimicrobial peptides and contributes to its virulence. *Microbiology* (2008). doi:10.1099/mic.0.2007/011114-0
26. Marlow, V. L. *et al.* Essential role for the BacA protein in the uptake of a truncated eukaryotic peptide in Sinorhizobium meliloti. *J. Bacteriol.* (2009). doi:10.1128/JB.01661-08
27. Andersson, D. I., Hughes, D. & Kubicek-Sutherland, J. Z. Mechanisms and consequences of bacterial resistance to antimicrobial peptides. *Drug Resist. Updat.* **26**, 43–57 (2016).

28. Nizet, V. Antimicrobial peptide resistance mechanisms of human bacterial pathogens. *Curr. Issues Mol. Biol.* **8**, 11–26 (2006).
29. McPhee, J. B., Lewenza, S. & Hancock, R. E. W. Cationic antimicrobial peptides activate a two-component regulatory system, PmrA-PmrB, that regulates resistance to polymyxin B and cationic antimicrobial peptides in Pseudomonas aeruginosa. *Mol. Microbiol.* (2003). doi:10.1046/j.1365-2958.2003.03673.x
30. Guo, L. *et al.* Regulation of lipid A modifications by Salmonella typhimurium virulence genes phoP-phoQ. *Science.* (1997). doi:10.1126/science.276.5310.250
31. Dalebroux, Z. D. & Miller, S. I. Salmonellae PhoPQ regulation of the outer membrane to resist innate immunity. *Current Opinion in Microbiology* (2014). doi:10.1016/j.mib.2013.12.005
32. Dalebroux, Z. D., Matamouros, S., Whittington, D., Bishop, R. E. & Miller, S. I. PhoPQ regulates acidic glycerophospholipid content of the Salmonella Typhimurium outer membrane . *Proc. Natl. Acad. Sci.* (2014). doi:10.1073/pnas.1316901111
33. Olaitan, A. O., Morand, S. & Rolain, J. M. Mechanisms of polymyxin resistance: Acquired and intrinsic resistance in bacteria. *Frontiers in Microbiology* (2014). doi:10.3389/fmicb.2014.00643
34. Stumpe, S., Schmid, R., Stephens, D. L., Georgiou, G. & Bakker, E. P. Identification of OmpT as the protease that hydrolyzes the antimicrobial peptide protamine before it enters growing cells of Escherichia coli. *J. Bacteriol.* **180**, 4002–6 (1998).
35. Guina, T., Yi, E. C., Wang, H., Hackett, M. & Miller, S. I. A PhoP-regulated outer membrane protease of Salmonella enterica serovar typhimurium promotes resistance to alpha-helical antimicrobial peptides. *J. Bacteriol.* (2000). doi:10.1128/JB.182.14.4077-4086.2000
36. Mattiuzzo, M. *et al.* Role of the Escherichia coli SbmA in the antimicrobial activity of proline-rich peptides. *Mol. Microbiol.* **66**, 151–163 (2007).
37. Narayanan, S. *et al.* Mechanism of escherichia coli resistance to pyrrhocoricin. *Antimicrob. Agents Chemother.* (2014). doi:10.1128/AAC.02565-13
38. Stensvåg, K. *et al.* Inner membrane proteins YgdD and SbmA are required for the complete susceptibility of Escherichia coli to the proline-rich antimicrobial peptide arasin 1(1–25). *Microbiology* **162**, 601–609 (2016).
39. Palmer, A. C., Chait, R. & Kishony, R. Nonoptimal Gene Expression Creates Latent Potential for Antibiotic Resistance. *Mol. Biol. Evol.* **35**, 2669–2684 (2018).
40. Cacace, E., Kritikos, G. & Typas, A. Chemical genetics in drug discovery. *Curr. Opin.*

Syst. Biol. **4**, 35–42 (2017).

41. Davies, J. & Davies, D. Origins and Evolution of Antibiotic Resistance. *Microbiol. Mol. Biol. Rev.* **74**, 417–433 (2010).
42. Liu, Y.-Y. *et al.* Emergence of plasmid-mediated colistin resistance mechanism MCR-1 in animals and human beings in China: a microbiological and molecular biological study. *Lancet Infect. Dis.* **16**, 161–168 (2016).
43. Cao, L., Li, X., Xu, Y. & Shen, J. Prevalence and molecular characteristics of mcr-1 colistin resistance in Escherichia coli: isolates of clinical infection from a Chinese University Hospital. *Infect. Drug Resist.* **Volume 11**, 1597–1603 (2018).
44. Pál, C., Papp, B. & Lázár, V. Collateral sensitivity of antibiotic-resistant microbes. *Trends Microbiol.* **23**, 401–407 (2015).
45. Imamovic, L. & Sommer, M. O. A. Use of Collateral Sensitivity Networks to Design Drug Cycling Protocols That Avoid Resistance Development. *Sci. Transl. Med.* **5**, 204ra132-204ra132 (2013).
46. Imamovic, L. *et al.* Drug-Driven Phenotypic Convergence Supports Rational Treatment Strategies of Chronic Infections. *Cell* **172**, 121-134.e14 (2018).
47. Baym, M., Stone, L. K. & Kishony, R. Multidrug evolutionary strategies to reverse antibiotic resistance. *Science.* **351**, aad3292–aad3292 (2016).
48. Lázár, V. *et al.* Antibiotic-resistant bacteria show widespread collateral sensitivity to antimicrobial peptides. *Nat. Microbiol.* **3**, 718–731 (2018).
49. Nichols, R. J. *et al.* Phenotypic Landscape of a Bacterial Cell. *Cell* **144**, 143–156 (2011).
50. Lee, A. Y. *et al.* Mapping the Cellular Response to Small Molecules Using Chemogenomic Fitness Signatures. *Science.* **344**, 208–211 (2014).
51. Ho, C. H. *et al.* A molecular barcoded yeast ORF library enables mode-of-action analysis of bioactive compounds. *Nat. Biotechnol.* **27**, 369–377 (2009).
52. Bredel, M. & Jacoby, E. Chemogenomics: an emerging strategy for rapid target and drug discovery. *Nat. Rev. Genet.* **5**, 262–275 (2004).
53. Wagih, O. *et al.* SGAtools: one-stop analysis and visualization of array-based genetic interaction screens. *Nucleic Acids Res.* **41**, W591–W596 (2013).
54. Hoon, S. *et al.* An integrated platform of genomic assays reveals small-molecule bioactivities. *Nat. Chem. Biol.* **4**, 498–506 (2008).
55. Parsons, A. B. *et al.* Integration of chemical-genetic and genetic interaction data links bioactive compounds to cellular target pathways. *Nat. Biotechnol.* **22**, 62–69 (2004).
56. Parsons, A. B. *et al.* Exploring the Mode-of-Action of Bioactive Compounds by Chemical-

Genetic Profiling in Yeast. *Cell* **126**, 611–625 (2006).

57. Giaever, G. *et al.* Genomic profiling of drug sensitivities via induced haploinsufficiency. *Nat. Genet.* **21**, 278–283 (1999).
58. Soo, V. W. C., Hanson-Manful, P. & Patrick, W. M. Artificial gene amplification reveals an abundance of promiscuous resistance determinants in Escherichia coli. *Proc. Natl. Acad. Sci.* **108**, 1484–1489 (2011).
59. Girgis, H. S., Hottes, A. K. & Tavazoie, S. Genetic architecture of intrinsic antibiotic susceptibility. *PLoS One* **4**, e5629 (2009).
60. Lázár, V. *et al.* Genome-wide analysis captures the determinants of the antibiotic cross-resistance interaction network. *Nat. Commun.* **5**, 4352 (2014).
61. Fleitas, O. & Franco, O. L. Induced Bacterial Cross-Resistance toward Host Antimicrobial Peptides: A Worrying Phenomenon. *Front. Microbiol.* **7**, 381 (2016).
62. Napier, B. A. *et al.* Clinical Use of Colistin Induces Cross-Resistance to Host Antimicrobials in Acinetobacter baumannii. *MBio* **4**, (2013).
63. Fox, J. L. Antimicrobial peptides stage a comeback. *Nat. Biotechnol.* **31**, 379–382 (2013).
64. Kitagawa, M. *et al.* Complete set of ORF clones of Escherichia coli ASKA library (A Complete Set of E. coli K-12 ORF Archive): Unique Resources for Biological Research. *DNA Res.* **12**, 291–299 (2006).
65. Notebaart, R. A. *et al.* Network-level architecture and the evolutionary potential of underground metabolism. *Proc. Natl. Acad. Sci.* **111**, 11762–11767 (2014).
66. Pierce, S. E., Davis, R. W., Nislow, C. & Giaever, G. Genome-wide analysis of barcoded Saccharomyces cerevisiae gene-deletion mutants in pooled cultures. *Nat. Protoc.* **2**, 2958–2974 (2007).
67. Robinson, D. G., Chen, W., Storey, J. D. & Gresham, D. Design and Analysis of Bar-seq Experiments. *G3: Genes|Genomes|Genetics* **4**, 11–18 (2014).
68. Rocke, D. M. & Durbin, B. Approximate variance-stabilizing transformations for gene-expression microarray data. *Bioinformatics* **19**, 966–972 (2003).
69. Anders, S. & Huber, W. Differential expression analysis for sequence count data. *Genome Biol.* **11**, R106 (2010).
70. Ronan, T., Qi, Z. & Naegle, K. M. Avoiding common pitfalls when clustering biological data. *Sci. Signal.* **9**, re6 (2016).
71. Babu, M., Gagarinova, A. & Emili, A. Array-Based Synthetic Genetic Screens to Map Bacterial Pathways and Functional Networks in Escherichia coli. in *Methods in Molecular Biology* 99–126 (2011). doi:10.1007/978-1-61779-276-2_7

72. Babu, M. *et al.* Genetic Interaction Maps in Escherichia coli Reveal Functional Crosstalk among Cell Envelope Biogenesis Pathways. *PLoS Genet.* **7**, e1002377 (2011).
73. Breslow, D. K. *et al.* A comprehensive strategy enabling high-resolution functional analysis of the yeast genome. *Nat. Methods* **5**, 711–718 (2008).
74. Babu, M. *et al.* Global landscape of cell envelope protein complexes in Escherichia coli. *Nat. Biotechnol.* **36**, 103–112 (2017).
75. Kumar, A. *et al.* Conditional Epistatic Interaction Maps Reveal Global Functional Rewiring of Genome Integrity Pathways in Escherichia coli. *Cell Rep.* **14**, 648–661 (2016).
76. Butland, G. *et al.* eSGA: E. coli synthetic genetic array analysis. *Nat. Methods* **5**, 789–795 (2008).
77. Babu, M. *et al.* Quantitative Genome-Wide Genetic Interaction Screens Reveal Global Epistatic Relationships of Protein Complexes in Escherichia coli. *PLoS Genet.* **10**, e1004120 (2014).
78. Wagih, O. & Parts, L. gitter: A Robust and Accurate Method for Quantification of Colony Sizes From Plate Images. *G3: Genes|Genomes|Genetics* **4**, 547–552 (2014).
79. Gasteiger, E. *et al.* Protein Identification and Analysis Tools on the ExPASy Server. in *The Proteomics Protocols Handbook* 571–607 (Humana Press, 2005). doi:10.1385/1-59259-890-0:571
80. Walsh, I., Seno, F., Tosatto, S. C. E. & Trovato, A. PASTA 2.0: an improved server for protein aggregation prediction. *Nucleic Acids Res.* **42**, W301–W307 (2014).
81. Team, R. D. C. & R Development Core Team, R. R: A Language and Environment for Statistical Computing. *R Found. Stat. Comput.* (2016). doi:10.1007/978-3-540-74686-7
82. Team, Rs. RStudio: Integrated Development for R. *[Online] RStudio, Inc., Boston, MA URL http://www. rstudio. com* (2015). doi:https://www.nrel.gov/docs/fy16osti/65298.pdf
83. Chen, H. *et al.* Genome-Wide Quantification of the Effect of Gene Overexpression on Escherichia coli Growth. *Genes (Basel).* **9**, 414 (2018).
84. Maere, S., Heymans, K. & Kuiper, M. BiNGO: a Cytoscape plugin to assess overrepresentation of Gene Ontology categories in Biological Networks. *Bioinformatics* **21**, 3448–3449 (2005).
85. Zhou, J. & Rudd, K. E. EcoGene 3.0. *Nucleic Acids Res.* **41**, D613–D624 (2012).
86. Hochberg, B. Controlling the False Discovery Rate: a Practical and Powerful Approach to Multiple Testing. *J. R. Stat. Soc.* (1995). doi:10.2307/2346101
87. Wiegand, I., Hilpert, K. & Hancock, R. E. W. Agar and broth dilution methods to determine the minimal inhibitory concentration (MIC) of antimicrobial substances. *Nat.*

Protoc. **3**, 163–175 (2008).

88. Peschel, A. *et al.* Inactivation of the dlt Operon in Staphylococcus aureus Confers Sensitivity to Defensins, Protegrins, and Other Antimicrobial Peptides. *J. Biol. Chem.* **274**, 8405–8410 (1999).
89. Rossetti, F. F. *et al.* Interaction of Poly(L-Lysine)-g-Poly(Ethylene Glycol) with Supported Phospholipid Bilayers. *Biophys. J.* **87**, 1711–1721 (2004).
90. Lazar, V. *et al.* Bacterial evolution of antibiotic hypersensitivity. *Mol. Syst. Biol.* **9**, 700–700 (2014).
91. Baba, T. *et al.* Construction of Escherichia coli K-12 in-frame, single-gene knockout mutants: the Keio collection. *Mol. Syst. Biol.* **2**, 2006.0008 (2006).
92. Pósfai, G., Koob, M. D., Kirkpatrick, H. A. & Blattner, F. R. Versatile insertion plasmids for targeted genome manipulations in bacteria: isolation, deletion, and rescue of the pathogenicity island LEE of the Escherichia coli O157:H7 genome. *J. Bacteriol.* **179**, 4426–4428 (1997).
93. Galardini, M. *et al.* Phenotype inference in an Escherichia coli strain panel. *Elife* **6**, (2017).
94. Mattiuzzo, M. *et al.* Proteolytic activity of Escherichia coli oligopeptidase B against proline-rich antimicrobial peptides. *J. Microbiol. Biotechnol.* (2014). doi:10.4014/jmb.1310.10015
95. Warner, D. M. & Levy, S. B. Different effects of transcriptional regulators MarA, SoxS and Rob on susceptibility of Escherichia coli to cationic antimicrobial peptides (CAMPs): Rob-dependent CAMP induction of the marRAB operon. *Microbiology* **156**, 570–578 (2010).
96. Stumpe, S., Schmid, R., Stephens, D. L., Georgiou, G. & Bakker, E. P. Identification of OmpT as the protease that hydrolyzes the antimicrobial peptide protamine before it enters growing cells of Escherichia coli. *J. Bacteriol.* (1998).
97. Trent, M. S. *et al.* Accumulation of a Polyisoprene-linked Amino Sugar in Polymyxin-resistant Salmonella typhimurium and Escherichia coli. *J. Biol. Chem.* **276**, 43132–43144 (2001).
98. Weatherspoon-Griffin, N. *et al.* The CpxR/CpxA Two-component System Up-regulates Two Tat-dependent Peptidoglycan Amidases to Confer Bacterial Resistance to Antimicrobial Peptide. *J. Biol. Chem.* **286**, 5529–5539 (2011).
99. Roland, K. L., Esther, C. R. & Spitznagel, J. K. Isolation and characterization of a gene, pmrD, from Salmonella typhimurium that confers resistance to polymyxin when expressed in multiple copies. *J. Bacteriol.* **176**, 3589–3597 (1994).

100. Pranting, M., Negrea, A., Rhen, M. & Andersson, D. I. Mechanism and Fitness Costs of PR-39 Resistance in Salmonella enterica Serovar Typhimurium LT2. *Antimicrob. Agents Chemother.* **52**, 2734–2741 (2008).
101. Matsumoto, K. *et al.* In vivo target exploration of apidaecin based on Acquired Resistance induced by Gene Overexpression (ARGO assay). *Sci. Rep.* **7**, 12136 (2017).
102. Dathe, M. & Wieprecht, T. Structural features of helical antimicrobial peptides: their potential to modulate activity on model membranes and biological cells. *Biochim. Biophys. Acta - Biomembr.* **1462**, 71–87 (1999).
103. Gerstel, U. *et al.* Hornerin contains a Linked Series of Ribosome-Targeting Peptide Antibiotics. *Sci. Rep.* **8**, 16158 (2018).
104. Hu, P. *et al.* Global Functional Atlas of Escherichia coli Encompassing Previously Uncharacterized Proteins. *PLoS Biol.* **7**, e1000096 (2009).
105. Gagarinova, A. *et al.* Systematic Genetic Screens Reveal the Dynamic Global Functional Organization of the Bacterial Translation Machinery. *Cell Rep.* (2016). doi:10.1016/j.celrep.2016.09.040
106. Ho, Y.-H., Shah, P., Chen, Y.-W. & Chen, C.-S. Systematic Analysis of Intracellular-targeting Antimicrobial Peptides, Bactenecin 7, Hybrid of Pleurocidin and Dermaseptin, Proline–Arginine-rich Peptide, and Lactoferricin B, by Using Escherichia coli Proteome Microarrays. *Mol. Cell. Proteomics* **15**, 1837–1847 (2016).
107. Malinverni, J. C. & Silhavy, T. J. An ABC transport system that maintains lipid asymmetry in the Gram-negative outer membrane. *Proc. Natl. Acad. Sci.* **106**, 8009–8014 (2009).
108. Nakamura, S. *et al.* Molecular Basis of Increased Serum Resistance among Pulmonary Isolates of Non-typeable Haemophilus influenzae. *PLoS Pathog.* **7**, e1001247 (2011).
109. Ekiert, D. C. *et al.* Architectures of Lipid Transport Systems for the Bacterial Outer Membrane. *Cell* **169**, 273-285.e17 (2017).
110. Roier, S. *et al.* A novel mechanism for the biogenesis of outer membrane vesicles in Gram-negative bacteria. *Nat. Commun.* **7**, 10515 (2016).
111. Prelich, G. Gene Overexpression: Uses, Mechanisms, and Interpretation. *Genetics* **190**, 841–854 (2012).
112. Papp, B., Pál, C. & Hurst, L. D. Dosage sensitivity and the evolution of gene families in yeast. *Nature* **424**, 194–197 (2003).
113. Chapman, M. R., Lam, K. L. H., Waring, A. J., Lehrer, R. I. & Lee, K. Y. C. The Origin of Antimicrobial Resistance and Fluidity Dependent Membrane Structural Transformation by Antimicrobial Peptide Protegrin-1. *Biophys. J.* **96**, 550a (2009).

114. Strahl, H. & Hamoen, L. W. Membrane potential is important for bacterial cell division. *Proc. Natl. Acad. Sci.* **107**, 12281–12286 (2010).
115. Aspedon, A. & Groisman, E. A. The antibacterial action of protamine: evidence for disruption of cytoplasmic membrane energization in Salmonella typhimurium. *Microbiology* **142**, 3389–3397 (1996).
116. Falla, T. J., Karunaratne, D. N. & Hancock, R. E. W. Mode of Action of the Antimicrobial Peptide Indolicidin. *J. Biol. Chem.* **271**, 19298–19303 (1996).
117. Spohn, R. *et al*. Integrated evolutionary analysis reveals antimicrobial peptides with limited resistance. (Under revision).
118. Li, W. *et al.* Proline-rich antimicrobial peptides: potential therapeutics against antibiotic-resistant bacteria. *Amino Acids* **46**, 2287–2294 (2014).
119. Bell, G. Arming the enemy: the evolution of resistance to self-proteins. *Microbiology* **149**, 1367–1375 (2003).
120. Habets, M. G. J. L. & Brockhurst, M. A. Therapeutic antimicrobial peptides may compromise natural immunity. *Biol. Lett.* **8**, 416–418 (2012).

10. List of publications

Number of scientific publications: 11 (+ 1 pre-print)
Number of citations: 83
H-index: 5
Total impact factor: 50.14
MTMT identification number: 10060960

*Kintses B[#], **Jangir PK[#]**, Fekete G[#], Számel M, Méhi O, Spohn R, Daruka L, Martins A, Hosseinnia A, Gagarinova A, Kim S, Phanse S, Csörgő B, Györkei Á, Ari E, Lázár V, Faragó A, Bodai L, Nagy I, Babu M, Pál C, Papp B. (2019). Chemical-genetic profiling reveals cross-resistance and collateral sensitivity between antimicrobial peptides. BioRxiv. doi: 10.1101/542548 **([#]equal first authors).** IF:NA

*Lázár V, Martins A, Spohn R, Daruka L, Grézal G, Fekete G, Számel M, **Jangir PK,** Kintses B, Csörgő B, Nyerges Á, Györkei Á, Kincses A, Dér A, Walter FR, Deli MA, Urbán E, Hegedűs Z, Olajos G, Méhi O, Bálint B, Nagy I, Martinek TA, Papp B, Pál C. (2018). Antibiotic-resistant bacteria show widespread collateral sensitivity to antimicrobial peptides. Nature Microbiology 3, 718–731. https://doi.org/10.1038/s41564-018-0164-0.
IF: 14.174

Trivedi VD[#], **Jangir PK[#]**, Sharma R, Phale PS. (2016). Draft Genome Sequence of Carbaryl-Degrading Soil Isolate *Pseudomonas* sp. Strain C5pp. Genome Announc. 9;4(3). doi: 10.1128/genomeA.00526-16. IF:NA **([#]equal first authors)**

*These publications serve as the basis of this PhD dissertation

Full papers (as a first or co-author) not included in the thesis:

Kintses B, Méhi O, Ari E, Számel M, Györkei Á, **Jangir PK,** Nagy I, Pál F, Fekete G, Tengölics R, Nyerges Á, Lik I, Bálint A, Molnár T, Bálint B, Vásárhelyi BM, Bustamante M, Papp B, Pál C. (2019). Phylogenetic barriers to horizontal transfer of antimicrobial peptide resistance genes in the human gut microbiota. Nature Microbiology 4, 447–458. IF: 14.174

Kumar R, **Jangir PK,** Das J, Taneja B, Sharma R. (2017). Genome Analysis of *Staphylococcus capitis* TE8 Reveals Repertoire of Antimicrobial Peptides and Adaptation Strategies for Growth on Human Skin. Scientific Reports 5;7(1):10447. doi: 10.1038/s41598-017-11020-7. IF: 4.25

Trivedi VD, **Jangir PK,** Sharma R, Phale PS. (2016). Insights into functional and evolutionary analysis of carbaryl metabolic pathway from *Pseudomonas* sp. strain C5pp. Scientific Reports 7;6:38430. doi: 10.1038/srep38430. IF: 4.25

Latka C, Dey SS, Mahajan S, Prabu R, **Jangir PK,** Gupta C, Das S, Ramachandran VG, Bhattacharya SN, Pandey R, Sharma R, Ramachandran S, Taneja B. (2015). Genome sequence of a clinical isolate of dermatophyte, *Trichophyton rubrum* from India. FEMS Microbiology Letters. 362(8):fnv039. doi: 10.1093/femsle/fnv039. IF: 1.85

Srivastav R, Singh A, **Jangir PK**, Kumari C, Muduli S, Sharma R. (2013). Genome Sequence of *Staphylococcus massiliensis* Strain S46, Isolated from the Surface of Healthy Human Skin. Genome Announc. 8;1(4). pii: e00553-13. doi: 10.1128/genomeA.00553-13. IF:NA

Karuthedath VS, Patowary A, Singh M, Periwal V, Singh AV, Singh PK, Garg P, Mohan Katoch V, Katoch K, **Jangir PK,** Sharma R; Open Source Drug Discovery Consortium, Chauhan DS, Scaria V, Sivasubbu S. (2013). Draft Genome Sequence of a Clinical Isolate of Multidrug-Resistant *Mycobacterium tuberculosis* East African Indian Strain OSDD271. Genome Announc.1;1(4). pii: e00541-13. doi: 10.1128/genomeA.00541-13. IF:NA

Jangir PK, Singh A, Shivaji S, Sharma R. (2012). Genome sequence of the alkaliphilic bacterium *Nitritalea halalkaliphila* type strain LW7, isolated from Lonar Lake, India. Journal of Bacteriology 194(20):5688-9. doi:10.1128/JB.01302-12. IF: 3.19

Bajpai R[#], Soni V[#], Khandrika L[#], **Jangir PK[#]**, Sharma R, Agrawal P. (2012). Genome sequence of a novel actinophage PIS136 isolated from a strain of *Saccharomonospora* sp. Journal of Virology 86(17):9552. doi: 10.1128/JVI.01529-12. IF: 5.07 **([#]equal first authors)**

Singh A[#], **Jangir PK[#],** Kumari C, Sharma R. (2012). Genome sequence of *Nitratireductor aquibiodomus* strain RA22. Journal of Bacteriology 194(22):6307. doi: 10.1128/JB.01510-12. IF:3.19 **([#]equal first authors)**

11. Summary

Antimicrobial peptides (AMPs) are crucial components of the host immune system. Because of their broad spectrum and rapid killing activity, they have been proposed as promising novel anti-infectives. However, there is a serious concern that therapeutic application of AMPs would drive bacterial resistance to our own immune peptides. This is an alarming issue as many AMP-based clinical applications are about to reach clinical trials while others are already in clinical use. As an example, resistance against polymyxins – a class of AMPs used as last-resort drugs – is spreading rapidly in pathogenic bacteria and the underlying resistance mechanisms have been shown to influence resistance to host-defense antimicrobials.

But are all classes of AMPs equally prone to induce such cross-resistance effects? Unfortunately, our knowledge on cross-resistance between AMPs remains extremely limited. To address this gap, we used chemical-genetic approaches to uncover the resistance determinants of *E. coli* against 15 different AMPs, and combined laboratory evolution approach to predict the cross-resistance interactions between AMPs.

We found that chemical-genetic profiles clustered the AMPs according to their broad mode of action. AMPs with similar broad modes of action and physicochemical properties show considerable similarity in their chemical-genetic profiles, suggesting that our chemical-genetic profiles can capture certain differences in how AMPs act on bacteria. Although generalizations about AMP resistance are quite common in the literature, we found that AMPs with different modes of action and physicochemical properties have largely distinct bacterial resistance determinants.

Next, we showed that resistance determinants often have antagonistic effects across different AMPs, a phenomenon called collateral sensitivity. For example, while many mutations caused resistance to membrane-targeting AMPs they induced collateral sensitivity to intracellular-targeting AMPs at the same time. These results suggest that mode of action lead to collateral sensitivity interactions between AMPs. We also offer a mechanistic explanation for such collateral sensitivity interactions that involve a clinically relevant and universal pathway in Gram-negative bacteria.

Finally, by integrating laboratory evolution approach, we demonstrated that chemical-genetic profiles inform on cross-resistance interactions between AMPs. We found that cross-resistance interactions were significantly overrepresented enriched between exclusively membrane-targeting AMPs or between exclusively intracellular-targeting AMPs. Importantly, the

chemical-genetic clustering provided additional insights into the cross-resistance patterns that could not have been predicted based on the known broad mode of action of AMPs.

In sum, our work revealed a wide diversity of resistance determinants across AMPs that largely depend on the mode of action of the specific AMP. As a consequence, the probability of cross-resistance between AMPs will be defined by the overlap in their chemical-genetic profiles and modes of action. We believe that these findings could inform future efforts to minimize cross-resistance between therapeutic and human-defense AMPs.

12. Összefoglaló

Az antimikrobiális peptidek (AMP-k) az immunrendszer ősi és létfontosságú összetevői. Széles hatásspektrumuk és gyors ölőhatásuk miatt ígéretes gyógyszerjelöltként tartják őket számon. Aggodalomra ad okot azonban, hogy az AMP-k terápiás alkalmazásával hozzásegíthetjük a baktériumokat az immunrendszerünk saját peptidjeivel szembeni ellenálló képesség kialakításához. Ez a probléma aktuálissá vált, mivel számos AMP alapú terapeutikum áll a klinikai tesztelés küszöbén, néhányat pedig már alkalmaznak a klinikumban. Ilyenek például a polimixinek, amelyeket jelenleg legvégső megoldásként alkalmaznak. Az ellenük kialakuló rezisztencia azonban gyorsan terjed a kórokozók között és kimutatták, hogy a háttérben húzódó rezisztenciamechanizmus keresztrezisztenciát biztosít az immunrendszer peptidjeivel szemben.

Kérdéses azonban, hogy a keresztrezisztencia kialakításának képessége minden AMP-re egyformán jellemző-e. Az e témában szerzett eddigi tudásunk sajnos erősen hiányos. Ennek bővítése érdekében kutatásunk során meghatároztuk, hogy az *Escherichia coli* baktérium mely génjei lehetnek felelősek a rezisztencia kialakításáért 15 különböző AMP-vel szemben, valamint feltérképeztük az AMP-k közötti keresztrezisztencia kapcsolatokat. Ehhez kemogenomikai és laboratóriumi evolúciós megközelítést alkalmaztunk.

Eredményeink azt mutatják, hogy a kemogenomikai profilok alapján az AMP-k hatásmechanizmusaik szerint csoportosíthatók. Azok az AMP-k tehát, amelyek hasonlóan változatos hatásmechanizmussal és fizikokémiai tulajdonságokkal rendelkeznek jelentős hasonlóságot mutatnak a kemogenomikai profiljukban is. Mindez azt mutatja, hogy a kemogenomikai profil képes felfedni az AMP-k baktériumokra gyakorolt hatásának különbségeit. Eredményeink szerint azon AMP-k esetén, amelyek különböző hatásmechanizmussal és fizikokémiai tulajdonságokkal rendelkeznek, a rezisztenciát meghatározó gének is jelentősen eltérnek. Ez a megfigyelés új megvilágításba helyezi az irodalomban gyakran olvasható általánosításokat az AMP rezisztenciát illetően.

Munkánk során kimutattuk azt is, hogy a rezisztenciát meghatározó géneknek különböző AMP-k esetén gyakran ellentétes hatásuk van. Ezt a jelenséget kollaterális szenzitivitásnak nevezzük. Számos mutációról kiderült, hogy míg a sejtmembránt célzó AMP-kkel szemben rezisztenciát biztosít, addig a sejten belüli célpontokkal rendelkező AMP-k esetén érzékenyítő hatása van. Ezek az eredmények arra utalnak, hogy a különféle hatásmechanizmusok kollaterális szenzitivitást okozhatnak az AMP-k között. Kutatásunk magyarázattal szolgál a

kollaterális szenzitivitás háttérmechanizmusáról is, amely egy klinikailag releváns, Gram-negatív baktériumokban általánosan jelen lévő biokémiai útvonalon alapul.

Végezetül, laboratóriumi evolúciós kísérletekkel kiegészülve demonstráltuk, hogy a kemogenomikai profilok információt nyújtanak az AMP-k közötti keresztrezisztencia kapcsolatokról is. Megfigyeltük ugyanis, hogy a keresztrezisztencia kapcsolatok szignifikánsan feldúsulnak a kizárólag sejtmembránt vagy a kizárólag sejten belüli célpontokat célzó AMP-k esetén. Így tehát a kemogenomikai csoportosítás segítségével olyan keresztrezisztencia kapcsolatokba nyertünk betekintést, amelyeket, az AMP-k széles hatásspektrumát figyelembe véve, más módon nem tudtunk volna megjósolni.

Összefoglalva, munkánk során az AMP-kkel szembeni rezisztenciamechanizmusok széles skáláját tártuk fel, amelyek nagymértékben függenek az adott AMP hatásmechanizmusától. Bemutattuk, hogy az AMP-k közötti keresztrezisztencia esélye meghatározható kemogenomikai profiljuk és hatásmechanizmusaik átfedései alapján. Eredményeink hasznos információkkal szolgálnak ahhoz, hogy a jövőben terápiás céllal alkalmazott és az immunrendszer által termelt AMP-k közötti keresztrezisztencia kialakulásának esélyét minimalizáljuk.

13. Appendix

Supplementary Table 1: List of literature curated AMP resistance genes in bacteria.

Resistance gene	Bacterial species	AMP resistance	Reference
apsS	*Staphylococcus aureus*	Nisin, indolicidin, LL37	PMID: 17961141
dltA (dlt operon)	*Staphylococcus aureus, Staphylococcus xylosus*	Human alfa-defensin1, 3, protegrins, tachyplesins, magainin II, gallidermin, nisin	PMID: 10085071
eptA	*Salmonella sp.*	Polymyxin B	PMID: 20384697
graR (GraRS)	*Staphylococcus aureus*	Polymyxin B	PMID: 17502406
hemB,C (hem operon)	*Staphylococcus aureus, SalmonellaTyphimurium*	LL-37, human beta-defensin 2, human beta-defensin 3, lactoferricin B, Protamine, colistin,	PMID: 24717245, 11934563
lpxF	*Bacteroides thetaiotaomicron, Porphyromonas gingivalis*	Polymyxin B	PMID: 20657724,25574022
marRAB	*Escherichia coli*	LL37	PMID: 19926649, 29795541
mcr1	*Escherichia coli, Klebsiella pneumoniae, Pseudomonas aeruginosa, Kluyvera ascorbata*	Colistin, polymyxin B	PMID: 26603172
mgrB	*Klebsiella pneumoniae*	Polymyxin B	PMID: 25190723, 28202493
mprF	*Staphylococcus aureus, Listeria monocytogenes, Brucella suis, Clostridium perfringens, Streptococcus agalactiae*	Defensins	PMID: 11342591
nlpE	*Escherichia coli*	Protamine	https://repository.asu.edu/attachments/110499/content/Griffin_asu_0010E_12909.pdf
ompT	*Enterobacteriaceae*	LL37, C18G, protamine	PMID: 22144482, 20646209, 9683502
pagP	*Salmonella typhimurium*	C18G, PGLA, protegrin	PMID: 9790526
pgtE	*Salmonella enterica Serovar Typhimurium, Shigella flexneri, Yersinia pestis*	C18G, LL37, CRAMP, peptide neuropilin-1, protegrin-1	PMID: 10869088
phoP (PhoPQ)	*Pseudomonas aeruginosa, Salmonella typhimurium, Escherichia coli*	Polymyxin B, protamine, defensins	PMID: 10567263, 7565089, 1465423, 10869088
pmrAB	*Pseudomonas aeruginosa, Salmonella Typhimurium*	Polymyxin B	PMID: 14702327
prfA	*Escherichia coli*	Apidaecin	PMID: 28939819
ptrB	*Escherichia coli*	*Bactenecin 5, PR39*	PMID: 24225368
qacA	*Staphylococcus aureus*	tPMP-1	PMID: 10508013

sapD	*Proteus mirabilis*	Protamine	PMID: 11408219
sbmA	*Escherichia coli, Salmonella Typhimurium*	Bactenecin7, PR39	PMID: 17725560
slyA	*Salmonella enterica serovar Typhimurium*	Magainin 2, polymyxin B	PMID: 15208313, 15813739
ugtL	*Salmonella enterica serovar Typhimurium*	Magainin 2, polymyxin B	PMID: 15208313
waaF	*Burkholderia genus*	Polymyxin B	PMID: 21811491
waaY	*Salmonella typhimurium, Escherichia coli*	LL37, CNY100HL, CAP18	PMID: 27180309
yejA (*yejABEF* operon)	*Salmonella enterica serovar Typhimurium*	Protamine, melittin, polymyxin B, human defensins	PMID: 18227269

Supplementary Table 2. Detailed information (based on literature mining) of the antimicrobial peptides (AMPs) used in this study.

AMP		Source	Pore formation	Mechanism of killing	Clinical relevance
Name	**Abbrev.**				
R8	R8	Synthetic (from linguistic model)	n.a.	n.a.	n.a.
Tachyplesin II	TPII	Japanese horseshoe crab	Yes[1]	Disrupts cell membrane[1]	n.a.
Polymyxin B	PXB	*Bacillus polymyxa*	Yes[2]	Disrupts cell membrane[2]	Yes[3]
				Induces ROS formation[4,5]	
Cecropin P1	CP1	Ascaris suum	Yes[6-8]	Disrupts cell membrane[8,9]	n.a.
Peptide Glycine-Leucine Amide	PGLA	Xenopus laevis; skin; stomach	Yes[10,11]	Disrupts cell membrane[12]	n.a.
Pexiganan	PEX	Synthetic; Magainin derivative	Yes[13]	Disrupts cell membrane[14]	Yes[15-17]
Pleurocidin	PLEU	Pleuronectes americanus	Yes[18]	Disrupts cell membrane[18]	n.a.
				Induces ROS formation[19]	
				Inhibits protein and DNA synthesis[20,21]	
LL-37 cathelicidin	LL37	Homo sapiens; neutrophils; skin; sweat	Yes[22]	Disrupts cell membrane[22-24]	Yes[23]
				Induces ROS formation[25,26]	
Human beta-defensin-3	HBD-3	Homo sapiens; synthetic	n.a.	Disrupts cell membrane[27]	n.a.
				Inhibits lipid II in peptidoglycan biosynthesis[28]	
Apidaecin IB	AP	Apis mellifera L.	n.a.	Inhibits DnaK[29],GroEL/GroES[30], FtsH[31]	Yes[33,34]
				Inhibits protein biosynthesis by targeting ribosome[32]	
CAP18	CAP18	Rabbit	Yes[35]	Disrupts cell membrane[35-37]	Yes[38]
Indolicidin	IND	Bos taurus; bovine neutrophils	Yes[39]	Disrupts cell membrane[39]	Yes[15,40,41]

				Inhibits septum formation[42]	
				Inhibits DNA and protein synthesis[42]	
Protamine	PROA	Herring	No[43]	Affects cellular respiration[43] and glycolysis[43,44]	n.a.
				Disrupts cell envelope[45]	
PR39	PR39	Pig	No[9]	Inhibits protein and DNA synthesis[9,46]	n.a.
				Inhibits folate biosynthesis[46]	
Bactenecin 5	BAC5	Bos taurus; bovine neutrophils	n.a.	Inhibits protein and RNA synthesis[47]	n.a.

Supplementary Table 3. Gene ontology (GO) enrichment analysis of the genes enhancing resistance and sensitivity to antimicrobial peptides (AMPs).

		Sensitivity-enhancing genes			Resistance-enhancing genes			
AMP	**GO-ID**	**p-value**	**corr p-value**	**Description**	GO-ID	p-value	corr p-value	Description
	5886	7.82E-31	1.09E-27	plasma membrane	3676	1.17E-05	0.00135	nucleic acid binding
	5887	6.82E-06	0.00095	integral to plasma membrane	3700	0.00119	0.0395	transcription factor activity
	6644	1.28E-05	0.00149	phospholipid metabolic process	6139	0.00081	0.0301	nucleotide and nucleic acid metabolic process
	6810	1.53E-05	0.00164	transport	6350	4.33E-06	0.000962	transcription
	8610	0.000312	0.0217	lipid biosynthetic process	9059	0.000985	0.0342	macromolecule biosynthetic process
	8654	8.84E-06	0.00112	phospholipid biosynthetic process	9251	0.00143	0.045	glucan catabolic process
AP	15075	0.000396	0.0251	ion transmembrane transporter activity	9889	6.61E-05	0.00362	regulation of biosynthetic process
					10467	5.42E-06	0.000962	gene expression
					16070	3.80E-06	0.000962	RNA metabolic process
					19222	3.37E-06	0.000962	regulation of metabolic process
					31323	1.63E-05	0.00154	regulation of cellular metabolic process
					32774	5.55E-06	0.000962	RNA biosynthetic process
					51171	2.28E-05	0.00177	regulation of nitrogen compound metabolic proce
	6974	0.000283	0.0301	response to DNA damage stimulus	154	2.45E-05	0.00669	rRNA modification
	9279	5.01E-12	5.49E-09	cell outer membrane	5527	0.000178	0.0292	macrolide binding
	30313	2.63E-09	4.80E-07	cell envelope	5528	0.000178	0.0292	FK506 binding
BAC5	30674	0.000178	0.0216	protein binding, bridging	5886	9.11E-15	1.49E-11	plasma membrane
	31230	1.82E-08	2.84E-06	intrinsic to cell outer membrane	6364	0.000198	0.0296	rRNA processing
	42884	0.000302	0.0301	microcin transport	16072	0.000355	0.0484	rRNA metabolic process
	44462	1.54E-09	4.22E-07	external encapsulating structure part	22613	9.08E-05	0.0186	ribonucleoprotein complex biogenesis
	45203	5.23E-06	0.000715	integral to cell outer membrane	42254	9.08E-05	0.0186	ribosome biogenesis
	3954	0.000528	0.0439	NADH dehydrogenase activity	166	0.000171	0.0178	nucleotide binding
	5886	3.39E-52	8.75E-49	plasma membrane	5622	0.000151	0.0174	intracellular
	5887	3.16E-10	7.73E-08	integral to plasma membrane	5737	2.59E-05	0.00628	cytoplasm
	6091	0.000307	0.0282	generation of precursor metabolites and energy	6082	0.000698	0.0371	organic acid metabolic process
	6629	0.000276	0.0264	lipid metabolic process	8198	0.000825	0.0408	ferrous iron binding
CAP18	6644	0.000607	0.0489	phospholipid metabolic process	8270	0.000453	0.0353	zinc ion binding
	8654	0.000346	0.0308	phospholipid biosynthetic process	16783	0.000714	0.0371	sulfurtransferase activity
	9055	1.72E-05	0.00211	electron carrier activity	19752	0.000612	0.0353	carboxylic acid metabolic process
	9061	7.27E-08	1.17E-05	anaerobic respiration	43436	0.000612	0.0353	oxoacid metabolic process
	22857	6.94E-11	1.99E-08	transmembrane transporter activity	51536	0.000516	0.0353	iron-sulfur cluster binding
	44255	0.00024	0.0244	cellular lipid metabolic process				
	45333	2.07E-05	0.00243	cellular respiration				
	5215	8.30E-07	0.000507	transporter activity	5886	2.88E-06	0.00384	plasma membrane
	5886	9.43E-05	0.0108	plasma membrane	8610	5.91E-05	0.0393	lipid biosynthetic process
	5887	0.00055	0.042	integral to plasma membrane				
CP1	9279	4.52E-05	0.00592	cell outer membrane				
	22857	8.25E-07	0.000507	transmembrane transporter activity				
	30313	0.000272	0.0238	cell envelope				
	31224	7.28E-06	0.00185	intrinsic to membrane				
	5215	9.70E-11	1.90E-08	transporter activity				
	5886	7.74E-37	8.33E-34	plasma membrane				
	5887	6.48E-10	1.07E-07	integral to plasma membrane				
	6091	0.000116	0.00734	generation of precursor metabolites and energy				
HBD3	6284	0.000738	0.0311	base-excision repair	no enrichment			
	8509	0.000406	0.0194	anion transmembrane transporter activity				
	8940	3.84E-05	0.00275	nitrate reductase activity				
	9055	0.000249	0.0127	electron carrier activity				
	9061	4.27E-07	4.83E-05	anaerobic respiration				
	55114	0.000498	0.0219	oxidation reduction				
	5215	5.76E-31	2.34E-28	transporter activity	166	0.000106	0.00908	nucleotide binding
	5345	0.00058	0.0223	purine transmembrane transporter activity	5737	0.000609	0.0333	cytoplasm
	5886	1.24E-88	2.51E-85	plasma membrane	6091	5.35E-05	0.0061	generation of precursor metabolites and energy
	5887	3.84E-25	6.01E-23	integral to plasma membrane	6396	0.00126	0.046	RNA processing
	8509	7.02E-06	0.000367	anion transmembrane transporter activity	6399	0.00106	0.043	tRNA metabolic process
	15562	6.14E-07	3.78E-05	efflux transmembrane transporter activity	6400	0.00128	0.046	tRNA modification
	22892	4.82E-27	9.80E-25	substrate-specific transporter activity	6629	4.47E-05	0.0061	lipid metabolic process
	45017	0.001	0.037	glycerolipid biosynthetic process	6631	0.000943	0.043	fatty acid metabolic process
IND	46943	4.38E-07	2.78E-05	carboxylic acid transmembrane transporter activity	8610	7.15E-05	0.00752	lipid biosynthetic process
	51119	3.04E-06	0.000172	sugar transmembrane transporter activity	9061	4.49E-07	0.000153	anaerobic respiration
					9375	0.000571	0.0325	ferredoxin hydrogenase complex
					10467	0.000939	0.043	gene expression
					16491	0.00034	0.0221	oxidoreductase activity
					34470	0.000376	0.0224	ncRNA processing
					34660	8.92E-05	0.00813	ncRNA metabolic process
					45333	2.32E-05	0.00453	cellular respiration
					51536	3.02E-09	2.06E-06	iron-sulfur cluster binding
	5215	9.29E-09	1.74E-06	transporter activity	1882	6.01E-05	0.00954	nucleoside binding
	5886	5.91E-32	5.00E-29	plasma membrane	6396	0.000197	0.0165	RNA processing
	5887	1.15E-07	1.22E-05	integral to plasma membrane	6730	4.71E-06	0.00325	one-carbon metabolic process
	6644	0.000529	0.028	phospholipid metabolic process	6808	0.000442	0.0316	regulation of nitrogen utilization
	8654	0.00038	0.023	phospholipid biosynthetic process	9451	0.000166	0.0148	RNA modification
LL37	9061	0.000331	0.0207	anaerobic respiration	19538	8.00E-04	0.0477	protein metabolic process
	46942	3.17E-05	0.00282	carboxylic acid transport	32259	6.82E-06	0.00325	methylation
	51179	5.87E-10	1.99E-07	localization	32553	0.000146	0.014	ribonucleotide binding
	51234	1.19E-09	2.87E-07	establishment of localization	34470	0.000547	0.0355	ncRNA processing
	55085	0.000449	0.0256	transmembrane transport	34660	0.000909	0.05	ncRNA metabolic process
					43412	1.61E-06	0.0023	macromolecule modification

PEX	5215	4.13E-12	5.36E-10	transporter activity				
	5575	6.49E-12	7.81E-10	cellular_component				
	5886	9.00E-56	7.59E-53	plasma membrane				
	5887	1.34E-17	2.82E-15	integral to plasma membrane				
	6655	0.000566	0.0298	phosphatidylglycerol biosynthetic process				
	9061	1.86E-06	0.000157	anaerobic respiration	no enrichment			
	44459	2.91E-18	7.02E-16	plasma membrane part				
	45333	0.000127	0.00794	cellular respiration				
	46471	0.000566	0.0298	phosphatidylglycerol metabolic process				
	51179	7.42E-14	1.14E-11	localization				
	55085	7.96E-06	0.000639	transmembrane transport				
PGLA	3954	8.24E-05	0.00379	NADH dehydrogenase activity	5543	3.89E-05	0.0204	phospholipid binding
	5215	4.30E-06	0.000274	transporter activity	5886	9.97E-06	0.0105	plasma membrane
	5886	3.37E-22	2.79E-19	plasma membrane				
	5887	2.23E-05	0.00119	integral to plasma membrane				
	6091	5.62E-07	5.18E-05	generation of precursor metabolites and energy				
	6857	0.000218	0.00922	oligopeptide transport				
	9055	2.40E-06	0.000159	electron carrier activity				
	9061	9.16E-12	5.06E-09	anaerobic respiration				
	45333	6.83E-08	8.09E-06	cellular respiration				
	51119	0.000228	0.00922	sugar transmembrane transporter activity				
	51536	7.16E-06	0.000424	iron-sulfur cluster binding				
	51539	0.000532	0.02	4 iron, 4 sulfur cluster binding				
PLEU	5886	2.37E-09	1.72E-06	plasma membrane				
	16020	2.21E-11	3.20E-08	membrane	no enrichment			
	30151	4.28E-06	0.00207	molybdenum ion binding				
PR39	41	0.000384	0.0178	transition metal ion transport	8483	1.88E-05	0.022	transaminase activity
	5215	2.55E-09	6.69E-07	transporter activity	16747	5.21E-05	0.0252	transferase activity, transferring acyl groups other than amino-acyl groups
	5543	0.00082	0.0314	phospholipid binding	16769	3.04E-05	0.022	transferase activity, transferring nitrogenous groups
	5886	4.42E-18	3.47E-15	plasma membrane				
	5887	7.16E-05	0.00563	integral to plasma membrane				
	9279	1.96E-07	2.56E-05	cell outer membrane				
	15682	0.00082	0.0314	ferric iron transport				
	15685	0.000181	0.00979	ferric-enterobactin transport				
	15688	0.000181	0.00979	iron chelate transport				
	15833	0.000206	0.0104	peptide transport				
	15892	0.000181	0.00979	siderophore-iron transport				
	33212	0.000148	0.00979	iron assimilation				
	33214	0.00082	0.0314	iron assimilation by chelation and transport				
	42884	0.000358	0.017	microcin transport				
	55052	0.000938	0.0343	ATP-binding cassette (ABC) transporter complex, substrate-binding subunit-containing				
PROA	41	0.00112	0.0271	transition metal ion transport				
	5215	1.23E-34	2.11E-32	transporter activity				
	5886	1.19E-139	0	plasma membrane				
	5887	3.27E-32	4.21E-30	integral to plasma membrane				
	6650	0.00172	0.0349	glycerophospholipid metabolic process				
	15833	2.13E-05	0.000865	peptide transport				
	17004	0.00182	0.0355	cytochrome complex assembly				
	19725	0.00199	0.0383	cellular homeostasis	no enrichment			
	42884	0.00155	0.0333	microcin transport				
	45017	0.000918	0.0225	glycerolipid biosynthetic process				
	46474	0.000918	0.0225	glycerophospholipid biosynthetic process				
	46915	0.00217	0.0404	transition metal ion transmembrane transporter activity				
	55052	9.52E-05	0.00367	ATP-binding cassette (ABC) transporter complex, substrate-binding subunit-containing				
	55085	1.07E-15	8.67E-14	transmembrane transport				
PXB	5215	2.49E-13	4.58E-11	transporter activity				
	5886	2.00E-35	1.66E-32	plasma membrane				
	5887	4.39E-11	5.60E-09	integral to plasma membrane				
	42592	0.000109	0.00669	homeostatic process				
	42623	0.000225	0.0124	ATPase activity, coupled	no enrichment			
	43190	0.000657	0.0311	ATP-binding cassette (ABC) transporter complex				
	50801	0.000892	0.039	ion homeostasis				
	51119	0.000231	0.0124	sugar transmembrane transporter activity				
	55085	2.78E-07	2.20E-05	transmembrane transport				
R8	5886	0.000237	0.0496	plasma membrane	154	6.56E-07	7.16E-05	rRNA modification
	9279	2.42E-05	0.00787	cell outer membrane	1510	7.89E-09	1.28E-06	RNA methylation
	16020	1.02E-06	0.00192	membrane	6139	4.02E-05	0.00276	nucleobase, nucleoside, nucleotide and nucleic acid metabolic process
	19867	1.69E-05	0.00787	outer membrane	6396	3.64E-11	3.25E-08	RNA processing
	30312	2.92E-05	0.00787	external encapsulating structure	6400	0.000556	0.0331	tRNA modification
	30313	2.19E-05	0.00787	cell envelope	10467	2.42E-06	0.000216	gene expression
					22613	1.38E-10	4.95E-08	ribonucleoprotein complex biogenesis
					31167	2.77E-07	3.80E-05	rRNA methylation
					42254	1.38E-10	4.95E-08	ribosome biogenesis
					43414	5.38E-10	1.14E-07	macromolecule methylation
					44260	1.34E-06	0.000126	cellular macromolecule metabolic process
TPII	5886	1.53E-07	7.14E-05	plasma membrane	154	9.35E-05	0.0122	rRNA modification
	9279	1.26E-07	7.14E-05	cell outer membrane	1510	0.000391	0.0383	RNA methylation
	16020	3.72E-11	6.93E-08	membrane	6364	1.57E-06	0.000733	rRNA processing
	19867	9.60E-08	7.14E-05	outer membrane	6396	2.99E-06	0.000733	RNA processing
	30312	4.97E-07	0.000116	external encapsulating structure	9451	5.46E-05	0.00916	RNA modification
	30313	3.43E-07	0.000102	cell envelope	22613	3.74E-06	0.000733	ribonucleoprotein complex biogenesis
					31167	0.000453	0.039	rRNA methylation
					32553	0.000155	0.0165	ribonucleotide binding
					34660	6.73E-05	0.00988	ncRNA metabolic process
					42254	3.74E-06	0.000733	ribosome biogenesis

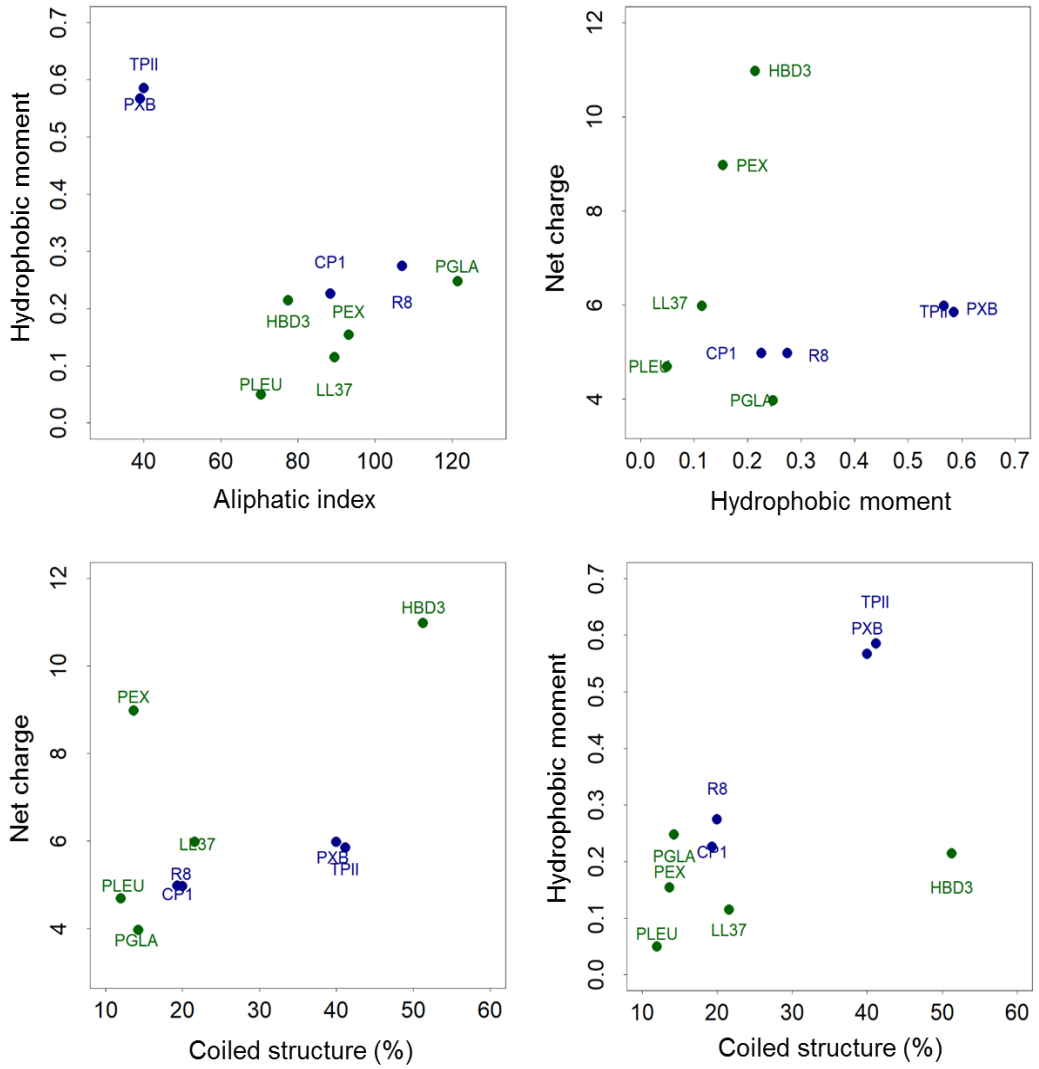

Supplementary Figure 1. C1 (blue) and C2 (green) peptides show differences in their physicochemical properties. Although AMPs in both C1 and C2 clusters belong to membrane-targeting peptides, they show differences in their chemical-genetic interactions. Reassuringly, some physicochemical properties, when considered together, separate C1 and C2 AMPs (P = 0.0186 from two-sided logistic regression for all four combinations).

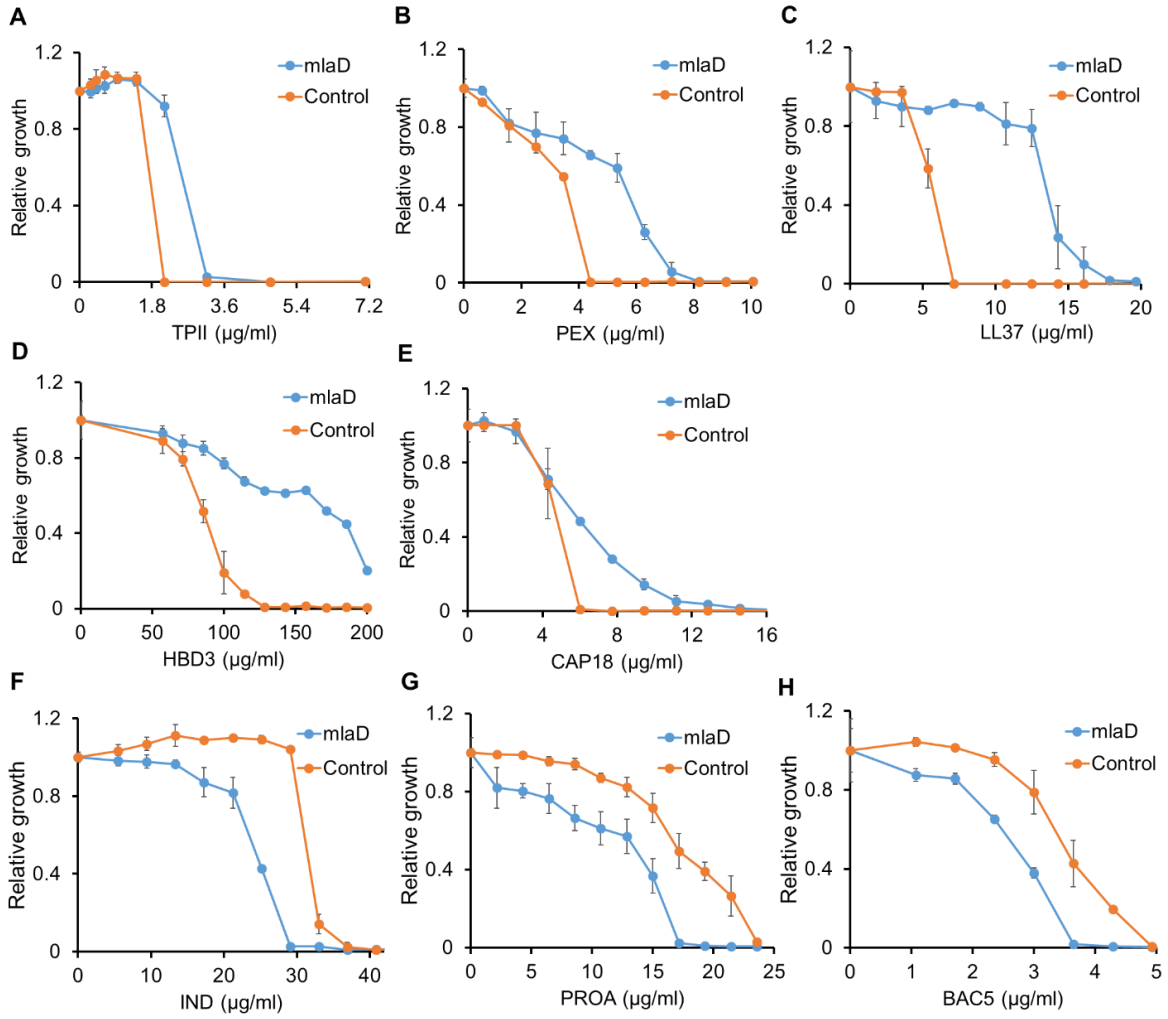

Supplementary Figure 2. Effect of *mlaD* overexpression on bacterial susceptibility to membrane- and intracellular-targeting AMPs. Overexpression of *mlaD* causes resistance to membrane-targeting **(A-E)** and sensitivity to intracellular-targeting AMPs **(F-H)**. Bacterial susceptibility to AMPs was tested by MIC determination. Growth is shown relative to growth in the absence of the given AMP. The blue line represents the *mlaD* overexpression strain and the orange line represents control strain (wild-type *E. coli* BW25113 containing the empty pCA24N vector). Error bars indicate the standard errors based on three biological replicates.

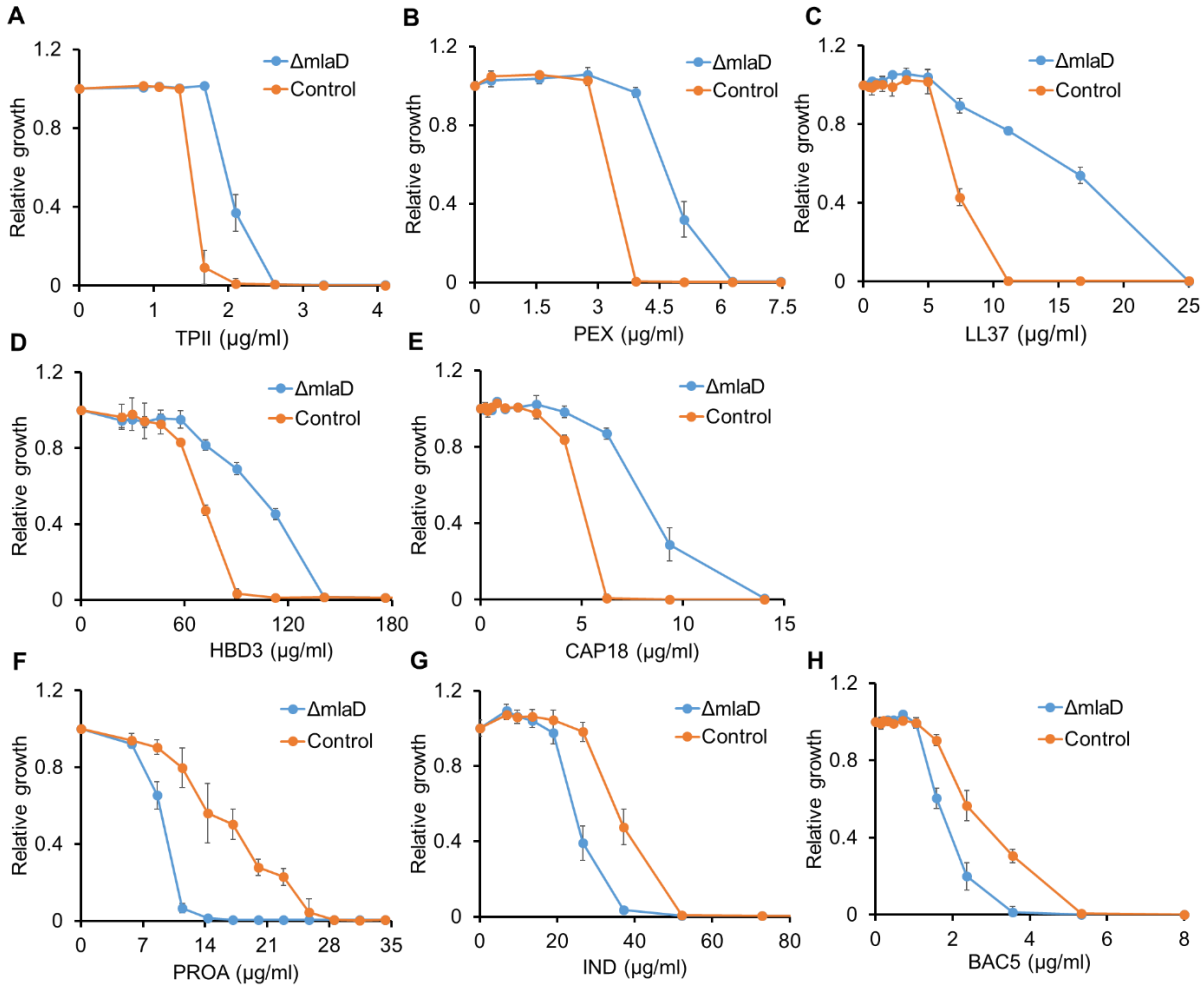

Supplementary Figure 3. Antimicrobial susceptibility of *mlaD* knockout mutant to membrane and intracellular-targeting AMPs. *mlaD* knockout mutant shows resistance to membrane-targeting **(A-E)** and sensitivity to intracellular-targeting AMPs **(F-H)**. The bacterial susceptibility of the mutant to AMPs was tested by MIC determination. Growth is shown relative to growth in the absence of the corresponding AMP. The blue line represents the *mlaD* knockout strain and the orange line represents control strain (wild-type *E. coli* BW25113). Error bars indicate the standard errors based on three biological replicates.

Supplementary references:

1 Matsuzaki, K. Why and how are peptide–lipid interactions utilized for self-defense? Magainins and tachyplesins as archetypes. *Biochim. Biophys. Acta - Biomembr.* **1462,** 1–10 (1999).

2 Daugelavicius, R., Bakiene, E. & Bamford, D. H. Stages of Polymyxin B Interaction with the *Escherichia coli* Cell Envelope. *Antimicrob. Agents Chemother.* **44,** 2969–2978 (2000).

3 Hirsch, E. B. & Tam, V. H. Detection and treatment options for *Klebsiella pneumoniae* carbapenemases (KPCs): an emerging cause of multidrug-resistant infection. *J. Antimicrob. Chemother.* **65,** 1119–1125 (2010).

4 Dong, T. G. *et al.* Generation of reactive oxygen species by lethal attacks from competing microbes. *Proc. Natl. Acad. Sci.* **112,** 2181–2186 (2015).

5 Sampson, T. R. *et al.* Rapid Killing of Acinetobacter baumannii by Polymyxins Is Mediated by a Hydroxyl Radical Death Pathway. *Antimicrob. Agents Chemother.* **56,** 5642–5649 (2012).

6 Kościuczuk, E. M. *et al.* Cathelicidins: family of antimicrobial peptides. A review. *Mol. Biol. Rep.* **39,** 10957–10970 (2012).

7 Sang, Y. & Blecha, F. Porcine host defense peptides: Expanding repertoire and functions. *Dev. Comp. Immunol.* **33,** 334–343 (2009).

8 Arcidiacono, S., Soares, J. W., Meehan, A. M., Marek, P. & Kirby, R. Membrane permeability and antimicrobial kinetics of cecropin P1 against *Escherichia coli*. *J. Pept. Sci.* **15,** 398–403 (2009).

9 Boman, H. G., Agerberth, B. & Boman, A. Mechanisms of action on *Escherichia coli* of cecropin P1 and PR-39, two antibacterial peptides from pig intestine. *Infect. Immun.* **61,** 2978–84 (1993).

10 Tremouilhac, P., Strandberg, E., Wadhwani, P. & Ulrich, A. S. Synergistic Transmembrane Alignment of the Antimicrobial Heterodimer PGLa/Magainin. *J. Biol. Chem.* **281,** 32089–32094 (2006).

11 Tremouilhac, P., Strandberg, E., Wadhwani, P. & Ulrich, A. S. Conditions affecting the re-alignment of the antimicrobial peptide PGLa in membranes as monitored by solid state 2H-NMR. *Biochim. Biophys. Acta - Biomembr.* **1758,** 1330–1342 (2006).

12 Hartmann, M. *et al.* Damage of the Bacterial Cell Envelope by Antimicrobial Peptides Gramicidin S and PGLa as Revealed by Transmission and Scanning Electron Microscopy. *Antimicrob. Agents Chemother.* **54,** 3132–3142 (2010).

13 Gottler, L. M. & Ramamoorthy, A. Structure, membrane orientation, mechanism, and function of pexiganan--a highly potent antimicrobial peptide designed from magainin. *Biochim. Biophys. Acta* **1788,** 1680–6 (2009).

14 Hallock, K. J., Lee, D.-K. & Ramamoorthy, A. MSI-78, an Analogue of the Magainin Antimicrobial Peptides, Disrupts Lipid Bilayer Structure via Positive Curvature Strain. *Biophys. J.* **84,** 3052–3060 (2003).

15 Hancock, R. E. W. & Sahl, H.-G. Antimicrobial and host-defense peptides as new anti-infective therapeutic strategies. *Nat. Biotechnol.* **24,** 1551–1557 (2006).

16 Zasloff, M. Antimicrobial peptides of multicellular organisms. *Nature* **415,** 389–395 (2002).

17 https://clinicaltrials.gov/ct2/results?cond=&term=pexiganan&cntry=&state=&city=&dist=

18 Saint, N., Cadiou, H., Bessin, Y. & Molle, G. Antibacterial peptide pleurocidin forms ion channels in planar lipid bilayers. *Biochim. Biophys. Acta - Biomembr.* **1564,** 359–364

(2002).
19 Choi, H. & Lee, D. G. Antimicrobial peptide pleurocidin synergizes with antibiotics through hydroxyl radical formation and membrane damage, and exerts antibiofilm activity. *Biochim. Biophys. Acta - Gen. Subj.* **1820,** 1831–1838 (2012).
20 Lee, J. & Lee, D. G. Concentration-Dependent Mechanism Alteration of Pleurocidin Peptide in *Escherichia coli*. *Curr. Microbiol.* **72,** 159–164 (2016).
21 Patrzykat, A., Friedrich, C. L., Zhang, L., Mendoza, V. & Hancock, R. E. W. Sublethal Concentrations of Pleurocidin-Derived Antimicrobial Peptides Inhibit Macromolecular Synthesis in *Escherichia coli*. *Antimicrob. Agents Chemother.* **46,** 605–614 (2002).
22 Senyurek, I. *et al.* Dermcidin-Derived Peptides Show a Different Mode of Action than the Cathelicidin LL-37 against *Staphylococcus aureus*. *Antimicrob. Agents Chemother.* **53,** 2499–2509 (2009).
23 Nagaoka, I. *et al.* Augmentation of the lipopolysaccharide-neutralizing activities of human cathelicidin CAP18/LL-37-derived antimicrobial peptides by replacement with hydrophobic and cationic amino acid residues. *Clin. Diagn. Lab. Immunol.* **9,** 972–82 (2002).
24 Rosenfeld, Y., Papo, N. & Shai, Y. Endotoxin (Lipopolysaccharide) Neutralization by Innate Immunity Host-Defense Peptides. *J. Biol. Chem.* **281,** 1636–1643 (2006).
25 Liu, W. *et al.* Effect of Intracellular Expression of Antimicrobial Peptide LL-37 on Growth of *Escherichia coli* Strain TOP10 under Aerobic and Anaerobic Conditions. *Antimicrob. Agents Chemother.* **57,** 4707–4716 (2013).
26 Choi, H., Yang, Z. & Weisshaar, J. C. Oxidative stress induced in E. coli by the human antimicrobial peptide LL-37. *PLOS Pathog.* **13,** e1006481 (2017).
27 Dhople, V., Krukemeyer, A. & Ramamoorthy, A. The human beta-defensin-3, an antibacterial peptide with multiple biological functions. *Biochim. Biophys. Acta - Biomembr.* **1758,** 1499–1512 (2006).
28 Sass, V. *et al.* Human -Defensin 3 Inhibits Cell Wall Biosynthesis in Staphylococci. *Infect. Immun.* **78,** 2793–2800 (2010).
29 Otvos, L. *et al.* Interaction between Heat Shock Proteins and Antimicrobial Peptide. *Biochemistry* **39,** 14150–14159 (2000).
30 Zhou, Y. & Chen, W. N. iTRAQ-coupled 2-D LC–MS/MS analysis of cytoplasmic protein profile in *Escherichia coli* incubated with apidaecin IB. *J. Proteomics* **75,** 511–516 (2011).
31 Zhou, Y. & Chen, W. N. iTRAQ-Coupled 2-D LC-MS/MS Analysis of Membrane Protein Profile in *Escherichia coli* Incubated with Apidaecin IB. PLoS ONE 6, e20442 (2011).
32 Le, C.-F., Fang, C.-M. & Sekaran, S. D. Intracellular Targeting Mechanisms by Antimicrobial Peptides. *Antimicrob. Agents Chemother.* **61,** (2017).
33 Ostorhazi, E., Nemes-Nikodem, E., Knappe, D. & Hoffmann, R. In Vivo Activity of Optimized Apidaecin and Oncocin Peptides Against a Multiresistant, KPC-Producing *Klebsiella pneumoniae* Strain. *Protein Pept. Lett.* **21,** 368–373 (2014).
34 Berthold, N. *et al.* Novel Apidaecin 1b Analogs with Superior Serum Stabilities for Treatment of Infections by Gram-Negative Pathogens. *Antimicrob. Agents Chemother.* **57,** 402–409 (2013).
35 Tossi, A., Scocchi, M., Skerlavaj, B. & Gennaro, R. Identification and characterization of a primary antibacterial domain in CAP18, a lipopolysaccharide binding protein from rabbit leukocytes. *FEBS Lett.* **339,** 108–112 (1994).
36 Larrick, J. W. *et al.* Human CAP18: a novel antimicrobial lipopolysaccharide-binding protein. *Infect. Immun.* **63,** 1291–7 (1995).
37 Chen, C. *et al.* The solution structure of the active domain of CAP18--a lipopolysaccharide binding protein from rabbit leukocytes. *FEBS Lett.* **370,** 46–52

(1995).
38 Saiman, L. *et al.* Cathelicidin Peptides Inhibit Multiply Antibiotic-Resistant Pathogens from Patients with Cystic Fibrosis. *Antimicrob. Agents Chemother.* **45,** 2838–2844 (2001).
39 Falla, T. J., Karunaratne, D. N. & Hancock, R. E. W. Mode of Action of the Antimicrobial Peptide Indolicidin. *J. Biol. Chem.* **271,** 19298–19303 (1996).
40 Melo, M., Dugourd, D. & Castanho, M. Omiganan Pentahydrochloride in the Front Line of Clinical Applications of Antimicrobial Peptides. *Recent Pat. Antiinfect. Drug Discov.* **1,** 201–207 (2006).
41 https://clinicaltrials.gov/ct2/results?cond=&term=omiganan&cntry=&state=&city=&dist=
42 Subbalakshmi, C. Mechanism of antimicrobial action of indolicidin. *FEMS Microbiol. Lett.* **160,** 91–96 (1998).
43 Aspedon, A. & Groisman, E. A. The antibacterial action of protamine: evidence for disruption of cytoplasmic membrane energization in *Salmonella typhimurium*. *Microbiology* **142,** 3389–3397 (1996).
44 Natasha Weatherspoon-Griffin. Identification of Novel Genetic Mechanisms Required for Bacterial Resistance to Antimicrobial Peptides. (https://repository.asu.edu/attachments/110499/content/Griffin_asu_0010E_12909.pdf)
45 Johansen, C., Verheul, A., Gram, L., Gill, T. & Abee, T. Protamine-induced permeabilization of cell envelopes of gram-positive and gram-negative bacteria. *Appl. Environ. Microbiol.* **63,** 1155–9 (1997).
46 Ho, Y.-H., Shah, P., Chen, Y.-W. & Chen, C.-S. Systematic Analysis of Intracellular-targeting Antimicrobial Peptides, Bactenecin 7, Hybrid of Pleurocidin and Dermaseptin, Proline–Arginine-rich Peptide, and Lactoferricin B, by Using Escherichia coli Proteome Microarrays. *Mol. Cell. Proteomics* **15,** 1837–1847 (2016).
47 Skerlavaj, B., Romeo, D. & Gennaro, R. Rapid membrane permeabilization and inhibition of vital functions of gram-negative bacteria by bactenecins. *Infect. Immun.* **58,** 3724–30 (1990).